2008

An investigation of the magnetic fabrics and the paleomagnetism of the Ghost Rocks Formation, Kodiak Islands, Alaska

Sean F. Gallen
Western Washington University

AN INVESTIGATION OF THE MAGNETIC FABRICS AND PALEOMAGNETISM OF THE GHOST ROCKS FORMATION, KODIAK ISLANDS, ALASKA

By

Sean F. Gallen

Accepted in Partial Completion

of the Requirements for the Degree

Master of Science

_____

Moheb A. Ghali, Dean of the Graduate School

ADVISORY COMMITTEE

_____

Chair, Dr. Bernard A. Housen

_____

Dr. Sarah M. Roeske

_____

Dr. Susan M. DeBari

MASTER'S THESIS

In presenting this thesis in partial fulfillment of the requirements for a master's degree at Western Washington University, I grant to Western Washington University the non-exclusive royalty-free right to archive, reproduce, distribute, and display the thesis in any and all forms, including electronic format, via any digital library mechanisms maintained by WWU.

I represent and warrant this is my original work, and does not infringe or violate any rights of others. I warrant that I have obtained written permissions from the owner of any third party copyrighted material included in these files.

I acknowledge that I retain ownership rights to the copyright of this work, including but not limited to the right to use all or part of this work in future works, such as articles or books.

Library users are granted permission for individual, research and non-commercial reproduction of this work for educational purposes only. Any further digital posting of this document requires specific permission from the author.

Any copying or publication of this thesis for commercial purposes, or for financial gain, is not allowed without my written permission.

Signature _____
Date _____

AN INVESIGATION OF THE MAGNETIC FABRICS AND THE PALEOMAGNETISM OF THE GHOST ROCKS FORMATION, KODIAK ISLANDS, ALASKA

A Thesis
Presented to
The Faculty of
Western Washington University

In Partial Fulfillment
Of the Requirements for the Degree
Master of Science

By
Sean F. Gallen
June 2008

Abstract

Recent tectonic models based on the hypothesized existence of the Resurrection plate between the Kula and Farallon plates have questioned the location(s) of trench-ridge-trench (TRT) triple junction(s) along the Northern Cordilleran margin during Paleocene to Eocene time. The Paleocene Ghost Rocks Formation, located in the Kodiak islands, Alaska (latitude ~57°N), consists of pillow lavas and hypabyssal sills interbedded with turbidites, and is interpreted to have formed in a trench slope or slope basin during the passage of a TRT triple junction. A previous paleomagnetic study (Plumley et al., 1983) on the volcanic flows of the Ghost Rocks Formation suggests these rocks formed at latitudes significantly south of their present-day locations, at a latitude of ~41ºN during Paleocene time. Tectonic models, based on the assumed existence of the Resurrection plate, reject the conclusions of Plumley et al.'s paleomagnetic study, and instead suggest that these rocks have been remagnetized. Our study revisited the Ghost Rocks Formation in an effort to resolve the disputed location of this TRT triple junction.

The focus of this thesis is on magnetic fabrics and paleomagnetism of two localities within the Ghost Rocks Formation: Jap Bay and Alitak Bay. More than 300 oriented core samples were obtained primarily from sedimentary rocks in two coherent sections of Jap Bay, Unit A and Unit B; and over 500 oriented core samples were taken from the turbidites and volcanic flows of Alitak Bay.

The anisotropy of magnetic susceptibility was used to study the magnetic fabrics of these rocks. The majority of the sedimentary rocks showed magnetic

fabrics typical of weakly deformed sediments with magnetic foliations oriented parallel to bedding, and cryptic magnetic lineations oriented perpendicular to the shortening direction. However, sediments from Unit B of Jap Bay showed a large portion of magnetic lineations oriented approximately parallel to the direction of slip on bedding parallel faults, becoming more pronounced in fold hinges. Magnetic lineations oriented parallel to the slip direction are not typical of weakly deformed sediments. The volcanic samples from Alitak Bay contained magnetic fabrics that can qualitatively be defined as foliated, lineated, and scattered.

The paleomagnetism of the majority of the sedimentary rocks were magnetically unstable. Those from Unit A however, exhibited good magnetic behavior but the high unblocking temperature components fail the fold test. The magnetic behavior of the volcanic flows from Alitak Bay was good. Results from a series of fold tests using various structural corrections yield inconclusive results. However, “rotation tests” show positive results. The “rotation corrected” directions from Alitak Bay and in-situ directions of Kiliuda Bay from Plumley et al. (1983) pass a regional fold test yielding a mean paleomagnetic direction for the Ghost Rocks Formation corresponding to a latitude of ~41º. However, the somewhat arbitrary nature of these rotation corrections and failed conglomerate tests suggest that remagnetization of the rocks at Alitak Bay is also a likely possibility.

Acknowledgements

Bernie Housen is responsible for allowing me to take part in such a wonderful project and helped extensively from start to finish. Without his help, guidance, support and patience this project would have never come to fruition. Sarah Roeske helped to refine my thoughts and ideas throughout this entire process. Many thanks to Sue DeBari for her keen editorial eye and fresh outside perspective on this thesis. Without Russ Burmester, this project would have never run so smoothly. I could always count on Russ for great discussions which helped to develop and clarify the work present in this thesis. I would also like to acknowledge Kristin O'Connell for helping me to get on my feet in the field and for bringing fresh ideas to the table. John Cooper was indispensable out in the field; without him we all would have done a great deal of swimming in the cold Alaskan waters. I would also like to acknowledge my friends and family, without their support and encouragement, I would never have come this far. A special thanks goes to my mother, Patricia Sullivan, for her moral and editorial support during my entire graduate career. This project would have never been possible without the financial support of the National Science Foundation, the Bureau of Faculty Research, and the Western Washington University Department of Geology.

Table of Contents

Tables

Figures

Introduction

Uncertainties in current tectonic plate reconstructions result in a range of possible latitudes for the Late Cretaceous-Mid Eocene location of the Kula-Farallon-North America trench-ridge-trench (TRT) triple junctions somewhere between the latitudes of present day Vancouver Island and Mexico (Engebretson et al., 1985). TRT triple junction interactions leave behind geologic anomalies that can be used to identify such an interaction long after it has taken place. Efforts to resolve the exact location of the Kula-Farallon-North America TRT triple junction using TRT geologic anomalies have been complicated. Evidence for two Paleocene to Eocene TRT triple junction interactions is found along the Northern Cordilleran margin, and various tectonic models have been developed to explain how this came to be.

The Paleocene Ghost Rocks Formation, located in south central Alaska (Fig. 1) consists of andesitic and basaltic flows, and mafic hypabyssal sills interbedded turbidites that most workers agree were deposited in a trench slope or slope basin during the passage of a TRT triple junction (e.g. Moore et al., 1983; Bradley et al., 2003). A previous paleomagnetic study on the volcanic flows of this Formation by Plumley et al. (1983) suggests that the TRT triple junction interaction recorded in these rocks took place at latitudes significantly south of their present day location, ~41^{o}N, during Paleocene time. Models based on this study and others like it suggest that only one TRT triple junction existed during the Paleocene-Eocene (Kula-Farallon-North America). These authors explain the presence of Paleocene-Eocene TRT rocks in two locations by suggesting that some of these units were translated >1000km northward to its present day location. Other models suggest the existence of

a third plate, the Resurrection plate which existed between the Kula and Farallon plates, thus allowing for the co-evolution of two different TRT triple junctions at the same time (Haeussler et al., 2003; Bradley et al., 2003). These models cast doubt on the conclusions of Plumley et al. (1983), suggesting that the Ghost Rocks Formation has been remagnetized and thus may have formed close to their present day location. The resolution of the disputed location of this TRT triple junction will allow further progression of tectonic plate reconstructions of the Northern Cordilleran for the Paleocene-Mid Eocene.

This thesis is a portion of a larger collaborative project between Western Washington University and the University of California at Davis to revisit and conduct an extensive paleomagnetic and structural study of the Paleocene Ghost Rocks Formation of the Kodiak Islands, Alaska. The focus of this thesis is on two localities of the Ghost Rocks Formation Jap Bay and Alitak Bay. The objectives of this thesis are: 1) To obtain a more detailed and extensive paleomagnetic data set than the previous study in an effort to resolve the controversial location of the Ghost Rocks Formation during the Paleocene. 2) To conduct a study of the magnetic fabrics of the Ghost Rocks Formation to aid in the structural investigation. A study of this kind, with the aid of the structural study conducted by our colleagues at the University at Davis, has helped put the controversy over the location of this TRT triple junction to rest.

Statement of the Problem

Background

Projections for the location of the Kula-Farallon-North America trench ridge-trench (TRT) triple junction were originally estimated from plate reconstructions, which place the triple junction at a kinematically reasonable orientation and location at a given point in time. These projections place the Kula-Farallon-North America TRT triple junction somewhere between the present-day latitudes of Vancouver Island and Mexico during Late Cretaceous-Middle Eocene time (Engebretson et al., 1985; Lonsdale, 1988; Stock and Molnar, 1988; Rosa and Molnar, 1988). The end-members of this range of possible latitudes became known as the "northern" and "southern" options. Most tectonics models for the Late Cretaceous-Middle Eocene time period have focused on either of these end-member options (e.g. Dickinson 2004), but a number of intermediate and different reconstructions have been put forward (e.g. Stock and Molnar, 1988; Breitsprecher et al., 2003).

The range of possible latitudes of the projected locations for the Kula-Farallon-North America triple junction prior to 40Ma is the result of uncertainties associated with predicting its location throughout the past. One source of uncertainty in these projections is the lack of direct evidence on the exact location and geometry of the Kula plate, as it has been entirely subducted. Therefore, estimates of its location and geometry must be extrapolated using the remaining magnetic anomalies and fracture zones on the Pacific plate. These estimates will only be as accurate as how precisely the remaining magnetic anomalies on the Pacific plate mirror those of

the Kula plate. A second source of uncertainty in some tectonic plate projections is the use of a fixed hotspot as a reference frame. Recent paleomagnetic (Tarduno et al., 2003) and sedimentalogical (Pares and Moore, 2005) evidence suggests relatively rapid southward movement of the Hawaiian hot spot. Therefore, the appropriate corrections must be made when using projections based on a fixed hotspot reference frame. Current plate reconstructions acknowledge these uncertainties and thus the location of the Kula-Farallon-North America TRT triple junction from Late Cretaceous through Middle Eocene time is ambiguous. One way to address these uncertainties is to study locations along the Northern Cordilleran margin that preserve geologic anomalies associated with the subduction of a ridge at a TRT triple junction, and fall between the Late Cretaceous-Middle Eocene age bracket.

Slab Windows

The orientation of and the angle at which a spreading ridge is subducted relative to the trench will determine the style of triple junction produced. A trench-ridge-trench (TRT) triple junction interaction occurs when a spreading ridge is subducted more or less perpendicular to a trench (Thorkelson and Taylor, 1989; Thorkelson, 1996; Sisson et al., 2003). When a hot buoyant spreading ridge is subducted, new ocean crust will cease to form beneath the overriding plate, resulting in the opening of an ever-widening gap, or “slab window,” beneath the overriding plate. Hence, a slab window is a location in which hot asthenosphere is in direct contact with the overlying crust and results in a drastic increase of heat flow into the overriding plate. The increased heat flow will change the thermal and mechanical properties of the overriding plate, resulting in several anomalous geologic phenomena

that are diagnostic of ridge subduction and slab windows (Dickinson and Snyder, 1979; Thorkelson, 1989, Thorkelson, 1996). The study of ridge-trench interactions and slab window processes in modern settings such as in Central America (Johnston and Thorkelson, 1997) and proposed ancient settings such as along the Northern Cordilleran margin (Thorkelson and Taylor, 1989; Sisson et al., 2003) has allowed for identification of the anomalous geologic processes unique to ridge-trench interactions and their slab windows. These anomalies include, but are not limited to, magmatism in the typically cold and amagmatic regions of the trench and forearc of subduction zones, cessation of arc magmatism anomalous backarc igneous activity, and coeval uplift and deformation (Thorkelson and Taylor, 1989; Thorkelson, 1996; Sisson et al., 2003) (Fig. 2). There is no other known explanation for these anomalous geologic signatures, thus when preserved can be used to identify the paleo-location of ridge-trench interactions such as TRT triple junctions long after this interaction has ceased to exist. Along the contemporary Northern Cordilleran margin, evidence for two Tertiary age TRT triple junctions are found.

Paleocene-Eocene trench-ridge-trench triple junctions of the Cordilleran

Two locations along the Northern Cordilleran margin preserve geologic signatures that are diagnostic of Paleocene-Eocene age TRT triple junctions (Fig. 3). One is located in the Cascades and Coast ranges of Oregon where anomalous igneous activity and structural evidence suggest a TRT interaction during Paleocene-Eocene time (Babcock et al., 1992; Breitspecher et al., 2003; Groome et al., 2003; Haeussler et al., 2003). Additionally, geophysical evidence from seismic tomography studies

suggests the presence of a slab window at this location beneath the North American plate during this time period (Bunge and Grand, 2000). The other location that most clearly shows evidence of a Paleocene-Eocene TRT triple junction is in the Chugach terrane, located on the southern margin of Alaska. It is here that a record of Tertiary age geologic anomalies are found, which include near-trench igneous rocks along the complete strike of the Chugach Terrane in the Sanak-Baranof belt (Marshak and Karig, 1977; Helwig and Emmit; 1981; Moore et al., 1983; Plafker et al., 1994; Bradley et al., 2003; Kusky et al., 2003; Haeussler et al., 2003), high-T low-P near trench metamorphism (Bowman et al., 2003; Weinberger and Sisson, 2003), motion on transverse strike-slip faults (Roeske et al., 2003; Pavlis and Sisson, 2003) and uplift of the accretionary prism (Pavlis and Sisson, 1995; Sample and Reid, 2003). Additionally, isotopic age data from the anomalous near-trench magmatism in the Sanak-Baranof belt shows a progressive decrease in age from west to east, which is most easily explained by the migration of a TRT triple junction along the margin during this time (Haeussler et al., 2003). The ages of the near trench magmatism of the Sanak-Baranof belt overlap with ages of the anomalous igneous units found in Oregon and Washington (Fig. 4). The location of the TRT triple junction interaction(s) responsible for the formation of the anomalous geologic units and processes found in Alaska has remained controversial for over twenty years with workers arguing for and against large-scale (>1000km) northward translations of the Chugach Terrane since Paleocene time.

Competing Models

Three competing tectonic models have been developed to explain the geologic and geophysical evidence of two Paleocene-Eocene age TRT triple junctions along the North American Margin (Fig. 5). The first model, Model A, is based on paleomagnetic and geologic studies of the anomalous geology associated with a Paleocene-Eocene TRT triple junction and suggests that the anomalous units of the Chugach terrane formed at latitudes significantly south of their present day location during Paleocene time (Plumley et al., 1983; Moore et al., 1983; Bol et al., 1992; Cowan, 2003; Roeske et al., 2003). This evidence places the Kula-Farallon-North America triple junction at a latitude of ~40°N during Paleocene-Eocene time and requires the large-scale (>1000km) translation of the anomalous igneous units and associated accretionary complex to their present location in Alaska (Fig. 6; 5a). A latitude of ~40°N for the Paleocene-Eocene Kula-Farallon-North America TRT triple junction interaction, suggested by Model A, is also consistent with most plate reconstruction models (Engebretson et al., 1985; Stock and Molnar, 1988; Breitsprecher et al., 2003).

The second model, Model B, is based on geologic evidence in Alaska, and suggests the Chugach terrane and its TRT anomalies formed and were emplaced near their present day position during the Paleocene with little to no subsequent movement relative to more inboard units. This hypothesis requires that the Kula-Farallon spreading ridge interacted with the North American margin at a latitude of ~58°N, migrating from northwest to southeast during the Paleocene-Eocene (Plafker et al., 1994; Bradley et al., 2003) (Fig. 7; 5b). This “extreme northern” option of the Kula-

Farallon-North America triple junction proposed by Model B has more or less become abandoned, as most plate reconstructions place this triple junction significantly further south from the Late Cretaceous through the Eocene. Additionally, Model B it ignores the geologic evidence of a TRT triple junction interaction of the same age found in Oregon and Washington.

An alternative to Models A and B has been proposed by Haeussler et al. (2003) and Bradley et al. (2003) and has been designated the Resurrection Plate Model (Fig. 8; 5c). This model is based on the geologic evidence of Paleocene-Eocene age TRT triple junction anomalies found in Oregon, Washington and Alaska and suggests that an oceanic plate, the Resurrection plate, existed between the Kula and Farallon plates. The existence of this third oceanic plate allows for the synchronous interaction of two TRT triple junctions along the Northern Cordilleran margin during Paleocene-Eocene time, the Kula-Resurrection-North America TRT triple junction migrating west to east along the SW Alaskan margin and the Resurrection-Farallon-North America TRT triple junction remaining more or less stationary around present day northwest Washington until ~47Ma (Haeussler et al., 2003; Bradley et al., 2003) (Fig. 8; 5c). One important aspect of the Resurrection plate model is that it calls for no significant translation of the Chugach terrane and associated TRT igneous units of the Sanak-Baranof belt. This poses a problem in that two existing studies (Plumley et al., 1983; Bol et al., 1992) using paleomagnetism have indicated that at least some significant portions of the TRT rocks were formed >1500km to the south. To address this problem, Haeussler et al. (2003) rejects the conclusions of these studies instead suggesting these rocks have been remagnetized.

These authors support this remagnetization by citing complications with each of the studies. Bol et al. (1992) used a two-stage structural correction on the paleomagnetic data set and Haeussler et al. (2003) point out the fact that there is ~3.6Ma time difference between the formation of the ophiolite studied by Bol et al. (1992) and its emplacement in the accretionary complex and thus even if the ophiolite has not be remagnetized it may not record the location of the accretionary complex. Haussler et al. (2003) casting doubt on the Plumley et al. (1983) study because a complex structural correction used at the Alitak Bay locality of the study, the relatively low (508ºC) unblocking temperatures of andesite samples, and the large discrepancies of magnetic directions between the two localities of the study.

In order to try to resolve the discrepancies between these models of location(s) of Paleocene to Eocene TRT triple junction(s) of the Northern Cordilleran, we revisited the Paleocene Ghost Rocks Formation of the Kodiak Islands, Alaska, the location of the previous paleomagnetic study by Plumley et al. (1983) (Fig. 1). The purpose of this collaborative study between Western Washington University and University of California at Davis was to do a more extensive and detailed paleomagnetic and structural study of the Ghost Rocks Formation in an effort to resolve problems of the study cited by Haeussler et al. (2003). The Ghost Rocks Formation consists of a sequence of turbidites interbedded with pillow lavas and is interpreted to have been deposited in a trench slope or slope basin during the passage of a TRT triple junction in Paleocene time (Moore et al., 1983; Bradley et al., 2003). The Ghost Rocks Formation was chosen because the previous paleomagnetic study by Plumley et al. (1983) reported good demagnetization behavior of the volcanic

units. The interbedded sedimentary units make identification of paleohorizontal relatively straightforward, suggesting that the Ghost Rocks Formation is ideal for paleomagnetic study.

Review of Previous Literature

Geologic setting

The Chugach terrane is an accretionary complex located along the southern margin of Alaska and records repeated episodes of accretion and subduction-related magmatism from at least the Early Jurassic to the present. The Kodiak Islands of Alaska represent an emergent portion of this accretionary complex exposing northeast trending southwest dipping belts of deep sea rocks. The Paleocene Ghost Rocks Formation crop out as a 160km long 15km wide belt on the southeast portion of the Islands. The Ghost Rocks are in fault contact with the Maastrichtian Kodiak Formation to the northwest and the Eocene Sitkalidak Formation to the southeast (Byrne, 1982; 1984) (Fig. 1).

The Ghost Rocks Formation consists of a sequence of turbidites interbedded with volcanic flows and scattered hypabyssal intrusions. The turbidites are deformed, primarily consisting of coherent beds of alternating sandstone and argillite, but locally grade from argillite to pebble conglomerate. Bedding thickness varies from thin (1-5cm) to thick (>10m) but is dominated by medium to thick beds of sandstone and argillite. Variable portions of the sedimentary units show stratal disruption, with map-scale sections qualifying as mélange (Byrne, 1984; Fisher and Byrne, 1987). Portions of the clastic sediments maintain primary depositional structures and are clearly

interbedded with igneous units including basaltic to andesitic pillows/flows, pillow breccia, tuff, dykes, and sills. Limestone is locally found primarily interbedded with or capping volcanic flows. Intrusive quartz diorite to tonalite bodies are also present, cross cutting the turbidites and volcanic flows of the Ghost Rock Formation, which most workers believe are satellite plutons of the Kodiak batholith found in the Kodiak Formation to the north (Byrne, 1984). Geochemical analysis of the cross-cutting igneous units of the Kodiak Formation has revealed a MORB (mid ocean ridge basalt) component. Compositional variation within the igneous units interpreted to be a result of various amounts of mixing of the magmatic source with the sedimentary units (Hill et al., 1981). It is generally accepted by most researchers that the Ghost Rocks Formation formed as a result of the passage of a trench-ridge-trench (TRT) triple junction through a trench slope or slope basin during Paleocene-Eocene time (Moore et al., 1983; Bradley et al., 2003).

The age of the Ghost Rocks Formation has been constrained by planktonic foraminifera fossils and isotopic ages from the quartz diorite to tonalite intrusives. Planktonic foraminifera occur locally in limestones, giving a maximum age of deposition that ranges from Late Cretaceous to Paleocene. Minimum ages of the formation are given by isotopic age dates from the intrusive plutons (Byrne, 1982; Moore et al., 1983; Byrne, 1984). A biotite granodiorite yeilds K-Ar biotite ages of 62.6, and 62.1+/-0.6Ma and a Rb/Sr biotite/plagioclase isochron yields an age of 63+/-3Ma (Moore et al., 1983). Additionally, a more recent study by Farris et al. (2006) reported a $^{40}Ar/^{39}Ar$ whole rock date of 60.15+/-0.86Ma from a pluton in the northeast end of the Ghost Rocks Formation. Thus, the minimum age of the Ghost

Rocks formation ranges from 60-63Ma. These dates constrain the age of the Ghost Rocks Formation to be between ~70Ma and 60Ma.

Peak metamorphic conditions experienced by the Ghost Rocks Formation have been determined from fluid inclusions of quartz veins formed during S1 and S2, yielding temperatures of 240-260+/-20ºC and pressures of 280-320+/-~25MPa (Vrolijk et al., 1988). Prehnite is present in quartz veins as is pumpellyite locally in volcaniclastic sandstones. This suggests that the regional metamorphism reached prehnite-pumpellyite facies. Contact metamorphic aureoles surrounding intrusive bodies are narrow and easily identifiable (Byrne, 1984; Vrolijk et al., 1988).

Review of Paleomagnetic Studies

Plumley et al. (1983) conducted a paleomagnetic study on the basalt and andesite flows of the Ghost Rocks Formation. The focus of their study was two localities separated by ~80km along strike, Alitak Bay and Kiliuda Bay (Fig. 1). A total of 29 sites were sampled, 13 sites from basalt and andesite flows at Kiliuda Bay and 16 sites from andesite flows at Alitak Bay. The reported demagnetization behavior was good, and a well-defined characteristic magnetization was found in the majority of the samples (with 11 acceptable sites at Kiliuda Bay and 16 acceptable sites at Alitak Bay). The secondary component of magnetization was concluded to be primary in origin, as both reverse and normal polarities were observed and great improvement in clustering was observed after tilt-corrections were applied to both localities. Plumley et al. (1983) determined the curie temperatures to be between 555°C-560°C for the basalts and 450°C-550°C for the andesites, concluding the

primary ferromagnetic mineral to be titanium-poor titanomagnetite for both rock types.

There were complications to the Plumley et al. (1983) study. The mean direction of the Kiliuda Bay locality is D=320.1º I=52.6º k=29.4 α_{95}=8.6º after application of a simple tilt-correction, while the mean direction of the Alitak Bay locality is D=82.1º I=65.0º k=25.8 α_{95}=7.4º after a complex two stage fold and tilt-correction was applied. The complex correction used on the Alitak data was necessary because Plumley et al. (1983) interpreted a regional scale 65º plunging fold to be present in Alitak Bay (Fig. 9). Thus the complex structural correction began by correction of bedding and directional data for the 65º plunging fold followed by a simple tilt-correction. Additionally, the tilt-corrected directions from the two localities are significantly different from one another, differing by 122º in declination and by 12º in inclination (Fig.10). Plumley et al. (1983) ascribed the differences in declination to possible block-rotations and suggested one of three possible factors that may be responsible for the discrepancies in inclinations. One factor is systematic differences in age, the second is possible systematic differences in initial dip, a consequence of the trench-slope or slope basin depositional environment, and the third is insufficient averaging of secular variation. The authors favored the third possibility as the largest contributor to the inclination discrepancies, as only reverse polarities were obtained from the Alitak Bay rocks; thus an insufficient amount of time may have been sampled to average secular variation accurately.

Despite the differences in the mean directions between the two localities, Plumley et al. (1983) employed two methods to obtain a mean inclination for the

Ghost Rocks Formation. One method required the somewhat arbitrary rotation of locality mean declinations so that locality means shared a common declination. Using Fisher (1953) statistics, a mean inclination was calculated, resulting in I=60º (Fig.10). The second method used, outlined by McFadden and Reid (1982), uses only inclination values; thus no arbitrary rotation of locality mean declinations was necessary. The results of the inclination only analysis showed I=58º. The similarity of results found using the two different methods led Plumley et al. (1983) to conclude that the Ghost Rocks Formation was magnetized at a latitude of ~40.3 +/- 6.2ºN during the Paleocene and has subsequently been displaced ~25 +/- 9º northward.

It is apparent from the above that the age of magnetization of the Ghost Rocks Formation is largely constrained by its structural corrections. To better constrain the relative age of magnetization I performed the fold test of Tauxe and Watson (1994) using the Plumley et al. (1983) paleomagnetic data from both Alitak Bay and Kiliuda Bay. The Alitak Bay data shows the maximum clustering of directions occurs between 66 and 90% untilting with a strong peak at ~75% (Fig. 11). This highlights the structural complications of Alitak Bay cited by Haeussler et al. (2003), but suggests that the results may pass the fold test if the structures can be better constrained. The fold test results from the structurally more simple Kiliuda locality, show that the maximum clustering of directions occurs between 96 and 131% un-tilting (Fig.12). This indicates that the results from this locality pass the fold test, but because they cluster best at 110% un-tilting, a re-examination of structures used for these corrections is necessary. The paleomagnetic data from Kiliuda from the Plumley et al. (1983) study appears to withstand the challenges presented by

Haeussler et al. (2003). The volcanic rocks from Kiliuda Bay pass the fold and reversal tests, and the basalt samples have a higher unblocking temperature of ~560ºC. Thus the complications of this study cited by Haeussler et al. (2003) used to suggest that the Ghost Rocks Formation has been remagnetized should be questioned.

A more detailed and expansive paleomagnetic and structural study of the Ghost Rocks Formation is needed to better constrain the age of magnetization of these units. Determination of age of magnetization will help distinguish between competing models A and C of Figure 4. If the magnetization is found to be primary and reveals latitudes of formation significantly south of their present location, Model A is correct. However, if the magnetization is primary and the paleolatitude of formation is not significantly different from the present day latitude, or the Ghost Rocks appear to have been remagnetized, Model C will more easily explain the data and is most likely correct. To accomplish this determination, the Western Washington University and University of California at Davis group studied and sampled rocks in areas of the Kodiak Islands. This thesis will present results from two of these areas, Alitak Bay and Jap Bay.

Review of Structural Studies

Byrne (1982; 1984) conducted a detailed structural study of the Ghost Rocks Formation primarily focusing on Jap Bay (Fig. 1 and 13; Jap Bay was apparently named for a Japanese family which lived there in the 1920s). The author describes the dominant rock types as being sandstone and mudstone but also includes local conglomerate, limestone, greenstone, and tuffaceous units. Byrne (1982; 1984) distinguished two structural units, which he describes as mélange terranes and

coherent terranes. The two units are lithologically indistinguishable. However, Byrne's structural studies and later work by Fisher and Byrne (1987) suggests that these units experienced different structural evolutions.

The mélange terranes exhibit a prolonged history of stratal disruption (S1), followed by a closely spaced steeply northwest dipping planar cleavage (S2). Textures associated with the S1 stratal disruption suggest that the rocks were not completely lithified at the time of deformation. S1 and S2 form a well developed intersection lineation that shallowly dips to the southwest. Folds associated with the S2 cleavage are present, but style and form are difficult to discern as S1 cannot be traced through fold closures, and fold hinges are commonly faulted out. However, D2 folds are found in one locality and indicate that the folds are open, asymmetric, and plunge moderately to the southwest. The mélange terranes have been interpreted to have been deposited in a trench basin with stratal disruption occurring as these units were underthrust, shearing along the décollment. The subsequent S2 pressure solution formed within the accretionary prism as the sediments progressively lithified (Byrne, 1984; Fisher and Byrne, 1987).

The coherent terranes are characterized by gently to tightly folded turbidites that can be traced for tens of meters, with a tectonic cleavage that is observed in both the argillite and sandstone units. Byrne (1982) subdivided the coherent terranes into two subunits that are in fault contact, Unit A and Unit B. This division is based on contrasting lithologies and structural and metamorphic histories.

The lithology of Unit A is indistinguishable from that of the mélange terranes and is consistent with the lithology of the majority of the Ghost Rocks Formation. It

is dominated by thick (tens of meters) to thin (less than 10cm) bedded sandstones and argillites, portions of which locally grade to conglomerate or pebbly mudstone. The sedimentary rocks are interbedded with volcanic and hypabyssal units. Portions of Unit A exhibit local hornfels metamorphism, which is more pronounced near the hypabyssal intrusions of Jap Bay. Two distinct structural styles are observed within Unit A: first, a seaward belt characterized by conjugate folds; and second, a landward belt distinguished by spaced cleavage. These features grade into one another (Byrne, 1982). Byrne (1982) attributed these two structural styles to different modes of deformation; the conjugate folds forming in partially lithified sediments and the spaced cleavage forming in completely lithified sediments, but both forming progressively in the D1 event. Byrne (1982) suggests that partially lithified sediment was experiencing a tectonic deformation forming the conjugate folds, and then as hypabyssal flows intruded it attenuated the lithification of sediments. As deformation continued in the now lithified sediments strain was accommodated by the development of the spaced cleavage. A shortening direction subparallel to bedding of ~318° was determined using the orientation of the conjugate fold axes and strike of spaced cleavage. A D2 event is expressed in Unit A by cross cutting thrust faults and defines a shortening direction of ~334°.

Byrne (1982) acknowledged the possibility that the conjugate fold belt may have been the result of gravity-induced slumping rather than tectonic processes. However, he described three field relationships that suggest that the latter interpretation is more likely. First, the folds grade into undeformed rocks of the same stratigraphic position, thus no discontinuity of slumping is suggested. Second, the

folds post-date the compaction of the sediments and the formation of calcareous concentrations. Therefore, deformation from gravity induced sliding would require a deep failure plane into partially lithified sediment. Third, the shortening direction determined from the conjugate fold belt is close to co-axial with a later deformation that is obviously tectonically induced.

The lithology and structural styles of Unit B are distinctly different from the majority of units in the Ghost Rock Formations. Unit B consists of medium (10-40cm) thick beds of sandstone and argillite; all other rock types common to the Ghost Rocks Formations are absent as is the hornsfels metamorphism observed in Unit A. Structures of Unit B do not show the multiple deformations recorded by the mélange terranes and Unit A coherent terranes. Unit B only records the D2 event as beds are typically tilted moderately to steeply to the northwest and locally folded by small scale asymmetric folds and cut by thrust faults. Bedding-parallel slickenlines indicate that the folding was accommodated though flexural-slip and the slip direction was perpendicular to the fold axes. Byrne (1982) determined a shortening direction for Unit B of ~334°, using fold axes orientation and bedding poles. The lack of evidence for D1 in Unit B, contrasting structural expressions of D2, and differing metamorphic histories led Byrne (1982) to conclude that Unit B is younger than the mélange terranes and Unit A coherent terranes and thus records only a younger deformation.

Methods

Field

Paleomagnetic samples were collected at 4 different localities within the Ghost Rocks Formation (Fig. 1). This thesis focused on the Jap Bay and Alitak Bay areas (Fig. 1). Most samples were obtained from coastal outcrops. Due to the rugged terrain of the Kodiak Islands and the isolated location of most of the target study areas, a float plane was required to transport equipment and supplies to and from most of the localities. A 15-foot Zodiak was used to transport equipment and access outcrops at each locality.

Over 1000 oriented core samples were taken at 167 sites from the 4 different localities during the 2006 and 2007 field seasons. I was a major participant in the 2007 field season. The majority of rock types sampled were pillow andesites, basalts and sandstones, but andesite sills, hypabyssal intrusions, mudstones and two plutons were also sampled. Sites were selected based on the quality of structural control and included sites to be used for fold tests, baked contact tests, and conglomerate tests to help constrain the age of magnetization of the Ghost Rocks Formation. Bedding measurements were taken on the clastic sedimentary beds and facing directions were determined to be used for structural corrections, to restore paleohorizontal on sites taken in both the sedimentary units and interbedded volcanic flows. Paleomagnetic sites generally consisted of 7 or more samples, some of which included oriented block samples, but samples were primarily obtained using a standard portable gasoline powered paleomagnetic drill and oriented using a Brunton compass and sun compass,

weather permitting. Latitudes and longitudes were taken with a recreational grade GPS unit.

More than 300 oriented samples came from a total of 46 sites within the Jap Bay area in the 2007 field season (Fig. 13). As Jap Bay primarily consisted of sedimentary rocks the majority of sites sampled were sedimentary rocks. However, two volcanic flows were sampled. Folded sedimentary units allowed for many sites to be collected for fold tests while large coherent sections allowed us to sample across strike to ensure enough of a time span was sampled to average out paleosecular variation (Fig. 14 and 15).

Over 500 oriented core samples were taken from a total of 72 sites from the Alitak Bay area in the 2006 and 2007 field seasons (Fig. 16). The geology of Alitak Bay was strikingly different from that of Jap Bay, consisting of large coherent sections abundant with pillow lavas interbedded with lesser amounts of sedimentary rocks. This allowed for ample sampling of the volcanic units, but sites also included sandstones, mudstones, conglomerates, and volcanic breccia (Fig. 17). This allowed for sites to be collected for the conglomerate test. The orientation of beds of Alitak Bay was very similar in strike and dip, and due to outcrop exposure, most of the sites were collected along strike.

Laboratory

All preparation and magnetic laboratory work was completed in the Pacific Northwest Paleomagnetism Laboratory at Western Washington University.

Magnetic Mineralogy and Curie Temperatures

To better understand the magnetic mineralogy of samples, a Princeton Measurements Co. Micromag^{tm} 3900 vibrating sample magnetometer (VSM) was used to obtain hysteresis loops to characterize the primary magnetic carriers. Additionally, on a representative group of sedimentary samples, bulk magnetic susceptibility was measured between thermal demagnetization steps using a Bartington susceptibility meter. An increase in magnetic susceptibility of a specimen during heating suggests the growth of new minerals, thus allowing for a better understanding of the effect of heating during later thermal demagnetization experiments on the magnetic mineralogy.

Anisotropy of Magnetic Susceptibility

Sample processing of paleomagnetic samples followed conventional methods. In the laboratory, the 2.4cm diameter cores oriented in the field were cut in to ~2.2cm in length, followed by measurements of magnetic anisotropy and susceptibility, using the AGICO KLY-3 Kappabridge Spinning Sample Magnetic Susceptibility Anisotropy Bridge. The data were reduced with the SUSAR program supplied with the instrument. Plots of the site data and their means and bootstrap confidence ellipses were generated using Tauxe's (1998) plotams.exe program. Flinn diagrams were generated using the raw data exported to Microsoft Excel.

Paleomagnetic

Natural remanent magnetization (NRM) was measured using a 3-axis 2-G 755 DC-SQUID magnetometer housed in a field-free room. Thermal demagnetization was accomplished using an ASC TD-48 magnetically shielded dual chamber thermal demagnetizer in steps of 10-40ºC. On select specimens, an ASC TD-48 magnetically shielded single chamber thermal demagnetizer in an argon environment was performed to retard possible effects of oxidation in steps of 10-40ºC. Alternating field (a.f.) demagnetization was conducted on selected samples using a D-Tech D-2000 a.f. demagnetizer in steps of 2.5-30mT. A combination of thermal and a.f. demagnetization was tried on specific samples. Thermal demagnetization produced the best results for both sedimentary and igneous samples and was used on the majority of samples. The remanent magnetization of acceptable samples was analyzed using principle component analysis (PAC) (Kirschvink, 1980) of visually identified linear and planar segments of thermal and a.f. demagnetization paths. Linear segments were fit with free lines using PCA.

Structural Analysis

It is clear from the previous paleomagnetic study by Plumley et al. (1983) that the age of magnetization of the Ghost Rocks Formation's characteristic magnetic direction is strongly constrained by its structural corrections. Therefore, in order to clear up uncertainties associated with the age of magnetization relative to deformation, the best structural constraints must be determined to ensure that the appropriate structural corrections are applied to the paleomagnetic data set. To achieve this we utilized information from the previous structural study on the Ghost

Rocks Formations by Byrne (1982, 1984) on Jap Bay, and conducted a more detailed structural analysis of Alitak Bay.

Jap Bay

The previous structural study conducted on the Ghost Rocks Formation by Byrne (1982, 1984) provided an extremely in-depth analysis of the Jap Bay area (Fig. 13). Review of this study suggested that the coherent terranes would be ideal targets to expand the scope of our paleomagnetic study of the Ghost Rocks Formation, as they have experienced relatively simple structural histories and thus relatively straightforward structural corrections can be applied. No field observations suggested the need for a more detailed structural study or reinterpretation of the results of Byrne (1982, 1984). Therefore, the majority of field work included paleomagnetic sampling and obtaining the appropriate structural data for correction of paleomagnetic data. The data and interpretations of Byrne (1982, 1984) proved to be a useful tool in helping determine areas best suited for paleomagnetic sampling. However, it is important to compare structural data between the previous study and ours to ensure consistency.

Unit B was extensively sampled for paleomagnetic analysis, thus most of our structural data was collected within Unit B. An equal area plot of poles to bedding from our study of Unit B, when compared with bedding poles from the Byrne (1982) study, shows similar results (Fig. 18). In Unit A, both the conjugate folds and spaced cleavage associated with D1 were observed, as well as the cross cutting thrust faults of D2. Limited outcrop exposure and locations for safe boat landings limited our collection of data from this unit. However, it should be noted that no observations

were made that suggested the need to reinterpret the structural evolution of Unit A made by Byrne (1982, 1984).

Alitak Bay

Plumley et al. (1983) interpreted the structure at Alitak Bay to consist of a regional scale 65° plunging fold (Fig. 9); thus a complex two-stage fold and tilt correction was necessary to restore bedding to paleohorizontal. The short review of the Plumley et al. (1983) study by Haeussler et al. (2003) cast doubt on this structural correction, thus one of the major objectives of this collaborative study was a more detailed structural study of the Alitak Bay region. The majority of the sample sites of the previous study were located on promontories between the coves within Alitak Bay and thus the structural data set used was not robust enough to accurately interpret the structures of Alitak Bay. Our colleagues at University of California at Davis performed a more detailed structural study, expanding into the coves of Alitak Bay while also re-visiting areas from the previous study. It was discovered that the structural interpretations of Plumley et al. (1983) were not entirely accurate (O'Connell, 2008; O'Connell et al., 2007).

A plot of poles to bedding from our colleagues at the University of California at Davis taken during this study shows a similar pattern to that of Plumley et al. (1983), and appears to form a weakly defined girdle. A cylindrical best fit to the apparent girdle of poles to bedding of this study has a pole whose trend and plunge is ~056º, 56º (Fig. 19); this is very similar to the trend and plunge of the interpreted regional scale fold axis of 46º,60º determined by Plumley et al. (1983) (Fig. 9 and 19). However, the identification of overturned beds, unrecognized in the previous

study, and numerous faults throughout the area suggest that Alitak Bay can more accurately be described as a group of coherent but isolated fault-bound blocks, as opposed to a regional scale fold (Fig. 19 and 20).

A total of 10 fault-bound blocks were identified in the study area, each showing differing amounts of rigid block-rotation relative to one another. Within individual blocks, minor folds and faults were observed in and cross-cutting bedding, suggesting that minor folding and faulting occurred prior to the major faulting and vertical axis rotation. The detailed structural study by our collaborators (O'Connell, 2008; O'Connell et al., 2007) suggests that the best correction of the paleomagnetic data would simply be rotation of crustal blocks about a vertical axis to a common strike, and the structural corrections used by Plumley et al. (1983) were erroneous. An equal area plot of poles to bedding after vertical axis rotation of individual blocks to a common orientation shows the bedding poles have a similar orientation, with the exception of a few outliers which can be explained by the minor folds observed within individual blocks (Fig. 20).

Anisotropy of Magnetic Susceptibility

Introduction

The study of magnetic fabrics through the measure of the anisotropy of magnetic susceptibility (AMS) in ancient accretionary prism rocks can be a useful compliment to other structural data, because it can be used to identify deformation patterns and in some cases to quantify deformation variation. AMS is particularly useful with regard to weakly deformed accretionary prism rocks, like those of the

Ghost Rocks Formation, because it allows for the detection of weak or incipient fabrics that may otherwise go unnoticed. Thus, an investigation of the AMS of the Ghost Rocks Formation gives a better understanding of the deformational histories of these units, provides a cross check to the previous structural study, help distinguish between different structural styles, and aid in the understanding of the magnetic behavior of these rocks.

Background

The ellipsoid of the anisotropy of low field magnetic susceptibility (AMS) is the aggregate measure of the preferred orientations of the diamagnetic, paramagnetic, and ferromagnetic mineral contributors to the magnetic anisotropy fabric. AMS is typically defined by either the grain-shape anisotropy of magnetite or the preferred crystallographic orientation of other minerals (Borradaile and Henry, 1997) and can be represented by an ellipsoid, defined by the three principle susceptibility axes (Kmax>Kint>Kmin) (Hrouda, 1982). AMS results are represented by its scalar data, defining the shape of the ellipsoid and its directional data, defined by the orientation of the three principle semi-axes.

The scalar component of AMS can be presented in a Flinn diagram, expressing the shape of the ellipsoid in terms of the amount of lineation (L=Kmax/Kint) vs. the amount of foliation (F=Kint/Kmin), in much the same way the shape of the strain ellipsoid is presented in structural studies. The directional component of AMS is presented on a lower-hemisphere equal area plot with the principal semi-axes of susceptibility, Kmax>Kint>Kmin, shown as squares, triangles, and circles respectively. The primary focus of this AMS study will be on the

directional components of AMS; the magnetic foliation, defined by the Kmax-Kint principal plane, and the magnetic lineation, defined by a cluster of Kmax, which can be can be compared to field measurements to better understand the structural history of deformed rocks.

In many cases the magnetic fabrics measured using AMS can be an accurate representation of a rocks bulk fabric, and some studies of deformed rocks have shown that the shape and orientation of the AMS ellipsoid can be qualitatively correlated to strain (e.g. Hrouda, 1982; Borradaile, 1987; Parés and van der Pluijm, 2002). Thus, AMS has been proved to be a useful tool to aid in structural studies because it allows for quick, accurate, and detailed analysis of rock fabrics (Hrouda, 1982). However, there are two caveats that complicate the use of AMS as a direct representation of the bulk rock fabric in the case of deformed rocks; the first is that the magnetic mineralogy of a rock controls its AMS and may not accurately reflect the bulk rock fabric and the second is the effect of multiple fabrics on the expression of AMS (Housen et al., 1993).

The first complication arises because AMS is the aggregate measure of the preferred orientation produced by all the magnetic contributors present in the rock, and ferromagnetic minerals have high susceptibilities relative to paramagnetic and diamagnetic minerals. Thus, ferromagnetic minerals have the ability to dominate the AMS signal, even in low concentrations (Borradaile, 1988). In some cases, the ferromagnetic minerals do not reflect the overall rock fabric; thus, if present in sufficient concentrations, the primary contributors to AMS may not accurately represent the rock fabric (Borradaile, 1987). It is therefore essential, when using

AMS, to first characterize the magnetic mineralogy of the rock to determine if the measured magnetic fabric is an accurate representation of the rock fabric.

The second complication is particularly important when using AMS to study weakly deformed rocks, such as those of the Ghost Rocks Formation. Studies have shown that if two planar fabrics are present in a rock, such as bedding and cleavage, the AMS will be a composite of those two fabrics, and result in magnetic lineations produced by intersection of those two planar fabrics (e.g. Housen et al., 1993; Parés and van der Pluijm, 2002). In weakly deformed rocks, the two fabrics responsible for magnetic intersection lineations are a primary fabric produced during a rock's formation and a tectonic fabric produced during deformation.

Undeformed sediments typically consist of a magnetic susceptibility ellipsoid that is oblate and a magnetic foliation plane (Kmax-Kint) that correlates to the bedding plane defined by a well clustered Kmin perpendicular to the bedding plane. These primary sedimentary fabrics are attributed to depositional and/or compaction processes (Cifelli et al., 2004). If a sedimentary rock experiences tectonic deformation, the primary fabric will be modified by the progressive development of the tectonic fabric (Housen et al., 1993; Parés et al., 1999). Tectonic fabrics are most often associated with magnetic lineations defined by a clustering of Kmax (Parés and van der Pluijm, 2002). As the rock is deformed, Kmin remains perpendicular to the bedding plane, preserving the primary sedimentary fabric, and Kmax will typically align either perpendicular to the shortening direction or parallel to the stretching direction, depending on the tectonic regime (Cifelli et al., 2004).

Weakly to moderately deformed sedimentary rocks in compressional regimes have magnetic lineations that are most often observed to be perpendicular to the shortening direction and parallel intersection lineations (see review by Borradaile, 1988). These magnetic lineations are attributed to the progressive tectonic overprinting of primary fabrics. A typical primary magnetic fabric for sedimentary rocks is defined by an oblate AMS ellipsoid, a strong magnetic foliation, the direction of a well clustered Kmin varying between ~0-15º from the bedding pole, and Kmax and Kint forming a girdle about Kmin (Tarling and Hrouda, 1993). During deformation this fabric will progressively change with increased deformation and cleavage development. First the AMS ellipsoid will shift from the oblate field to the prolate field and be accompanied by an increase in the clustering of Kmax and Kint as the influence of the tectonic fabric increases. With continued deformation and cleavage development, the tectonic fabric will dominate the AMS signal and the ellipsoid will shift back to the oblate field. A well developed magnetic lineation will be formed and Kint and Kmin will form a girdle (Fig. 21; Housen et al., 1993; Parés et al., 1999). These progressive changes observed in weakly deformed sediments can be tracked by AMS and distinguish between different structural styles. Thus, a major goal of this AMS study was to use these observed changes in the AMS to distinguish between the different structural styles in the weakly deformed sediments found through out the Ghost Rocks Formation.

The majority of volcanic rocks sampled for the entire project were pillow lavas; AMS studies of pillow lavas are limited, and as such, their primary magnetic fabrics and the effects tectonism on these fabrics are poorly understood. However, it

would be expected that a similar process of the progressive overprinting of a tectonic fabric on the primary (igneous) fabric would occur. Studies of submarine basalt flows have been observed as having AMS in which the fabrics are random (Ellwood, 1978; Tarling and Hrouda, 1993). Thus, it may be expected that the overprinting of such a fabric in weakly deformed rocks may resemble a poorly defined tectonic fabric or may go unrecognized. Because of this another goal of this AMS study was to investigate the AMS of the pillow lavas and see how their magnetic fabrics relate to the structural geology.

Characterization of magnetic mineralogy

In order to characterize the primary contributors to susceptibility in the sedimentary and volcanic units of the Ghost Rocks Formation, hysteresis loops were obtained on representative samples from both Jap Bay and Alitak Bay rocks using a Vibrating Sample Magnetometer (VSM). The hysteresis loops from all samples are small, narrow and have positive high field slopes, regardless of lithology or sample locality (Fig. 22). This evidence suggests that paramagnetic minerals are the primary contributors to susceptibility in a low field (<1 mT) in both the sedimentary and volcanic rocks of the Ghost Rocks Formation. This is important because the AMS will primarily be controlled by the paramagnetic minerals and thus will most likely be an accurate approximation of the bulk rock fabrics.

Jap Bay

The coherent units, which were the focus of the Jap Bay portion of this study, were previously interpreted to have different lithologies and structural histories

(Byrne, 1982). These differences suggest that a division of Unit A and Unit B results is appropriate because both lithology and structural history greatly influence the AMS of rocks.

Results

Unit A

A Flinn diagram of AMS scalar data from specimens of Unit A sites shows differences in the AMS between each rock type (Fig. 23). The volcanic sites have a low degree of anisotropy and are quite triaxial, the sandstones are more anisotropic and fall into the prolate field, and the mudstones are the most anisotropic and have very oblate shaped ellipsoids. The mudstones show a trend towards the prolate field and can be divided into two sub-groupings, a less anisotropic group and a more anisotropic group.

Differences between the three rock types are also observed in the magnetic fabrics defined by the AMS directional data. The sandstones and mudstones show clear evidence of a magnetic lineation with Kmax in all sites clustering shallowly to the SW (Fig. 24). However, clustering of Kint and Kmin varies between the two lithologies. The sandstones have the tightest clustering of Kmax with Kint and Kmin directions forming a loosely defined girdle (Fig. 24). All three principal AMS semi-axes of mudstones cluster tightly, thus Kmax defines a magnetic lineation and Kmin a magnetic foliation (Fig. 24). The volcanic sites show great scatter of all AMS axes, but the direction of scatter is not random. Kmin is directed more steeply to the SW with Kmax and Kint oriented shallowly to the N and W respectively (Fig. 24). No

clear magnetic foliation or lineation can be identified from the volcanic rocks as is expected by the near triaxial shapes of their AMS ellipsoids.

Unit B

A Flinn diagram of the AMS ellipsoids of specimens from Unit B shows that a wide variety of ellipsoid shapes exist in the sandstones, ranging from very oblate to very prolate shapes, with a small bias towards the oblate field (Fig. 23). The range of AMS ellipsoid shapes can be summarized by sites falling somewhere between the two end-member cases; sites with oblate shapes and sites with prolate shapes (Fig. 25). The AMS directional data of sites show distinct differences in the magnetic fabrics of the oblate and prolate end-members. The oblate end-member shows a clear magnetic foliation, defined by a tightly clustered Kmin and Kmax and Kint, forming a girdle perpendicular to the Kmin direction (Fig. 25A). The prolate end-member shows a clear magnetic lineation, defined by tightly clustered Kmax and Kint and Kmax forming a girdle perpendicular to the Kmax direction (Fig. 25B). The AMS of the majority of sites is more similar to the oblate end-member but tends to be more triaxial in shape and has less defined magnetic foliations, showing slightly better clustering of Kmax and Kint (Fig. 25C). In summary, the AMS of sandstones from Unit B fall between an oblate end-member with a magnetic foliation and a prolate end-member with a magnetic lineation, with the majority of sites' AMS being more similar to the oblate end-member but tending to be more triaxial in shape and have a more weakly defined magnetic foliation.

Analysis and Discussion of Results

Unit A

The AMS of the sandstones and mudstones has a well defined magnetic lineation while evidence for a resolvable magnetic foliation is absent, or in the case of some mudstones, cryptic at best. This evidence suggests that tectonic deformation has overprinted the primary sedimentary fabric. This interpretation is supported by the prolate shapes of the sandstone AMS ellipsoids and the trends of mudstone AMS ellipsoids toward the prolate field (Fig. 24).

A comparison of the AMS results from the sedimentary rocks of Unit A and the results of Byrne (1982) is necessary to understand what is controlling this magnetic lineation. Byrne describes a well developed spaced cleavage that is approximately axial planar to the conjugate folds in Unit A, and forms a well developed intersection lineation that plunges shallowly to the SW. Thus, it is reasonable to assume the intersection of the planar bedding and cleavage fabrics could be responsible for the magnetic lineation, which has the same orientation (Fig. 26).

A remaining question with regard to the sedimentary rocks is why there are two-subgroups within the mudstones defined by large differences in the degree of anisotropy. The differences between the sub-groups can be attributed to one or both of the following reasons: 1) Spatial differences of ~ 150m exist between the sample locations and thus may have experienced somewhat different geologic histories or 2) possible differences in magnetic mineralogy, as even a small difference in the amount of magnetic minerals in a rock can profoundly influence a rock's magnetic

anisotropy. Because some sites are located closer to a hypabyssal sill, they were likely to have experienced greater heating resulting in greater mineralogical changes and changes in rheology. The anisotropy difference may have been caused by a combination of both of these possibilities.

The AMS results of the volcanic units are very different from that of the sedimentary units, showing more triaxial shapes and lack evidence of a clear tectonic fabric. The differences in the shape of the AMS ellipsoids may be explained by differences in mineralogy and the primary AMS fabrics between the two lithologies. However, mineralogical and primary AMS fabric differences cannot explain the lack of a tectonic fabric in the volcanic units and thus another explanation is required. Assuming that the interpreted sequence of structural events describe by Byrne (1982) is correct, the different structural histories of the two lithologies can account for lack of clear evidence for a tectonic fabric in the AMS of the volcanic rocks samples. Byrne (1982) interpreted the hypabyssal sills to have intruded during deformation, and thus experienced a somewhat different stain history. Additionally, differences in the rheology of the volcanic and sedimentary units is likely another contributing factor in the lack of a developed tectonic fabric in the volcanic units.

Unit B

The AMS of Unit B is different from that of Unit A (Fig. 23 and 27). Samples from Unit B are much less anisotropic than those from Unit A (Fig. 23). This is likely due to the lesser amounts of deformation and strain observed in Unit B and differences in magnetic mineralogy between the two units. The majority of sites from Unit B show a typical sedimentary fabric with oblate ellipsoid shapes and well-

clustered Kmin principal directions (Fig. 25A). Comparison of site mean AMS directional data and poles to bedding shows a clear relationship, which is expected with preservation of the sedimentary fabric (Fig. 28A and C). However, the trend of specimen scalar data from individual sites shows a trend toward to prolate field, suggesting a tectonic overprint of the sedimentary fabric. Additional evidence for a tectonic influence on the AMS comes from the distinct magnetic lineations observed in some of the sites (Fig. 25B).

Evidence for the tectonic overprint of the primary fabrics of the sandstones of Unit B warrants a comparison of the AMS results with results and conclusions from the previous structural study of Byrne (1982).

A lower-hemisphere equal area plot of the Kmin principal directions of individual specimens shows that they correlate with the shortening and transport directions determined from structural data of Byrne (1982) (Fig. 28). This relationship is expected, as the Kmin of Unit B is directly related to bedding. Thus when plotted on in-situ coordinates, the specimens should define a girdle roughly parallel to the direction of maximum shortening (Fig. 27 and 28; Cifelli et al., 2004). A plot of Kmax directions of individual specimens from Unit B shows a large scatter, but the directions are primarily constrained to the west and south west quadrant of the equal area plot, with a locality mean plunging moderately to the west with the 95% confidence ellipse smearing to the SW and NE (Fig. 28B). A comparison of the Kmax results with the fold axes orientations of Byrne (1982) shows that only a portion of the Kmax directions correlate to the orientation of the fold axes, as was observed in Unit A (Fig. 28B and C). This is important because it suggests that many of the Kmax

orientations within Unit B are likely a result of intersection lineations (due to the intersection of bedding and a crypto-cleavage, similar to the magnetic lineations found in Unit A). However, the orientations of the Kmax directions that do not correspond to the fold axes require another explanation. One suggestion is that the orientations of these Kmax directions is the result of sedimentary processes. However, this interpretation is unlikely as the evidence suggests that the tectonic overprint of the sedimentary fabric, and thus deformational processes are more likely responsible for the Kmax directions that do not correlate to fold axes.

Comparison of individual specimen Kmax directions and slickenline and fault plane data from Byrne (1982) show a loosely defined pattern, with Kmax directions trending in a similar direction as the slip direction from Byrne's data (Fig. 28B and D). This suggests that the magnetic lineations that do not correspond to the fold axes may be related to the direction of slip on faults. Byrne (1982) describes folding in Unit B as being accommodated by flexural-slip on bedding parallel faults and is a possible mechanism that can explain the orientation of these magnetic lineations. The simple shear resulting from flexural slip on the fault planes may result in the alignment of grains parallel to the slip direction, producing magnetic lineations parallel to the transport and slip direction. Magnetic lineations parallel to the tectonic transport and slip direction in sedimentary rocks are more common extensional regimes (e.g. Cifelli et al., 2004). However, magnetic lineations parallel to the transport and slip direction, though uncommon, have been observed in weakly deformed sediments in compressional regimes as well (Aubourg et al., 1999). Thus, it is likely the magnetic lineations and the Kmax directions within Unit B that are sub-

parallel to the slip direction are the result of flexural-slip on bedding parallel faults. This process may be thought of as similar to the development of a stretching lineation due to the progressive overprinting of the sedimentary fabric by a tectonic fabric. This hypothesis is supported by more developed magnetic lineations being found in the more highly strained hinges of folds (Fig. 29).

It is evident that the AMS fabrics of Unit A and Unit B are different from each other. From the discussions above, these differences can be explained by the different structural styles that accommodate deformation within each unit. Additionally, the AMS of Unit A and Unit B nicely compliments the previous structural study by Byrne (1982). This is important because it shows that the AMS can be used to distinguish between different the structural styles of the weakly deformed sedimentary rocks of Jap Bay.

Alitak Bay

Results

Sedimentary Units

The AMS of the large majority of the mudstones and sandstones is very similar. Both rock types generally have oblate AMS ellipsoids,, with the sandstone being slightly more triaxial and less anisotropic than the mudstones (Fig. 30). The AMS directional data from both sedimentary units show well defined magnetic foliations, defined by well clustered Kmin directions. The Kmax and Kint principal directions show varying degrees of cluster about the Kmin direction, ranging from a smeared girdle to well clustered directions (Fig. 31). The evidence of well clustered

Kmax directions found in some samples suggests the presence of a weak tectonic fabric, resulting in an intersection lineation similar to the sedimentary units of Alitak Bay. The differences in AMS ellipsoid shape between the two rock types can be attributed to either different mineralogical controls on the AMS between the two rock types, differences in the development of a tectonic fabric caused by rheological differences, or both.

Volcanic Units

The shape of the AMS ellipsoid from volcanic specimens shows a near triaxial ellipsoid shape with a slight bias toward the oblate field (Fig. 30). In general, the orientations of the AMS principle axes show more scatter than the sedimentary units; however, three different categories of weakly defined magnetic fabrics can be identified: foliated, lineated, and scattered. The orientations of different AMS axes influence the shape of the ellipsoid, with the foliated and lineated fabrics falling further into the oblate and prolate fields and scattered fabrics tending to be more triaxial (Fig. 32).

Analysis and discussion of results

Sedimentary Units

An equal area projection of AMS directional data from all sedimentary specimens show constancy in the orientations of the AMS principal semi-axes throughout the entire sample area (Fig. 33). A comparison of Kmin with all of the measured poles to bedding from Alitak Bay shows a direct relationship; this is

evidence that a sedimentary fabric is preserved in the mudstones and sandstones (Fig. 33).

Kmax has a relatively consistent orientation throughout the locality and thus begs the question of whether this is controlled by the primary (sedimentary) fabric or reflects the overprint of a tectonic fabric (Fig. 33). In some sedimentary fabrics the orientation of Kmax is controlled by the orientation of more prolate grains deposited perpendicular to the transport direction or slope of the depositional environment (Tarling and Hrouda, 1993). While it is possible that the consistent orientation of Kmax in the sedimentary rocks of Alitak Bay is the result of sedimentary processes, it is unlikely because they show evidence for weak tectonic fabrics. Most literature on the AMS of weakly deformed sediments suggests that the orientation of Kmax will be a function of the intersection of two magnetic foliation fabrics, the primary (sedimentary) fabric and the tectonic fabric (i.e., Parés and van der Pluijm, 2002). Thus, it is more likely the orientation of Kmax is controlled by the intersection of the sedimentary fabric and a weak cryptic tectonic fabric, as Kmax is oriented approximately perpendicular to the poles to bedding. This is a similar scenario to the magnetic lineations present in the sedimentary rocks in Unit A of Jap Bay. However, these sediments have experienced less deformation; thus the magnetic lineations in Alitak Bay are less defined. Additional support for this comes from the mudstones showing a triaxial AMS ellipsoid. The primary AMD fabrics of mudstone AMS are typically very oblate (Housen and van der Pluijm, 1991), thus suggests that a tectonic overprint is responsible for the triaxial AMS ellipsoid in these mudstones.

The AMS results from the sedimentary units can be used to cross check the structural interpretations as they maintain a strong sedimentary fabric. However, the amount of sedimentary sites collected is small and does not encompass enough of the crustal blocks to help distinguish between the possible structural interpretations. The AMS results of the sedimentary rocks from Alitak Bay are different from those of both coherent units from Jap Bay. This is most likely a result of the distinctly different structural style observed within Alitak Bay. Thus, the AMS of sedimentary units from both coherent units within Jap Bay and those from Alitak Bay shows that AMS can be used to distinguish between different structural styles in the weakly deformed sediments within the Ghost Rocks Formation.

Volcanics Units

Little AMS work has been conducted on pillow lavas. However, studies of subaqueous basalts suggest that the AMS of such flows is generally random (Ellwood, 1978). The majority of the AMS data from the pillow lavas at Alitak Bay show random fabrics. However, small groupings with weakly foliated and weakly lineated fabrics have been identified (Fig. 32). It is unclear how these fabrics form but it is important to see if the pillow lava magnetic fabrics at Alitak Bay are related to the structural geology in any way. Equal area projections of specimen data, qualitatively subdivided by the magnetic fabrics described above, suggest that the lineated fabrics have Kmax directions that may relate to bedding, but the foliated and scatter fabrics show no such relationship (Fig. 34). Whether these relationships between the different AMS fabrics of these pillows and the structures are even important is unclear because of the limited understanding of the nature of how these

fabrics form. Thus, this evidence only suggests that the fabric of pillow lavas may not be entirely random and that further work is needed on the study of the primary magnetic fabrics of pillow lavas.

Paleomagnetism

One of the primary goals of this collaborative study was to conduct a more detailed and extensive paleomagnetic study of the Ghost Rocks Formation than had previously been performed by Plumley et al. (1983). The previous paleomagnetic study by Plumley et al. (1983) was conducted using samples from the volcanic flows at two localities, Alitak and Kiluida Bays. To clear up uncertainties in the previous paleomagnetic study, we conducted a more detailed study of both Altiak Bay and Kiluda Bay and expanded to other portions of the Ghost Rocks Formation. The coherent sections were chosen for this expansion of the study as they are the best targets for a paleomagnetic study because they are less likely to have been remagnetized and allow for the best structural constrains to be placed on a paleomagnetic data set. In addition to expanding the scope of this paleomagnetic study to other localities, we expanded paleomagnetic sampling to sedimentary rocks. Volcanic rocks are the best targets for paleomagnetic study. However, over the past 25 years, since the previous study, improvements in the sensitivity of equipment has allowed for more accurate measurement of weakly magnetic rocks. The improvement in equipment sensitivity has allowed us to measure the weakly magnetic sedimentary rocks of the Ghost Rocks Formation, an opportunity not available during the study by Plumley et al. (1983). As such, our paleomagnetic study expanded to include sedimentary rocks of the Ghost Rocks Formation.

Jap Bay

The previous structural study by Byrne (1982, 1984) suggests that Jap Bay is an ideal location to expand upon the previous paleomagnetic study for three reasons: 1) large coherent sections of sedimentary rocks are found within Jap Bay, 2) it contains two sub-divisions of the coherent sections of differing geologic histories, and 3) the previous study by Byrne (1982, 1984) provides a wealth of useful structural data and interpretations.

The coherent terranes of Jap Bay, described by Byrne (1982), were the targets of this paleomagnetic study. The majority of sites collected came from Unit B (Fig. 13). The reason for this bias of sampling was due to two factors: First, Byrne (1982) described Unit B as lacking a hornfels metamorphism that is observed in Unit A, suggesting that it is a better target for paleomagnetic sampling as it is less likely to have been remagnetized. Second, more outcrop exposure and locations for safe boat landings were found in Unit B outcrops.

The paleomagnetic results from Unit A and Unit B have been divided for three reasons: 1) The two units have experienced different geologic histories, 2) they are interpreted to be of relatively different ages, and 3) they exhibit two distinctly different magnetic behaviors, as will be shown below.

Unit A

Results

A total of 8 sites were collected within Unit A on the east coast of Jap Bay (Fig. 13). These sites were in close proximity to a hypabyssal sill. Efforts to avoid

sampling near the sill proved difficult because of limited outcrop exposure and safe boat landing locations. Lithologies sampled from the 8 sites included two volcanic flows and six fine to medium grained sandstones and mudstones.

Stepwise thermal and a.f. demagnetization methods were performed on samples from Unit A. Both methods proved effective in providing stable demagnetization paths on most samples, with 7 of 8 acceptable sites being obtained (Fig. 35). Thermal demagnetization yielded the best results and thus was the method of choice on most samples. A minimum of 7 samples per site was demagnetized from Unit A. Thermal and a.f. demagnetization paths show two components of demagnetization, a first removed component ranges from ~80-290ºC or ~2.5-30mT for thermal or a.f. demagnetization respectively and a second removed component ranges from ~325-500ºC or ~35-200mT for thermal or a.f. demagnetization, with the second removed component decaying to the origin (Fig.29). Directions of the high temperature components were obtained using principal component analysis (PCA). From the seven acceptable sites within Unit A, site mean directions of the high temperature component were calculated using the method of Fisher (1953) (Table 1).

Stability Tests

To constrain the age of magnetization, the fold test of Tauxe and Watson (1994) was performed using the high temperature directions from the seven acceptable sites found within Unit A (Fig. 36). Sites within Unit A fail the fold test with best clustering of site mean directions between -2-58% un-tilting, suggesting remagnetization. The largest degree of clustering at ~40% un-tilting suggests a syn-deformational magnetization. This fold test suggests the characteristic magnetization

within Unit A was acquired during deformation. It is unlikely that the failure of sites collected from Unit A to pass the fold test is due to a more complicated structure because 1) there were no observed large scale structures in which the site were located, and 2) the previous structural study by Byrne (1982) was very detailed and does not suggest a large scale complex structure in Unit A that would necessitate a complex multi-stage correction of the paleomagnetic data.

The syn-deformational magnetization recorded in sites collected from Unit A is not surprising because of their close proximity to a hypabyssal sill. If the interpretation of Byrne (1982) is correct and the hypabyssal sill intruded as the sediments were being deformed, it would be expected that sediments in close proximity to the intrusion would be remagnetized during deformation. Therefore, while this magnetization it not primary in origin, the results of this fold test suggest that it is likely to still be very ancient and that the mean paleomagnetic direction of Unit A at the point best clustering may record the latitude at which the magnetization was acquired. The mean paleomagnetic direction of Unit A at 40% untilting, the point of maximum cluster of site mean directions, is D=233º I=-57º, k=189, α95=4.4º, n=7, corresponding to a paleolatitude of 38º +5/-4.

Unit B

Results

A total of 38 sites were collected from Unit B (Fig. 13). All sites were in fine to medium grained sandstones. Large exposures of tilted beds allowed for extensive sampling across strike to ensure that an adequate amount of geologic time was

sampled to average out secular variation (Fig. 14). Open to tight folds are predominant in Unit B allowing for the collection of many sites to be used for fold tests to aid in constraining the age of magnetization of the Ghost Rocks Formation (Fig. 14).

A minimum of 3 samples per site were demagnetized using thermal, alternating field (a.f.), or a combination of both demagnetization methods. Inspection of orthogonal vector plots of the demagnetization paths shows no samples that decay to the origin, thus no characteristic components of magnetization could be resolved. All samples become magnetically unstable after heating above ~355ºC. However, the demagnetization paths of samples from Unit B show some magnetic characteristics worth noting. Sites within Unit B exhibit two distinct thermal demagnetization behaviors, a majority grouping of sites exhibits semi-stable low temperature paths ranging from 80ºC up to ~280-355ºC, and a minority group of sites shows no stability during demagnetization. The majority group shows a distinct low unblocking temperature component, ranging from ~80-210ºC and a hint of a second component ranging from ~215-330ºC (Fig. 37). Efforts to better resolve the second removed component using a.f. and combinations of thermal and a.f. demagnetization proved ineffective, thus no resolvable components could be derived from Unit B.

To try to better understand why samples from Unit B do not maintain magnetic stability during thermal demagnetization, the bulk susceptibility was tracked between each magnetization step for a representative group of specimens (Fig. 38). A large increase in bulk magnetic susceptibility is observed between 310-330ºC. The

increase in susceptibility generally indicated a reaction of some other ferromagnetic mineral to magnetite, thus resulting in unstable demagnetization paths.

Discussion

The fold test of Tauxe and Watson (1994) performed on the high temperature directions from Unit A suggests that these rocks have been remagnetized during deformation, which can be explained by site locations in close proximity to a hypabyssal sill. The mean paleomagnetic direction of Unit A at peak clustering of site mean directions upon simple untilting corresponds to a paleolatitude of 38º +5/-4. It is difficult to argue that this is definitively the latitude at which the characteristic magnetization of Unit A was acquired. However, it is important to note that it overlaps within error of the paleolatitude calculated using the Kiliuda Bay results from Plumley et al. (1983) of 38º +5º/-4º.

The Unit B samples provided no resolvable primary component. Thus no information can be gathered to provide an answer to the question of the paleolatitude of the formation of the Ghost Rocks Formation. However, interesting questions arise as to why Unit B does not preserve a resolvable primary component of magnetization. The temperature at which samples from Unit B become unstable, between 310-355ºC, and the observed increase in bulk susceptibility, between 310-330ºC, are close to the unblocking temperature of the iron sulfide pyrrhotite of 320ºC. Thus, we suspect that the presence of pyrrhotite or some other iron sulfide present in Unit B is the culprit responsible for the unstable demagnetization paths of Unit B. The distinctly different magnetic behavior of the behavior of two coherent sub-units can most easily be

explained by the close proximity of samples taken from Unit A to a hypabyssal sill and their clear remagnetization.

Alitak Bay

Due to the controversy over the paleomagnetism of Alitak Bay, a primary goal of this study, in conjunction with the more detailed structural analysis, was to obtain a more extensive paleomagnetic data set in an effort to clear up uncertainties of the previous study by Plumley et al. (1983). A total of 72 sites, amounting to over 500 samples, were collected within Alitak Bay in the 2006 and 2007 field seasons. Sites sampled included 37 volcanic flows, 26 sedimentary units, 8 conglomerate and volcanic breccia, and one pluton. Both Thermal and a.f. demagnetization methods were used on samples from Alitak Bay. Thermal demagnetization provided the best results and thus was the method of choice. Efforts using low temperature demagnetization to try to remove the effects of multi-domain grains proved minimally effective, and thus were only performed on a handful of samples.

Results

Sedimentary Units

The sedimentary units sampled primarily consisted of fine to medium grained sandstones, but minor amounts of mudstone were sampled as well. The sedimentary units exhibited three distinct magnetic behaviors. A majority group showed stable demagnetization paths to ~280-355ºC, whereupon the magnetic vectors become erratic and irresolvable (Fig. 39B). Two minority groups exhibited different behaviors, one with completely unstable magnetization paths and a second with

demagnetization paths that are stable to ~450-560ºC, show two components of demagnetization, and decay to the origin (Fig. 39A). The sedimentary units which decay to the origin all were collected from sedimentary beds that lie in close proximity (~0-3m) to volcanic flows, suggesting that the magnetization recorded in these sites may not be a primary magnetization but one that was acquired through contact metamorphism by the volcanic flows. The magnetic behavior of sedimentary rocks from Alitak Bay is similar to the magnetic behaviors found in the sedimentary rocks of both of the coherent terranes within Jap Bay.

Volcanic Units

The volcanic sites primarily consisted of pillow andesites, while a few sites sampled included andesitic sills, all of which were interbedded with turbidite sequences (Fig. 14A,B). The magnetic behavior of the volcanic units falls into two general groups, a minority group showing no stable demagnetization paths and a majority group which remains stable to ~450-580ºC and decays to the origin. The demagnetization paths of the majority group typically have two components of magnetization (Fig. 40A), but a minority of samples show demagnetization paths with three components of magnetization (Fig. 40B). The low unblocking temperature components of both the two and three component vectors range from ~80-300°C. Samples with two components of magnetization show a high unblocking temperature component that typically ranges from ~330-480°C. Samples with three magnetic vectors show a second removed component that ranges from ~330-440°C and a high unblocking temperature component typically ranging from 460-500°C.

A total of 35 sites provided sets of samples with well defined demagnetization paths. PCA was performed on the last removed components of specimens that show demagnetization decaying towards the origin, and site mean directions were calculated using the methods of Fisher (1953) (Table 2). Sites with k values less than 20 and sites with poor or questionable structural constraints were discarded, leaving 19 acceptable sites. A variety of corrections using the high unblocking temperature components were performed in an effort to constrain the age of magnetization and are discussed below.

Stability tests

The first correction applied to the paleomagnetic data involved simple untilting of in-situ directions using the fold test of Tauxe and Watson (1994)(Fig. 41). The results show that the paleomagnetic directions cluster best between 54-77%, with a strong peak at ~65%. This fold test suggests a syn-deformational magnetization. However, this fold test does not take into account complexities in the structural geology such as block-rotations or plunging folds. Two methods can be employed in an effort to overcome the complex structural geology of Alitak Bay and constrain the age of the characteristic magnetization. One is the use of inclination-only statistics, which only takes into account the paleomagnetic inclinations and is thus “immune” to structural complexities. The second method is to perform a multi-stage correction of the paleomagnetic data using the structural constrains determined by our colleagues at UC Davis (O’Connell et al., 2007; O’Connell, 2008).

An inclination-only analysis allows one to calculate statistics from just the inclinations and allows for the comparison of the in-situ paleomagnetic mean

inclination and the 100% tilt corrected paleomagnetic mean inclination. When using inclination-only analysis to constrain the relative age of magnetization with respect to deformation the important statistic is the kappa or k value, which is a precision value. The higher the k value, the more precise or clustered and the less random the data are. Thus, a significant increase in the k value of paleomagnetic mean directions after inclination-only analysis suggests that the magnetization may be primary. Conversely, if the k value decreases significantly after tilt correction, remagnetization is suggested. Using the inclination-only method of McFadden and Reid (1982), we found the in-situ mean inclination of Alitak Bay to be I=-38º, k=14, α95=9.1º, n=19 and tilt corrected mean inclination to be I=-60.1º, k=12, α95=11º, n=19. These statistics show that the inclinations of the in-situ and tilt corrected means are significantly different, but that the k values are not significantly different. Therefore, this inclination-only analysis is inconclusive. However, whether or not these inclinations are reasonable can be tested. The dipole equation ($\tan I = 2 \tan \lambda$, where I=inclination and λ=latitude) can be used to determine the hypothetical paleolatitude of magnetization. The in-situ mean inclination of Alitak Bay shows a latitude of 21º +7/-6 and is unreasonably shallow. The tilt corrected mean inclination correlates to a latitude of 41º +14/-11 and is a reasonable paleolatitude of formation for the units of Alitak Bay. Comparison of the tilt corrected Alitak Bay paleolatitude and the paleolatitude found using the better constrained Kiliuda Bay tilt corrected results (D=143.5º, I=-52.5º, k=33, α95=8.5º; paleolatitude of 33º +9º/-7º) shows that they overlap within error. It is important to note that while the inclinations do not differ significantly, they are not identical. The differences of inclination can be attributed to

the same three possibilities cited by Plumley et al. (1983): 1) age difference between the unit sampled in the two localities, 2) inherited differences in initial dip of the depositional surface in the trench slope of slope basin, or 3) because all Alitak Bay sites sampled were reverse-polarity, the data set inadequately samples enough geologic time to average out secular variation. The last option is the most likely, as only reverse polarities were found.

The paleomagnetic direction after inclination-only analysis corresponds to a reasonable paleolatitude of magnetization. This is important because it supports the suggestion that the characteristic component of magnetization found in the volcanic rocks of Alitak Bay may be primary. However, the inconclusive results above do not rule out the possibility that the magnetization was acquired during deformation. The best way to test whether the magnetization of Alitak Bay is a primary or syn-deformational magnetization is to use the second method and to determine the paleomagnetic directs using structural constraints to correct the palemagnetic data, hereby restoring bedding to paleohorizontal.

Our collaborators at UC Davis (O'Connell et al., 2007; O'Connell, 2008) conducted a detailed structural analysis of Alitak Bay and identified at least 10 coherent isolated blocks, which are interpreted to have been rotated by varying amounts relative to one another (Fig. 20). Thus, this structural interpretation suggests that to properly correct the paleomagnetic data would first require the rotation of the rigid blocks to a common attitude, followed by simple untilting. To execute vertical axis rotation corrections we first calculated the mean bedding attitude for each of the individual blocks identified by our collaborators. Next we rotated block means to a

common reference attitude of 250° and finally performing the classic fold test, unitlting about a horizontal axis. The selection of a common bedding attitude of 250° was chosen because it is the approximate trend of the entire Ghost Rock Formation over a >100km swath of Kodiak Island, and therefore, it may be a reasonable approximation of a pre-rotation orientation of the beds of Alitak Bay.

To perform the rotation corrections, I used a modified version of the fold test of Tauxe and Watson (1994), which performs vertical axis rotations of strike as opposed to the classic fold test, which untilts bedding about a horizontal axis. The vertical axis "rotation test" shows the best clustering of paleomagnetic directions between 60-106% block-rotation within 95% confidence with a strong peak of the maximum eigenvalue at ~101%, signifying best clustering of directions and thus passes the "rotation test (Fig. 42B). This evidence shows that simple vertical-axis rotations greatly improve clustering of directions and suggests that the magnetization was acquired before rigid block-rotation. Simple untilting of the block rotated directions shows the best clustering of paleomagnetic directions between 30-91% untilting with maximum eigenvalues peaking near 50%, suggesting a syn-tilting magnetization (Fig. 42C). However, this correction does not take into account the minor rotation of beds within coherent blocks. Thus, these corrections are incomplete and it is appropriate to additionally rotate all bedding attitudes for individual sites, to the common reference strike of 250° before untilting to take into account this deformation and properly restore bedding to paleohorizontal.

To rotate all bedding to the common reference strike of 250°, we performed the vertical axis "rotation test" on individual site directions using the block-rotated

data from the previous rotation correction. This was done to test whether the clustering of paleomagnetic directions continued to improve with further vertical axis rotation. The “block-rotation test” shows the best clustering of paleomagnetic directions between 45-130% rotation corrected within 95% confidence, with the peak in clustering between 90-100% rotation (Fig. 42D). While the increase in clustering of directions is not overwhelmingly large it still passes the “rotation test.” The small increase in clustering of paleomagnetic directions is expected, as the bedding attitudes of sites within blocks yielding primary magnetic directions did not vary much from the block mean. Thus, rotation of individual bedding attitudes to a common strike after block-rotations will not result in much change. However, small the increase in clustering it is still important as it accounts for deformation experienced pre-rigid block-rotation and suggests that the magnetization was acquired prior to minor within-block rotation.

Untilting of the site-corrected paleomagnetic directions yields inconclusive fold test results (Fig. 42E). Inconclusive results upon untilting can be attributed to the fact that all of the dips of beds within Alitak Bay are very similar with most falling between 70-90º. However, the inconclusive fold test after bedding is corrected for rigid block-rotation and minor folding still suggests that this magnetization was either acquired prior to, during, or post tilting. The question of whether or not the untilted and tilt-corrected paleomagnetic directions are reasonable can be checked in the same way as the inclinations found using the inclination-only analysis were checked by finding their corresponding paleolatitude. The Alitak Bay mean direction after rotation corrections but before untilting bedding is D=334.4º, I=-42.7º, k=14.63,

α95=9.1º, yielding a paleolatitude of 25 º +8º/-6º. The mean direction after rotation corrections and untilting is D=168.4º, I=-60.2º, k=12.7, α95=9.8º yielding a paleolatitude of 41º +13º/-10º. A latitude of ~25º appears to be extremely low and an unreasonable latitude for the acquisition of a possible secondary magnetization of the Alitak Bay rocks. A latitude for ~41º, while shallow, may be a reasonable latitude for the primary magnetization of these units during the formation of these units. A comparison of the tilt-corrected paleolatitude with that of the better constrained Kiliuda Bay mean locality direction after tilt-corrected (D=143.5º, I=-52.5º, k=33, α95=8.5º; paleolatitude of 33º +9º/-7º.) shows that these paleolatitudes overlap with in error. The locality mean inclinations of Kiliuda Bay and Alitak Bay, using this multi-stage correction, are the same but not identical, differences that can be attributed to the same reasons as stated above in the inclination-only analysis. Also important is that the locality mean inclination found using the multi-stage block-rotation corrections, which is ~-60.2º, is almost identical to that found with the inclination only analysis, which is ~-60.1º.

The conglomerate test can be used to constrain the age of magnetization in addition to the fold test. The volcanic clasts collected from volcanic breccia behaved well during thermal demagnetization, decaying to the origin, similar to the pillow lavas (Fig. 43). The volcanic clasts should have directions that are random if the characteristic magnetization is primary. However, the directions of the volcanic clasts are relatively well-clustered and generally have only slightly greater amounts of dispersion (lower k values) than the majority of sites collected (Table 2; Fig. 43). The evidence from the volcanic breccia sites collected from Alitak Bay shows that the

characteristic magnetization was acquired after breccia emplacement. However, the volcanic breccia units are in thick sections of pillows, so failure of the conglomerate test may only indicate that the volcanic breccia clasts were magnetized at the time of the last episode of pillow emplacement and thus can still be a very ancient magnetization. This hypothesis is supported by evidence of similar paleomagnetic directions of the volcanic breccia sites and the nearby volcanic flows (Fig. 45) and by slightly lower k values found in most of the volcanic breccia sites.

Discussion

It is apparent from the stability tests above that the units of Alitak Bay may have been remagnetized, as they yield inconclusive results for both the fold test and conglomerate test. This would suggest that Model C or the Resurrection hypothesis proposed by Haeussler et al. (2003) and Bradley et al. (2003) may be correct (Figs.4c and 7). However, the Kiliuda Bay results from Plumley et al. (1983) pass both the fold and reversal tests (Fig. 11). This suggests that the magnetization of Kiliuda Bay is primary. It is possible that Alitak Bay has been remagnetized and Kiliuda Bay has not, based on three lines of reasoning: 1) they are spatially separated by ~80km, 2) they show distinctly different structural histories, and 3) the basalts sampled at Kiliuda Bay have higher unblocking temperatures and thus may be more resistant to being magnetically reset. This suggests that both localities could have experienced very different geologic histories and that even if conditions were similar, Alitak Bay could have acquired a secondary magnetization and Kiliuda Bay would have been resistant to resetting. However it is also possible that characteristic magnetization of

Alitak Bay may be primary given that the fold tests are inconclusive and the failed conglomerate tests can be explained in other ways.

The fold test results may be biased by inaccurate interpretation of the structures of Alitak Bay. Two of the blocks identified at Alitak Bay require rotations >110º for the block-rotation corrections (Table 3), which may be unreasonably large rotations and may suggest that a different or more complex structural geology of the area. Comparison of the structural interpretations of this structural study and the structural interpretations of Plumley et al. (1983) show that the two blocks requiring >110º rotations fall on the hinge and on the opposite limb of Plumley et al.'s (1983) interpreted regional scale fold. A plot of poles to bedding from this study weakly defines a girdle, and suggests that the structural interpretation of a regional scale plunge fold by Plumley et al. (1983) could be correct (Fig. 9 and 19).

Correcting the paleomagnetic directions from this study, assuming a regional-scale fold with a fold axis plunging 56º at an azimuth of 056º, by first unplunging the fold axis to horizontal, and then untilting the beds about strike, as Plumley et al. (1983) had done, yields an increase in best clustering of directions between 45-91% untilting within 95% confidence (Fig. 45). These results suggest a syn-deformational magnetization. However, two "normal polarity" directions are found that are not antipodal to the reverse-polarity sites, suggesting that this structural correction may also not be accurate or that the structure may be more complicated. If the latter is true, it would suggest that the rotation-based structural interpretations from this study and Plumley et al. (1983) may both be correct, representing end-member possibilities for the structure of Alitak Bay, and some combination of the two most appropriately

describes the structural geology of Alitak Bay. However, the results of the inclination-only analysis (I=-60.1º, k=12, α95=11º, n=19), and those found after structural corrections applied (D=168.4º, I=-60.2º, k=12.7, α95=9.8º) are reasonably similar and suggest the same paleolatitude of ~41º, with a slightly different amount of uncertainty for Alitak Bay after tilt correction. The congruence of these results suggests that the structural corrections used are, on the whole, accurate. The accuracy of these corrections is additionally supported by the field observations, structural data, the results of the rotation tests performed above, and the fact that the inclusive fold test after rotation corrections could simply be due to the fact that the dip of beds at Alitak Bay do not show much variation.

The presence of all reverse-polarity data from Alitak Bay may be the result of inadequate sampling of geologic time. This is a likely possibility, as many of the beds at Alitak Bay have similar strikes and the majority of sampling was along strike, a sampling bias due to outcrop exposure.

Failed conglomerate tests may be the result of the volcanic breccia being magnetized during the last episode of pillow emplacement, and thus the character magnetization is unlikely primary in origin but still maintains a very ancient magnetization related to the magnetization of the pillow flows.

The vertical axis “rotation tests” suggest that the characteristic magnetization in volcanic units within Alitak Bay was acquired pre ridged-block rotation and pre intra block folding and faulting. However, because of the inconclusive inclination only analysis and the inconclusive fold test after rotation corrections applied the relative age of magnetization remains uncertain. The reason for the inclusive results

of these two stability tests may be attributed to the fact that the bedding dips of sites which yielded reliable paleomagnetic directions do not show sufficient variation to distinguish if paleomagnetic directions cluster better in-situ or tilt corrected. However, if the data set was larger and contained sites with different bedding dips a proper fold test could be preformed. Fortunately other paleomagnetic data exists from Plumley et al. (1983).

The exact location of the sites taken by Plumley et al. (1983) at Alitak Bay could not be determined and thus because we could not pinpoint the block they corresponded to we could not use them to expand our Alitak Bay data set. However, we were able to expand out data set to Plumley et al.'s Kiliuda Bay data. We performed a regional fold test using our rotation-corrected Alitak Bay directions and the in-situ Kiliuda Bay direction from the previous study by Plumley et al. (1983). The results of this fold test show the best clustering of directions between 68-128% untilting within 95% confidence, with a peak in the eigenvalue at ~100% (Fig. 46). When all directions are corrected to reverse polarity, the mean paleomagnetic direction is D=160.2º, I=-60.3º k=18.1, α95=6.5º, yielding a paleolatitude for the Ghost Rocks Formation of 41º +8º/-7º (Fig. 47). If this correction is assumed valid, these results suggest that the Ghost Rocks Formation passes the paleomagnetic fold test on a regional basis and were formed at latitudes significantly south of their present location, having subsequently translated northward to their present day location, and thus would support Model A (Figs.4a and 5).

It may be suggested that the results of the regional scale fold test are not accurate. This is because the validity of the regional scale fold test hinges on the

assumptions that the structural corrections used to rotate the Alitak Bay paleomagnetic directions are accurate and that the common reference strike of 250º is the appropriate pre-rotation orientation. However, three line of evidence suggest that this approach is reasonable. First, the structures observed in the field are consistent with the "Block Model." Second, these corrections result in remarkable improvement in clustering of the paleomagnetic data as shown by the "rotation test." Finally, the selection of the common reference strike of 250º is a reasonable value to choose because it may be assumed that prior to deformation, the entire Ghost Rocks Formation more or less had a similar strike, as is common in many modern accretionary prism rocks. Thus, it may be appropriate to rotate data to a strike that is common to the Ghost Rocks Formation. Because the regional trend of the formation is ~ 250º, it seems that this reference value is reasonable. With this said, the selection of a reference strike, however reasonable it may seem, is still rather arbitrary and therefore the comparison of paleomagnetic declinations between Alitak Bay and Kiliuda Bay is subject to uncertainty.

Conclusions

Jap Bay

Field observations and structural data from Jap Bay support the findings of the previous structural study on Jap Bay by Byrne (1982, 1984). The study of the AMS of rocks from ancient accretionary prisms is important because the results can be useful compliments to other structural data. AMS can be used to both define patterns of variable deformation and to detect weak or incipient fabrics. The AMS results from

this study highlight these points. Within Jap Bay, it is observed that the AMS can define variable patterns if deformation between the coherent terranes, Unit A and Unit B, supporting the findings of Byrne (1982, 1984) that the two units experienced different deformational histories. The magnetic fabrics of sedimentary rocks from Unit A are more strongly overprinted by tectonic fabrics than those of Unit B, and have a magnetic lineation approximately parallel to the orientation of the fold axes. The results from the relatively less deformed sandstones of Unit B suggest that the orientation of Kmax can be associated with the tectonic transport direction confirming the findings of other studies of weakly deformed sedimentary rocks (e.g. Cifelli et al., 2004; Aubourg et al., 1999).

Unit A shows good demagnetization behavior with resolvable characteristic components. The characteristic components of Unit A fail the fold test, and suggests that sites collected within Unit A of Jap Bay have been remagnetized syn-deformation. The magnetic components of Unit B are irresolvable, but marked increases in bulk susceptibility are noted when magnetic directions become unstable and suggest the presence of iron sulfides in these samples.

Alitak Bay

The structural interpretations of Plumley et al. (1983) were inaccurate and Alitak Bay can be more accurately described as a group of fault bound blocks rotated relative to one another as apposed to a regional scale fold.

The sedimentary rocks of Alitak Bay show magnetic fabrics which are less tectonically overprinted than Unit A of Jap Bay, but a weak tectonic fabric is observed within these rocks. The magnetic fabrics of the sedimentary units may

possibly be used to cross-check structural interpretations, but a more robust data-set is needed. However, the AMS data is large enough to show it can be used to distinguish between the structural style here and the two coherent units of Jap Bay. The volcanic units of Alitak Bay show magnetic fabrics are not always random with some of which are more lineated and others more foliated. However, the understanding of these fabrics is extremely limited and Alitak Bay may prove to be a useful location for the study of the magnetic fabrics of pillow lavas

The magnetization contained in the sedimentary rocks of Alitak Bay exhibits similar behavior to the sedimentary units of Unit A and Unit B of Jap Bay, the majority exhibiting behavior characteristic of Unit B. However, sites in close proximity to volcanic flows show stable magnetization paths similar to Unit A and reveal primary directions similar in orientation to flows in close proximity. The volcanic units generally show good magnetic behavior. The timing of magnetization of these units is unclear. However, it has been determined to have been acquired either before or syn-tilting. At this juncture, the results from this paleomagnetic study are inconclusive and therefore cannot be used to confidently distinguish between the competing models. However, it would be a remarkable coincidence that the structurally corrected Alitak Bay data of this study and the Kiliuda Bay data of Plumley et al. (1983) pass the fold test. Thus, it is likely that Ghost Rocks Formation preserves a primary magnetization and that the inclination is shallow for their present day latitude (~57°N). This suggests that the Ghost Rocks Formation formed at a latitude of ~41°N +8°/-7° and have subsequently translated large (> 1500km) northward since Paleocene time supporting Model A (Fig. 5a and 6).

Table 1: Paleomagnetic results from the Jap Bay Locality of the Paleocene Ghost Rocks Formation

	Geographic		Stratigraphic						Bedding	
Site	D	I	D	I	k	N	R	a-95	Strike	Dip
07tg89	240.1	-51	214.4	-31.2	42.252	7	6.858	9.4	171	34
07tg90	244.4	-40	224.6	-24.2	119.28	9	8.9329	4.7	171	34
07tg92	219.6	-51.6	183.3	-49.1	103.919	6	5.9519	6.6	116	29
07tg93	232.9	-49	203.5	-59.6	120.631	6	5.9586	6.1	102	23
07tg94	225	-46.6	196.6	-54.7	211.104	6	5.9763	4.6	102	24
07tg95	226	-42.4	197.8	-52	179.117	9	8.9553	3.9	102	27
07tg96	219.6	-49.3	188.2	-52.5	97.406	7	6.9384	6.1	107	25

Notes for Table 1: D, declination; I, inclination; k, Fisher's precision parameter; N, is the number of samples; R, Fisher's resultant vector length; a-95, 95% confidence circle.

Table 2: Paleomagnetic results from the Alitak Bay locality of the Paleocene Ghost Rocks Formation

		geographic						Bedding		
	Site	D	I	k	N	R	a-95	Strike	Dip	
Block 1	06tg12	6.3	-26.1	51.175	7	6.8828	8.5	117	100	*
Block 1	06tg14	359.9	-51.6	11.425	5	4.6499	23.6	263	75	x
Block 1	07tg48	353.9	-20.7	722.657	3	2.9972	4.6	262	68	
Block 1	07tg49	339.8	-26.9	25.808	8	7.7288	11.1	258	68	
Block 2	07tg7	354.6	-48.2	21.962	9	8.6357	11.2	264	61	
Block 3	06tg25	319.7	-49.3	30.503	5	4.8689	14.1	241	74	
Block 4	06tg23	11.9	-36.5	15.405	10	9.4158	12.7	320	75	x
Block 4	06tg24	7.8	-30.6	151.987	9	8.9474	4.2	305	80	
Block 5	06tg20	8.6	-14.2	166.646	10	9.946	3.8	104	85	*
Block 6	06tg4	326.4	-23.2	4.765	3	2.5803	64.2	237	74	x *
Block 6	06tg5	335	-33.5	40.159	3	2.9502	19.7	250	82	
Block 6	06tg6	341.1	-25.8	6.204	4	3.5165	40.2	314	34	x *
Block 6	07tg2	333.3	-48.6	91.227	9	8.9123	5.4	252	74	
Block 6	07tg3	339.9	-43.8	103.923	7	6.9423	5.9	252	74	
Block 6	07tg10	296.6	-79.2	59.312	8	7.882	7.3	247	74	
Block 6	07tg11	293.4	-62.9	21.876	6	5.7714	14.6	246	74	
Block 7	07tg22	330	-18.1	81.652	7	6.9265	6.7	254	80	
Block 7	07tg23	335.5	-28.9	15.583	3	2.8717	32.3	254	80	x *
Block 7	07tg27	331	-42.1	10.101	5	4.604	25.3	255	83	x
Block 7	07tg28	344.7	-40.4	35.841	8	7.8047	9.4	253	80	
Block 7	07tg30	338.3	-32.2	46.149	7	6.87	9	248	80	
Block 8	07tg35	324	-33.4	13.848	8	7.4945	15.4	249	75	x
Block 8	07tg37	332.2	-28.6	14.113	7	6.5749	16.6	249	75	x
Block 8	07tg38	321.1	-33.7	21.188	15	14.3392	8.5	238	75	
Block 8	07tg39	331.7	-34.3	22.069	8	7.6828	12.1	238	75	
Block 8	07tg40	330.4	-43.3	4.612	8	6.4824	29	250	78	x
Block 8	07tg41	343.2	-42.9	18.774	7	6.6804	14.3	256	85	x
Block 8	07tg42	347.3	-16.4	5.437	5	4.2643	36.1	263	79	x *
Block 9	06tg15	121.6	-67.4	40.983	10	9.7804	7.6	292	81	
Block 9	06tg18	152.4	-54.7	10.651	5	4.6244	24.6	63	95	x
Block 10	07tg32	145.5	-61.2	17.695	6	5.7174	16.4	53	95	x
Block 10	07tg45	144.7	-27.6	66.191	7	6.9094	7.5	53	75	
Block 10	07tg46	144.7	-41.4	29.888	10	9.6989	9	53	89	
Block 10	07tg47	159.5	-29.4	7.606	6	5.3426	26	84	89	x
Volcanic Beccia sites										
Block 2	06tg19	134.7	-43.4	11.463	5	4.651	23.6	63	95	
Block 5	06tg21	261.6	-45.9	9.257	3	2.7839	43.1	109	96	
Block 6	07tg13	318.4	-32	1.827	7	3.7153	64.7	3	71	
Block 3	07tg15	308.2	-43.2	8.906	10	8.9894	17.1	18	74	
Block 10	07tg31	155.9	-44.8	64.945	6	5.923	8.4	63	85	

Notes for Table 2: D, declination; I, inclination; k, Fisher's precision parameter; N, is the number of samples; R, Fisher's resultant vector length; a-95, 95% confidence circle. The "x" indicates sites with k>20 and "*" indicates sites with questionable structural constraints.

Table 3: Paleomagnetic results from acceptable sites from Alitak Bay

		geographic						Bedding		Amounts rotated for corrections	
	site	D	I	k	N	R	a-95	Strike	dip	A	B
Block 1	07tg48	353.9	-20.7	722.657	3	2.9972	4.6	262	68	2.6	-12
Block 1	07tg49	339.8	-26.9	25.808	8	7.7288	11.1	258	68	2.6	-8
Block 2	07tg7	354.6	-48.2	21.962	9	8.6357	11.2	264	61	-17.4	-14
Block 3	06tg25	319.7	-49.3	30.503	5	4.8689	14.1	241	74	7.1	9
Block 4	06tg24	7.8	-30.6	151.987	9	8.9474	4.2	305	80	-58.9	-55
Block 5	06tg20	8.6	-14.2	166.646	10	9.946	3.8	284	85	-38	-34
Block 6	06tg5	335	-33.5	40.159	3	2.9502	19.7	250	82	-11.9	0
Block 6	07tg2	333.3	-48.6	91.227	9	8.9123	5.4	252	74	-11.9	-2
Block 6	07tg3	339.9	-43.8	103.923	7	6.9423	5.9	252	74	-11.9	-2
Block 6	07tg10	296.6	-79.2	59.312	8	7.882	7.3	247	74	-11.9	3
Block 6	07tg11	293.4	-62.9	21.876	6	5.7714	14.6	246	74	-11.9	4
Block 7	07tg22	330	-18.1	81.652	7	6.9265	6.7	254	80	-13.1	-4
Block 7	07tg28	344.7	-40.4	35.841	8	7.8047	9.4	253	80	-13.1	-3
Block 7	07tg30	338.3	-32.2	46.149	7	6.87	9	248	80	-13.1	2
Block 8	07tg38	321.1	-33.7	21.188	15	14.3392	8.5	238	75	-1.3	12
Block 8	07tg39	331.7	-34.3	22.069	8	7.6828	12.1	238	75	-1.3	12
Block 10	07tg31	155.9	-44.8	64.945	6	5.923	8.4	84	95	170	-4
Block 10	07tg45	144.7	-27.6	66.191	7	6.9094	7.5	53	75	170	27
Block 10	07tg46	144.7	-41.4	29.888	10	9.6989	9	53	89	170	27

Notes for Table 3: D, declination; I, inclination; k, Fisher's precision parameter; N, is the number of samples; R, Fisher's resultant vector length; a-95, 95% confidence circle. Column "A" corresponds to the amount of rotation needed to correct the calculated block mean strike and the reference strike of 250º. Column "B" corresponds to the amount of rotation needed to rotate the strike of an individual site to strike and the reference strike of 250º. Column "B" corresponds to the amount of rotation needed to rotate the strike of an individual site to the strike of 250º after the block rotations (of column "A") were applied. For Columns "A" and "B" positive numbers correspond to clockwise rotation and negative numbers correspond to counterclockwise rotation.

Table 4: Paleomagnetic combine mean results from Alitak Bay after corrections

	D	I	k	a-95	N
In-situ	339.5	-39.7	14	10.3	19
Simple tilt correction	179.7	-74.6	8	12.6	19
Block rotated	325.6	-42.2	16.834	8.4	19
Block and Strike rotated	334.4	-42.7	14.63	9.1	19
Block rotated-tilt corrected	153.9	-63.6	9.169	11.7	19
Block then strike rotated-tilt corrected	168.4	-60.2	12.727	9.8	19
un-plunge and tilt corrected	218	-62.3	10	11.6	19

Notes for Table 3: D, declination; I, inclination; k, Fisher's precision parameter; a-95, 95% confidence circle; N, is the number of samples.

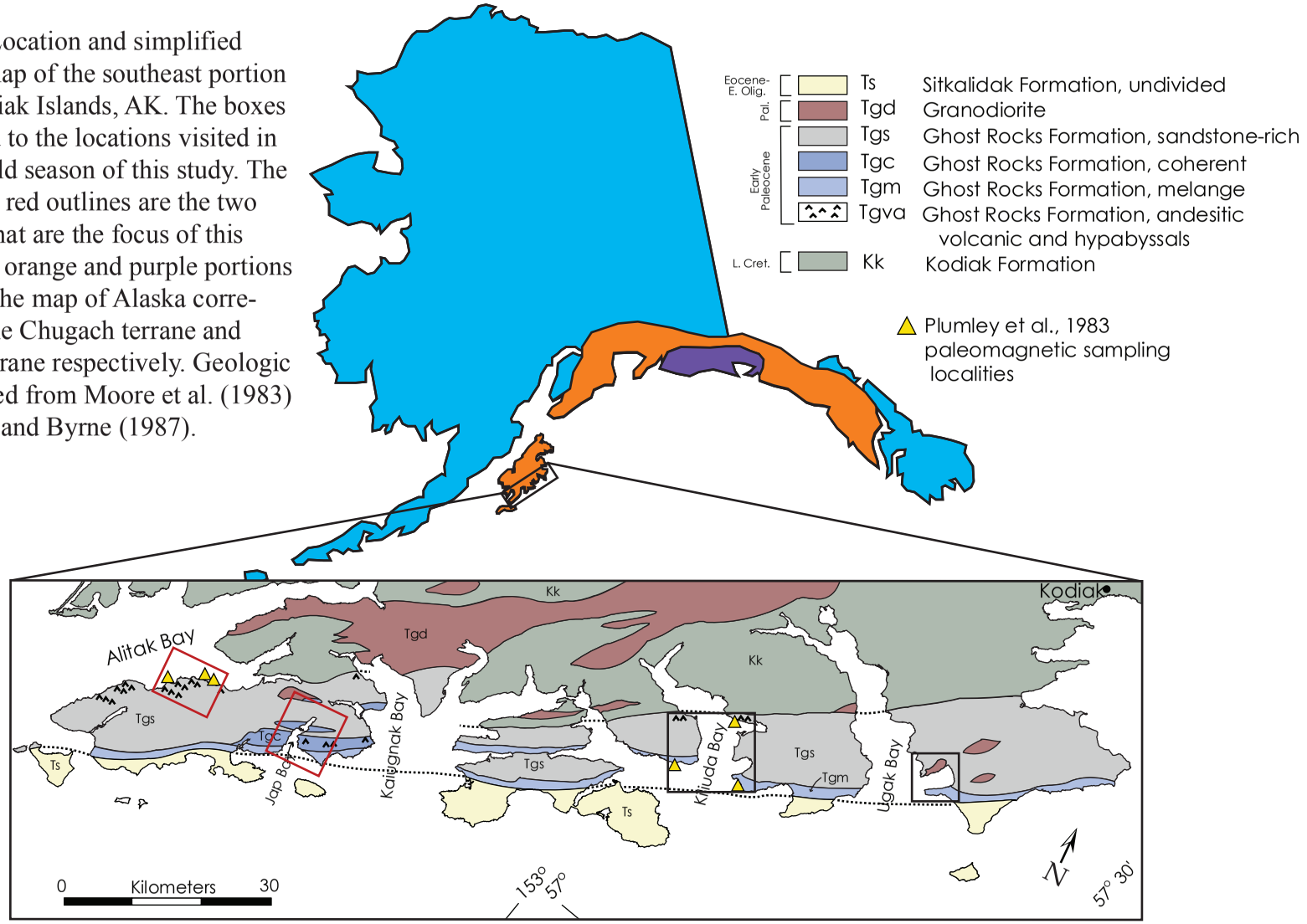

Figure 1: Location and simplified geologic map of the southeast portion of the Kodiak Islands, AK. The boxes correspond to the locations visited in the two field season of this study. The boxes with red outlines are the two locations that are the focus of this thesis. The orange and purple portions shown on the map of Alaska correspond to the Chugach terrane and Yakutat terrane respectively. Geologic map adapted from Moore et al. (1983) and Fisher and Byrne (1987).

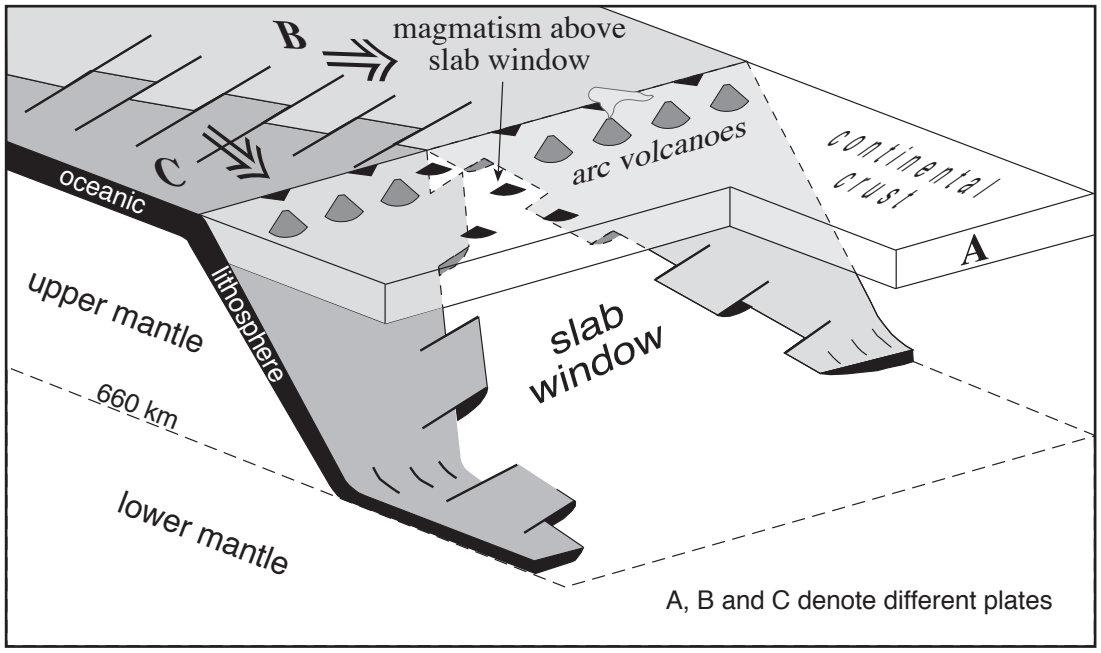

Figure 2: Schematic block diagram showing a trench-ridge-trench (TRT) triple junction, highlighting some of the geologic anomalies unique to this geologic interaction. Adapted from Thorkelson (1996).

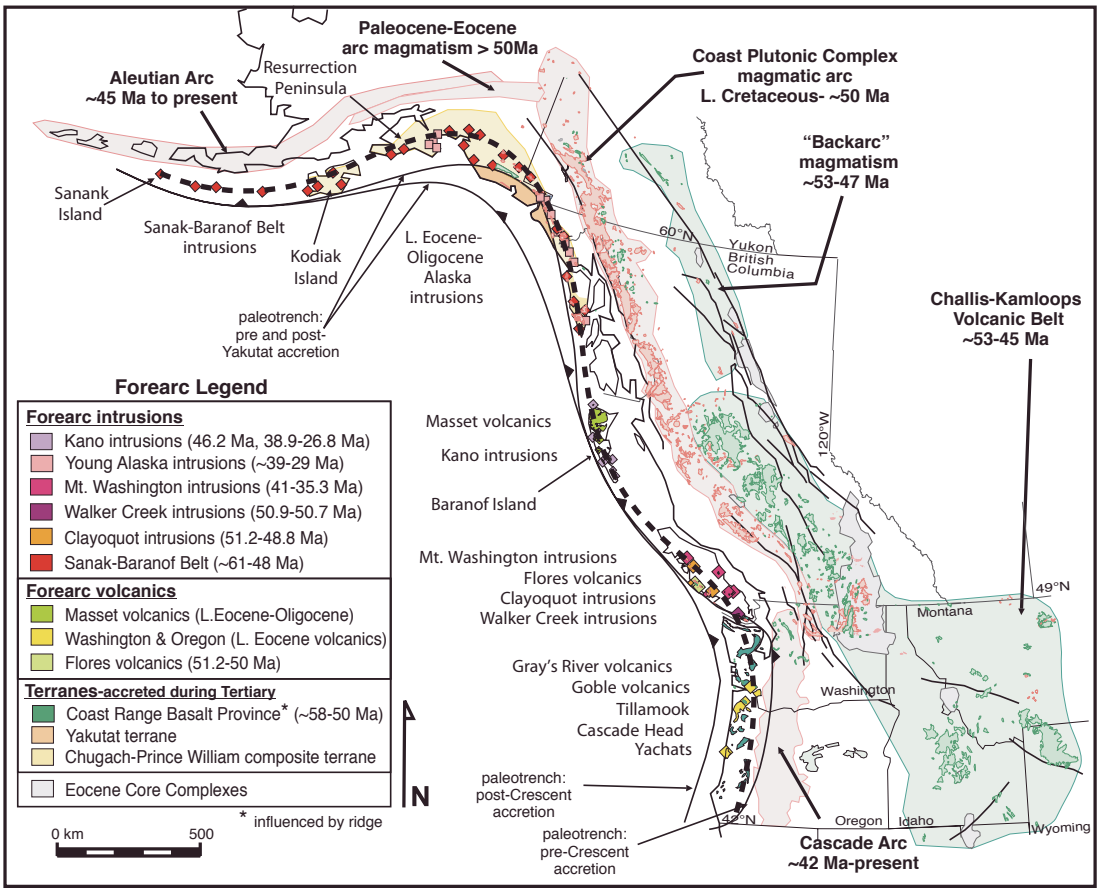

Figure 3: Paleocene-Oligocene forearc, arc and backarc magmatism of the contemporary Northern Cordilleran margin. Also highlighted are the Coast Range Basalt Province, and the Chugach and Yakutat terrane, which accreted to the fore arc during the Tertiary. Where igneous exposures are small, they are shown as diamonds or squares. Major strike-slip faults are shown as thin black lines. The bold dashed line corresponds to figure 4. Modified from Madsen et al. (2006).

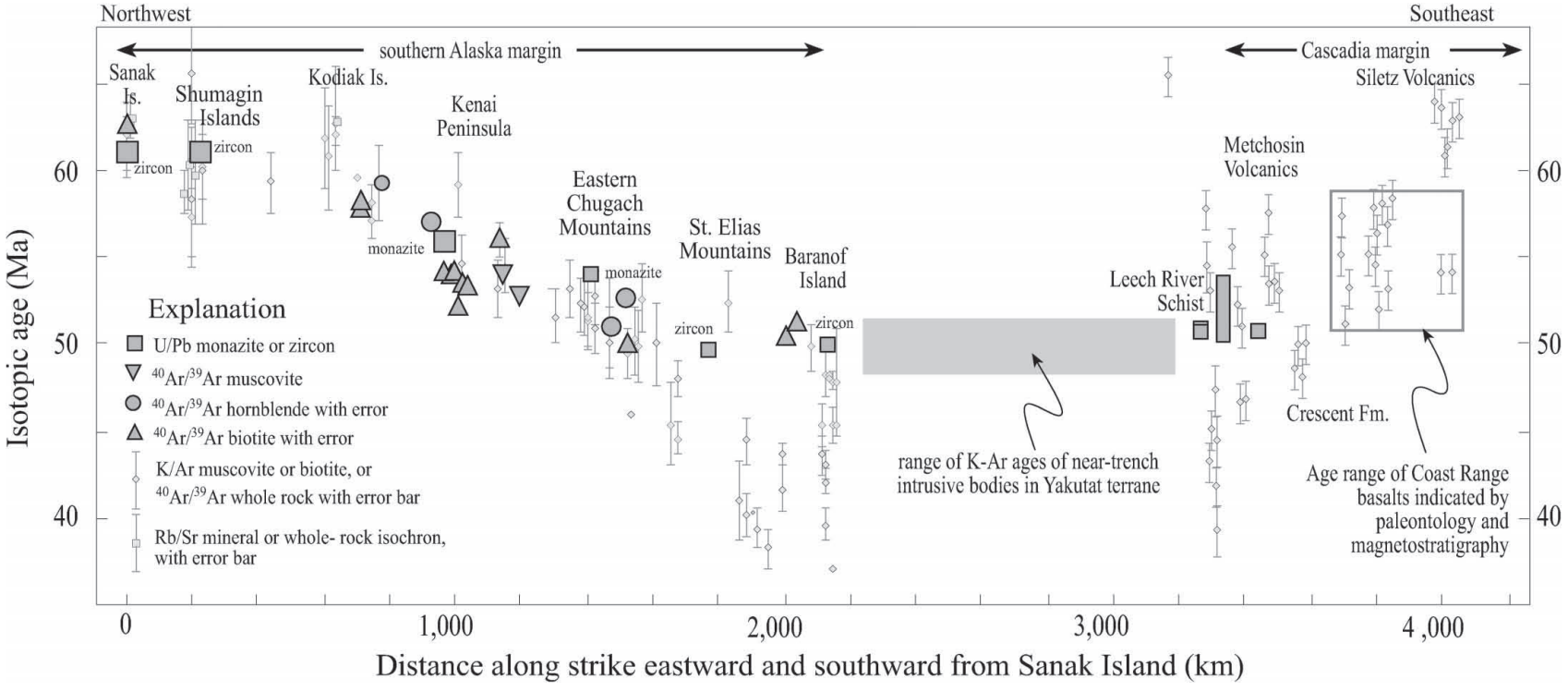

Figure 4: Plot of age vs. distance of near-trench magmatism from Sanak Island to Oregon along the dashed bold line in figure 3. From Haeussler et al. (2003).

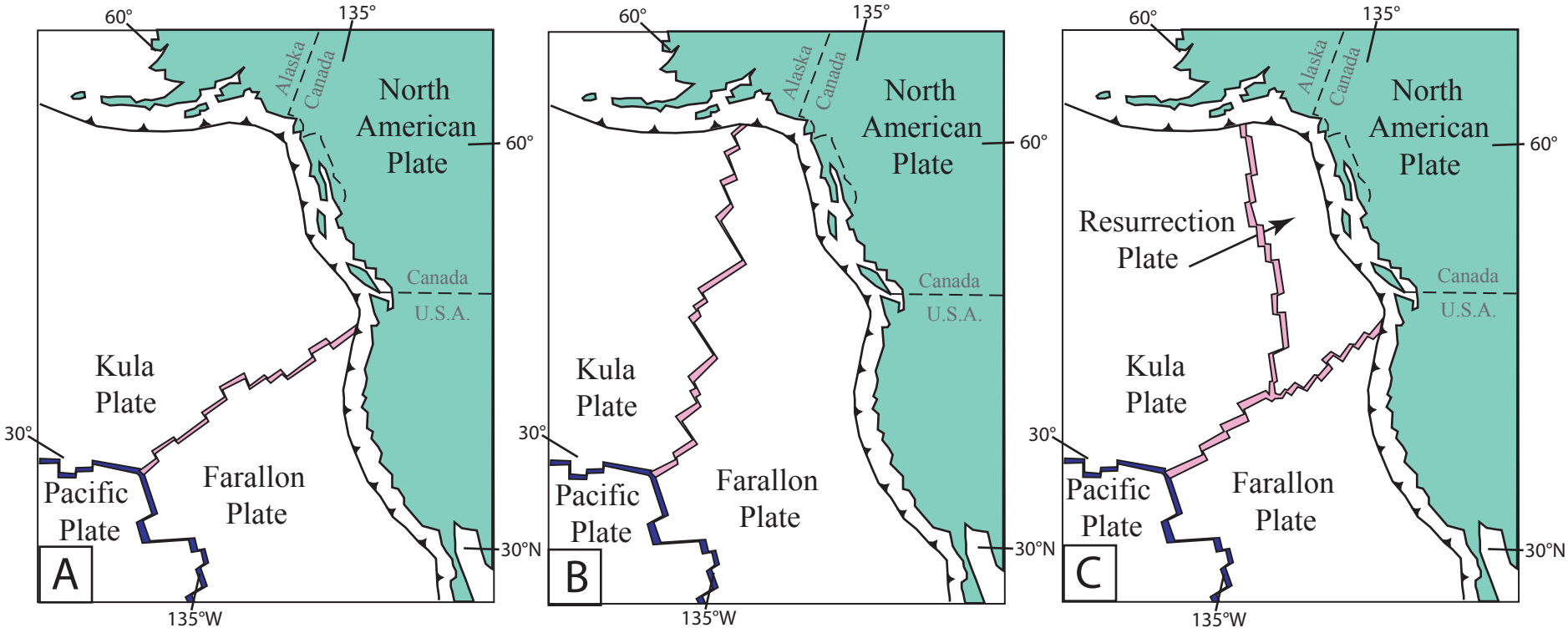

Figure 5: Schematic showing the three hypothesized location(s) of TRT triple junction(s) along the Northern Cordilleran at ~56.1Ma. See text for explanation. Hypotheses A, B, and C correspond to figures 6,7, and 8 respectively. From Haeussler et al. (2003) and Bradley et al. (2003).

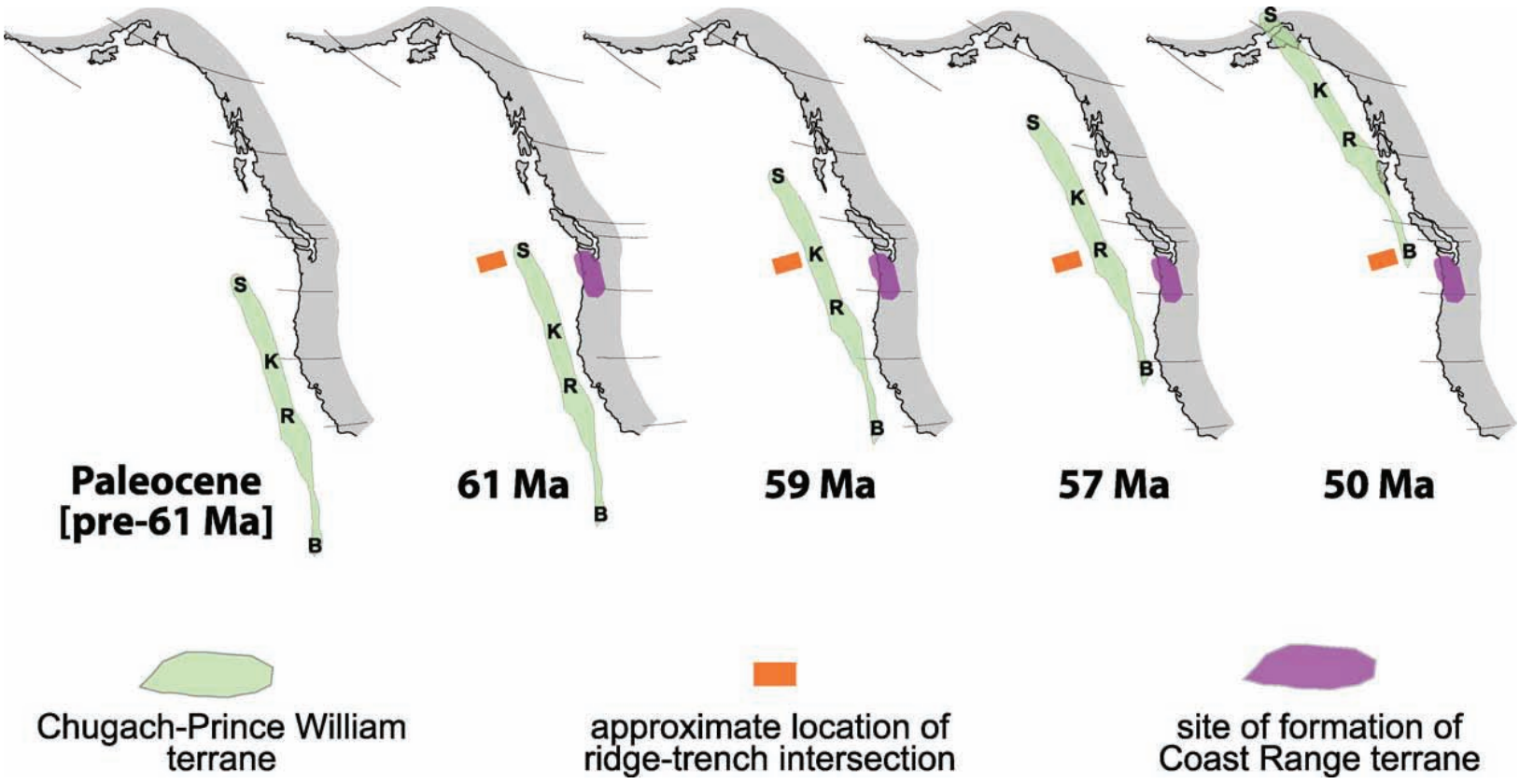

Figure 6: Schematic showing hypothesized latitudinal northward translation of the Chugach terrane during the early Tertiary. The Chugach terrane is shown restored to its hypothesized orientation prior to the oroclinal bending of Alaska, which is thought to have occurred sometime between ~66-44Ma (Bradley et al., 2003). This model is based on paleomagnetic and geologic data. The letters S, K, R, and B on the Chugach terrane are the portions of Sanak Island, Kodiak Island, Resurrection Peninsula, and southern Baranof Island respectively. From Cowan (2003).

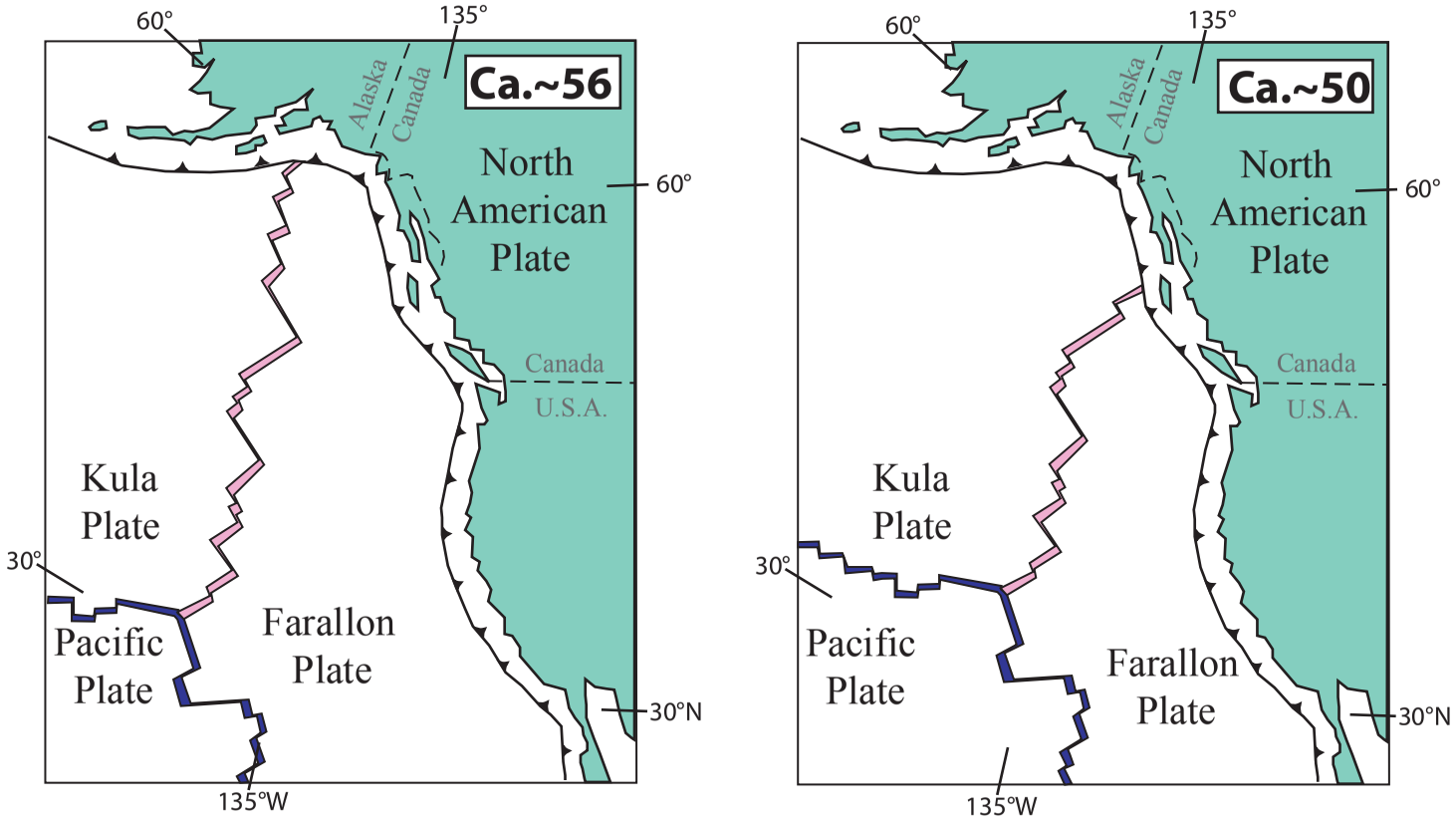

Figure 7: Schematic showing the hypothesized W-E migration of the "extreme-northern option" of Kula-Farallon spreading ridge along the North American margin. After Haeussler et al. (2003).

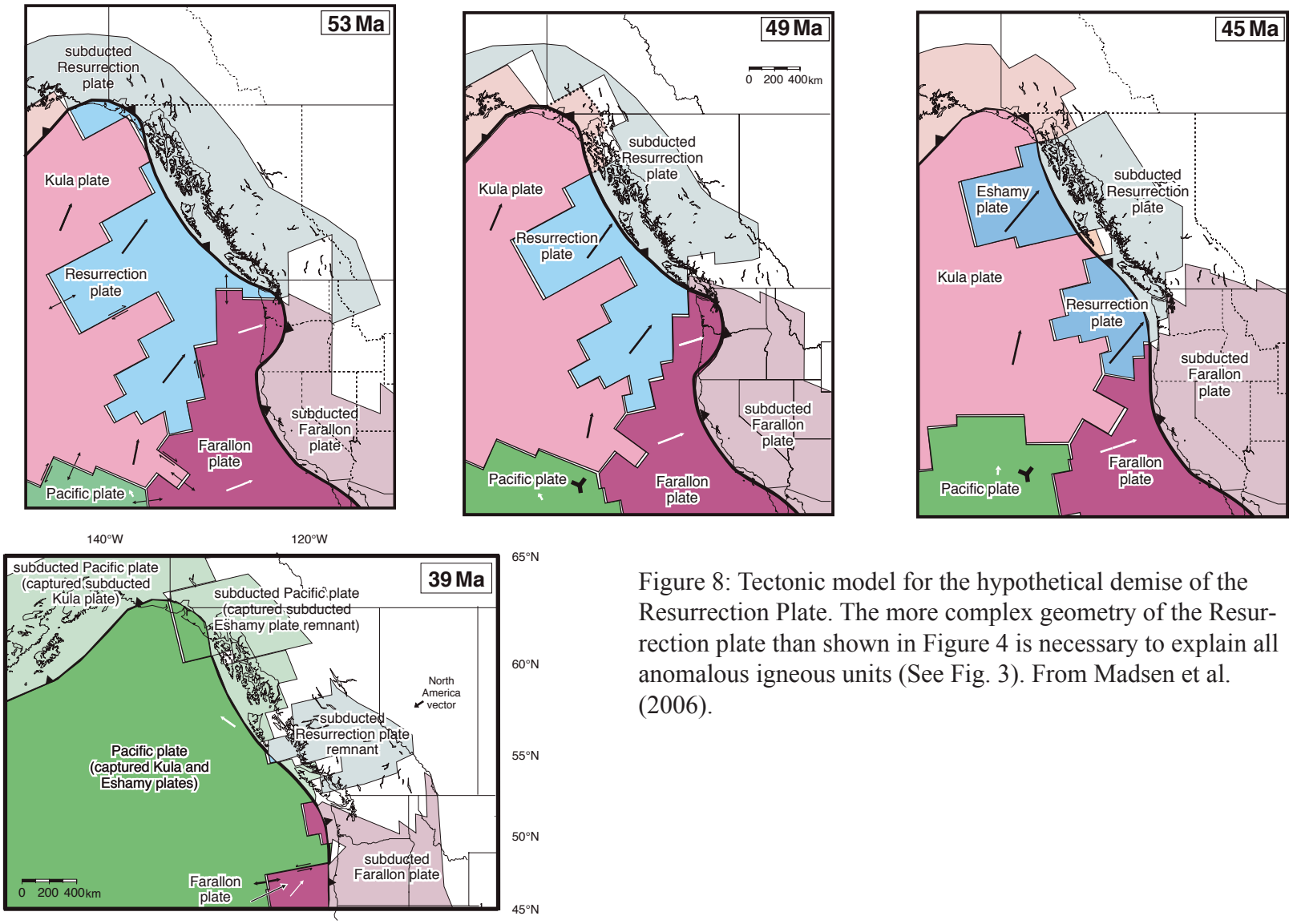

Figure 8: Tectonic model for the hypothetical demise of the Resurrection Plate. The more complex geometry of the Resurrection plate than shown in Figure 4 is necessary to explain all anomalous igneous units (See Fig. 3). From Madsen et al. (2006).

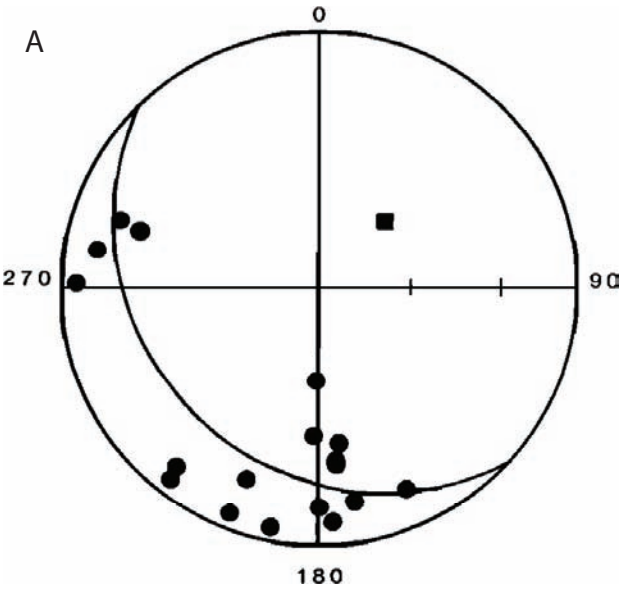

Figure 9: Structural data and interpretation of the Alitak Bay region by Plumley et al. (1983) A. equal area projection of Alitak Bay poles to bedding (circles) with cylindrical best fit and interpreted fold axis (square) plunging 60° along an azimuth of 45°. B. Map showing interpreted regional scale fold and paleomagnetic site locations.

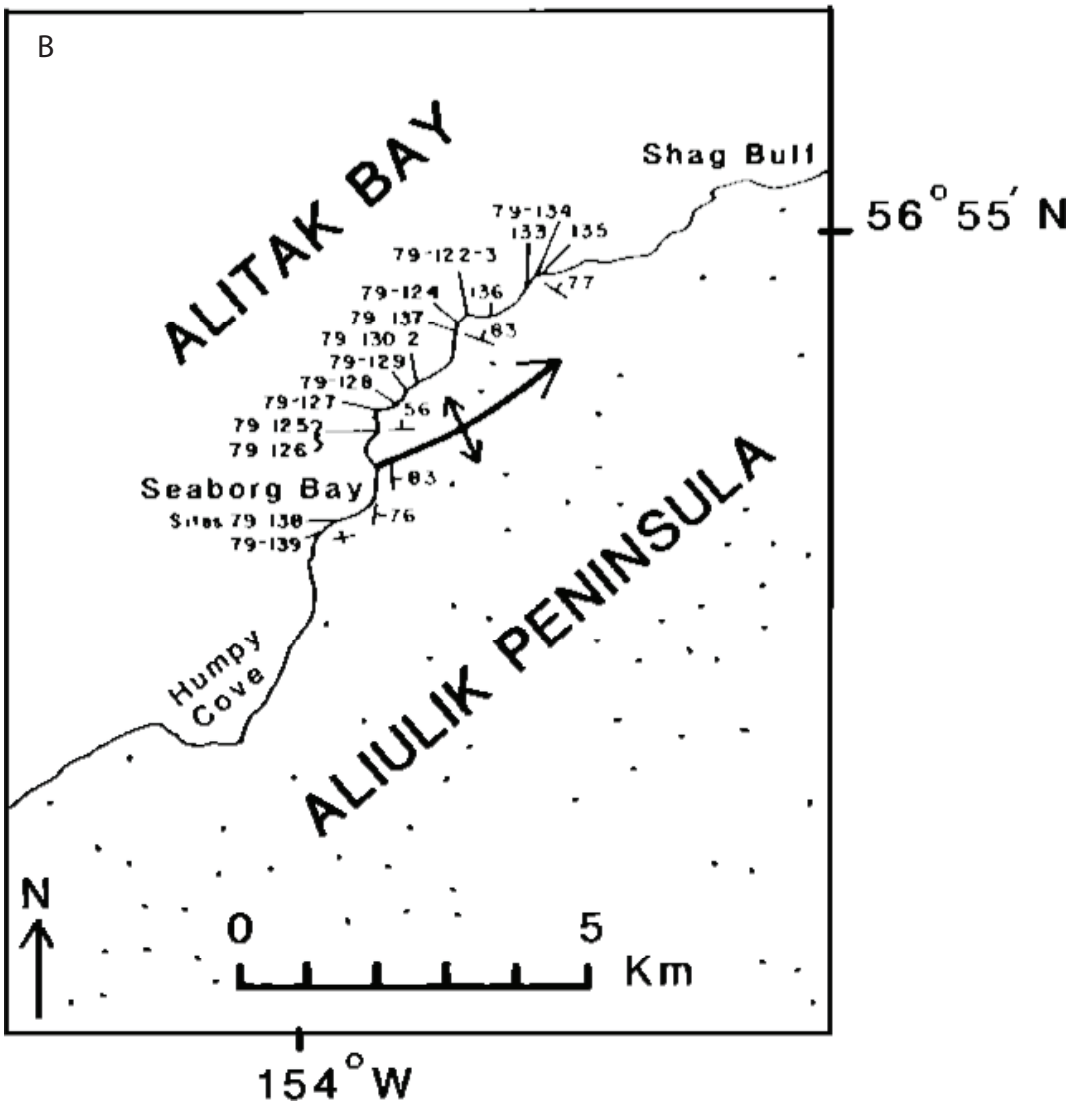

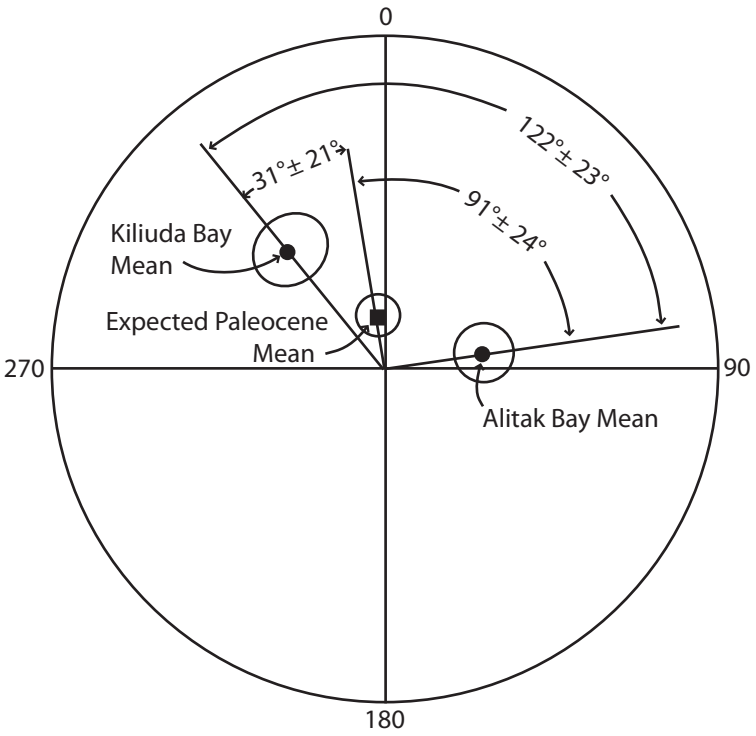

Figure 10: Equal area plot of locality means from Kiliuda bay and Alitak bay and the expected mean of the entire Ghost Rocks Formation from the Plumley et al. (1983) study. All paleomagnetic directions have been changed to normal polarity for easy comparison. See text for explanation.

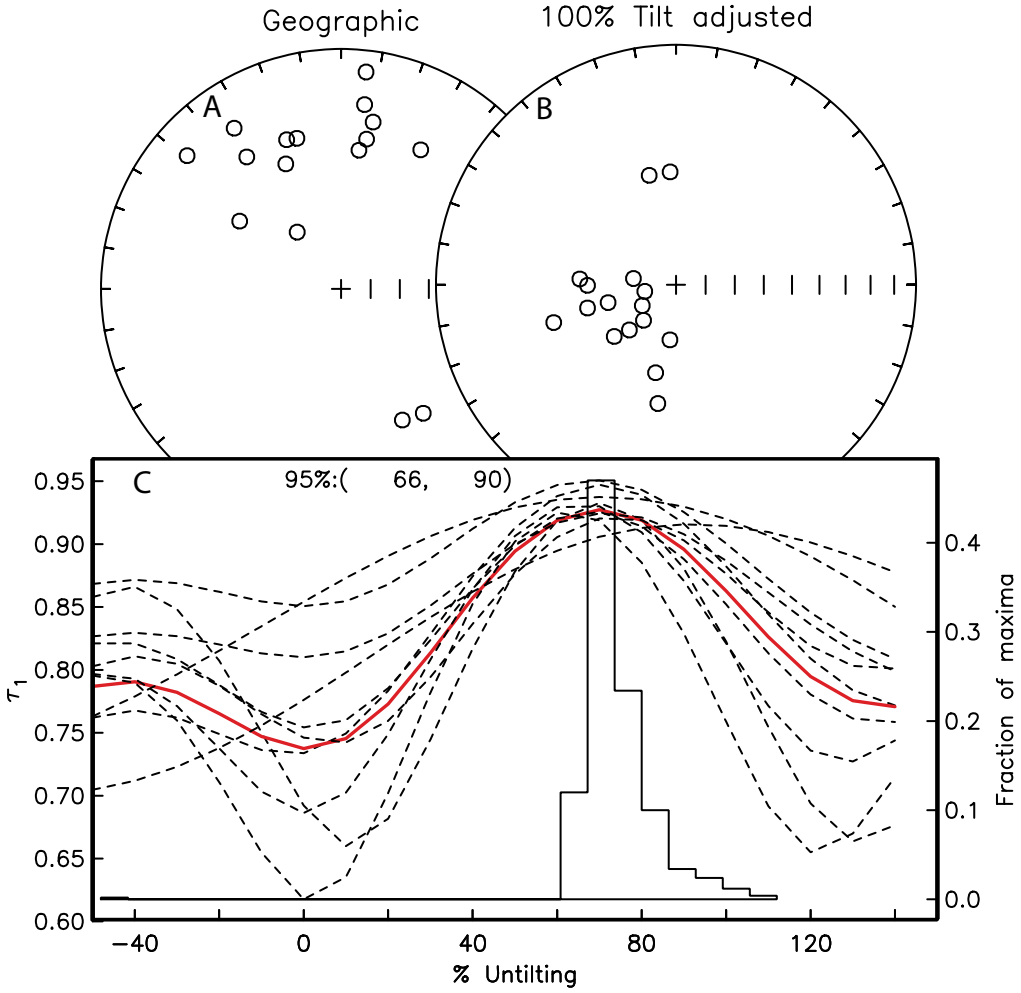

Figure 11: Plumley et al. (1983) paleomagnetic results from the volcanic flows of the Alitak Bay area. Equal area projections of site mean directions A. in-situ coordinates and B. tilt-corrected coordinates. C. Results of the Tauxe and Watson (1994) fold test, the red line shows the best fit correction and dash lines represent bootstrap trials.

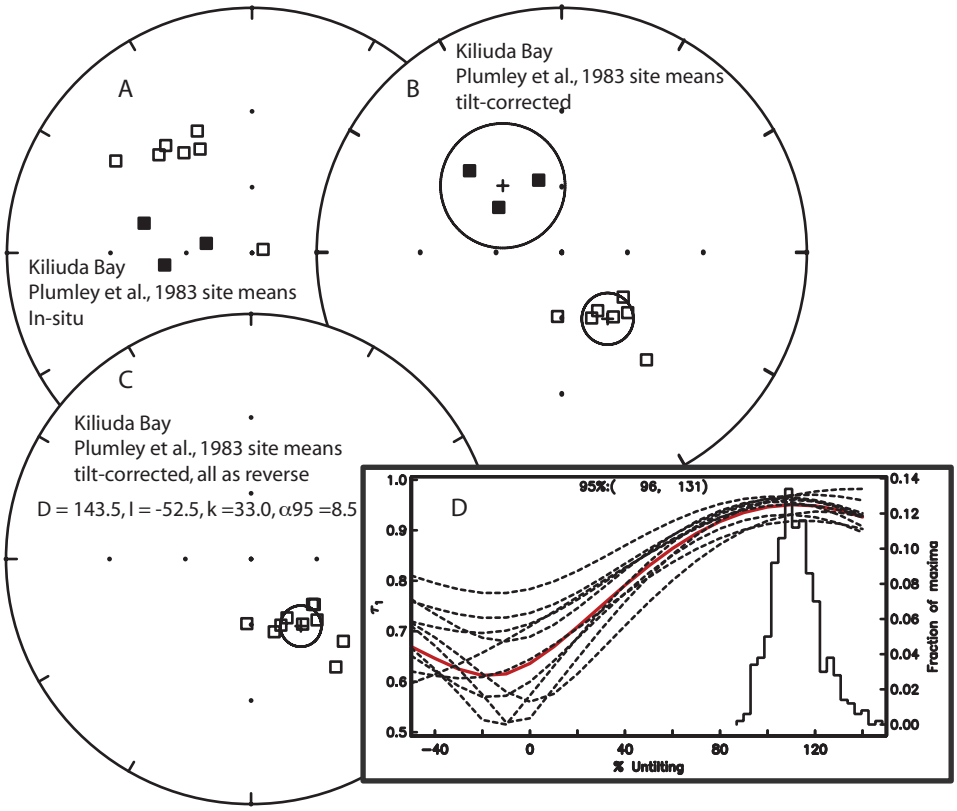

Figure 12: Plumley et al., 1983 Paleomagnetic results from the volcanic flows of the Kiliuda Bay area. For this analysis we discarded one additional site that has a k value not significantly different from random, so N=10. A. Site means in-situ coordinates and B. tilt-corrected coordinates. C. Locality mean direction after all directions are changed to reverse-polarity, in tilt-corrected coordinates. D. Results of the Tauxe and Watson (1994) fold test, the red line shows the best fit correction and dash lines represent boot-strap trials. Large open circles show the 95% confidence ellipses of the tilt corrected mean directions.

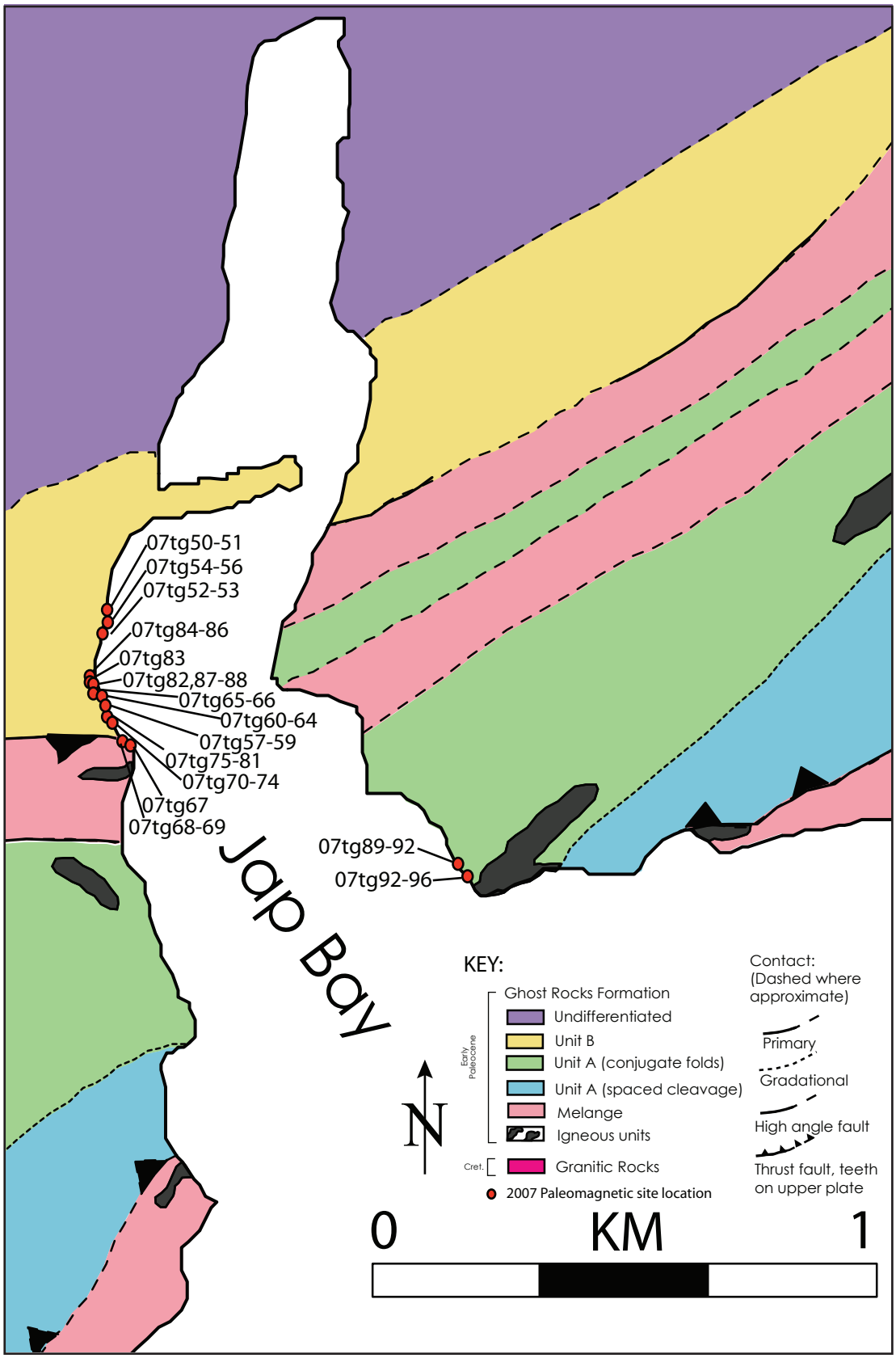

Figure 13: Simplified geologic map of the Jap Bay area showing paleomagnetic site locations from this study. Adapted from Byrne (1982).

A

B

C

Figure 14: Photos of typical outcrop exposures of thin to medium sandstone and mudstone beds with in Unit B of Jap Bay. A. Open folds, sites 07tg54-56, B. tight folds sites 07tg65-66, C. coherent section with little to no folding, site 07tg57

A

B

C

Figure 15: Photos showing typical outcrop exposures with in Unit A of Jap Bay. A. Sandstone and mudstone beds with in the “spaced cleavage” portion of Unit A as describe by Byrne (1982). B. Fine-grained sandstone sites 07tg94-96. C. Volcanic flow, site 07tg91, note the mudstone above and below the flow.

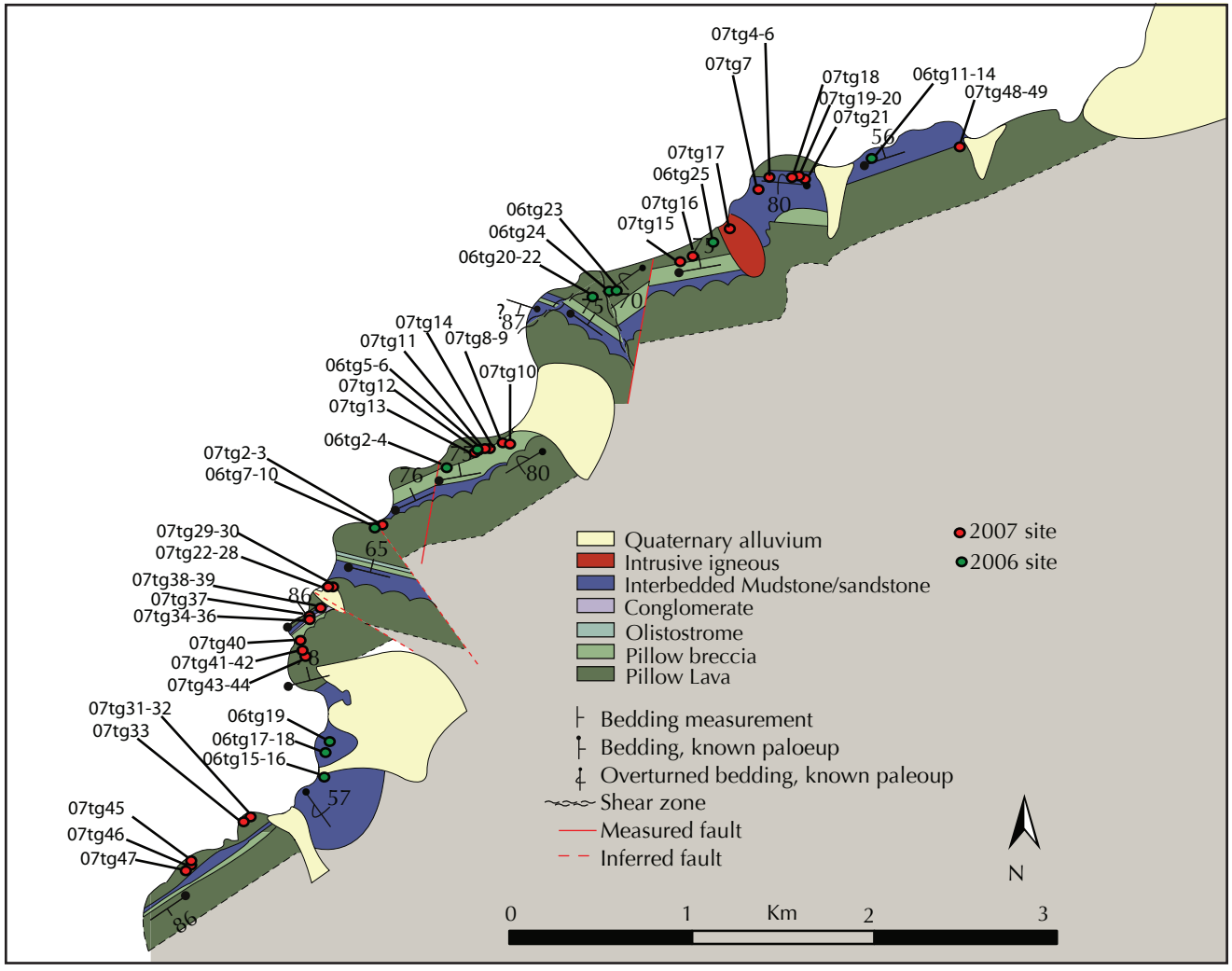

Figure 16: Simplified geologic map of the Alitak Bay area with the 2006 and 2007 paleomagnetic site locations. Modified from O'Connell et al. (2007).

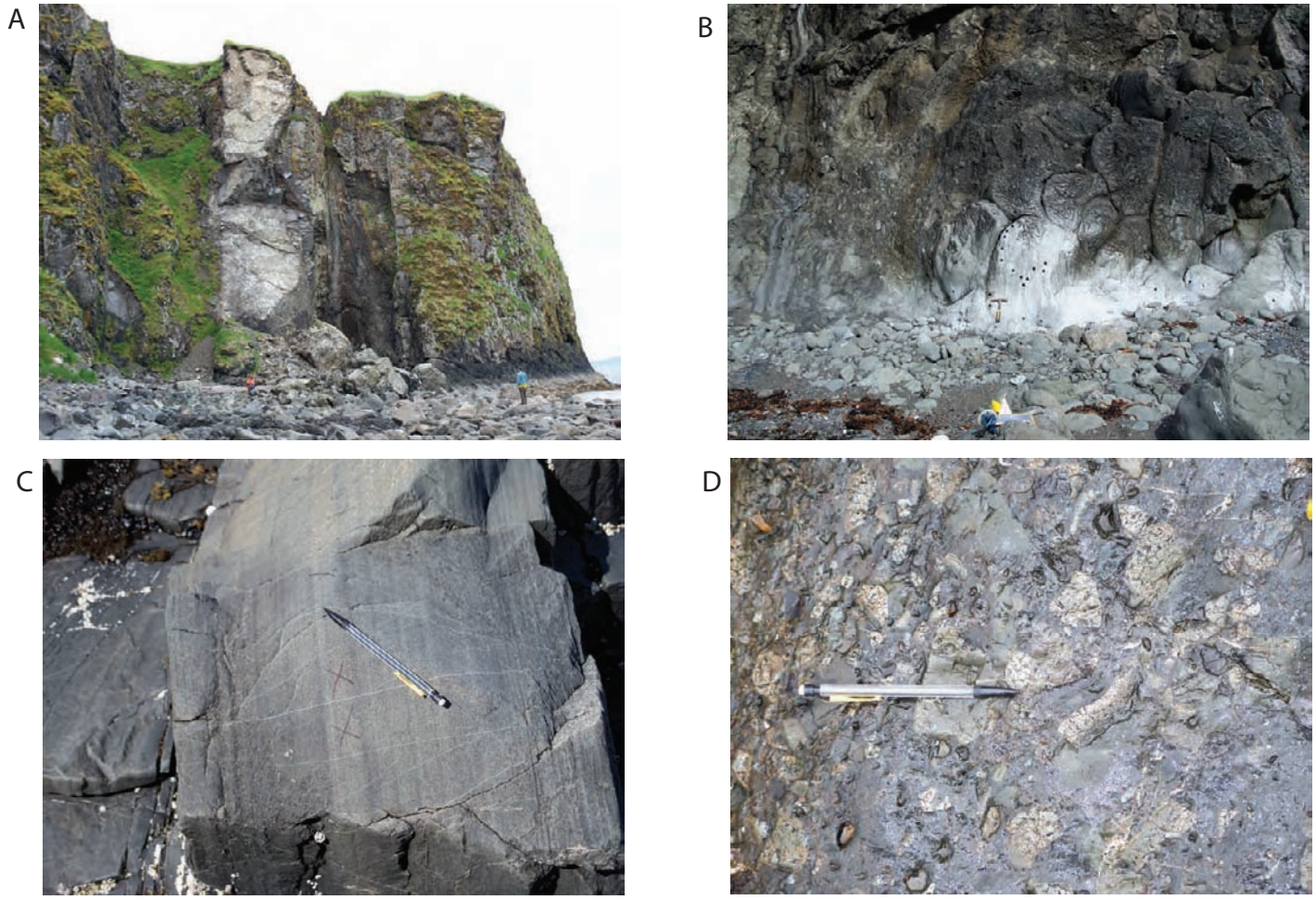

Figure 17: Photos from Alitak Bay study area. A. Example of the scale of the coherent "blocks" identified by O'Connell (2007, 2008), showing a sequence of sedimentary beds stratigraphically overlain by pillow lavas. People for scale. B. Typical outcrop at Alitak Bay showing pillows interbedding with turbidites, sites 07tg38-39. C. Typical sedimentary site, not the preservation of sedimentary structures. D. Typical volcanic breccia in Alitak Bay.

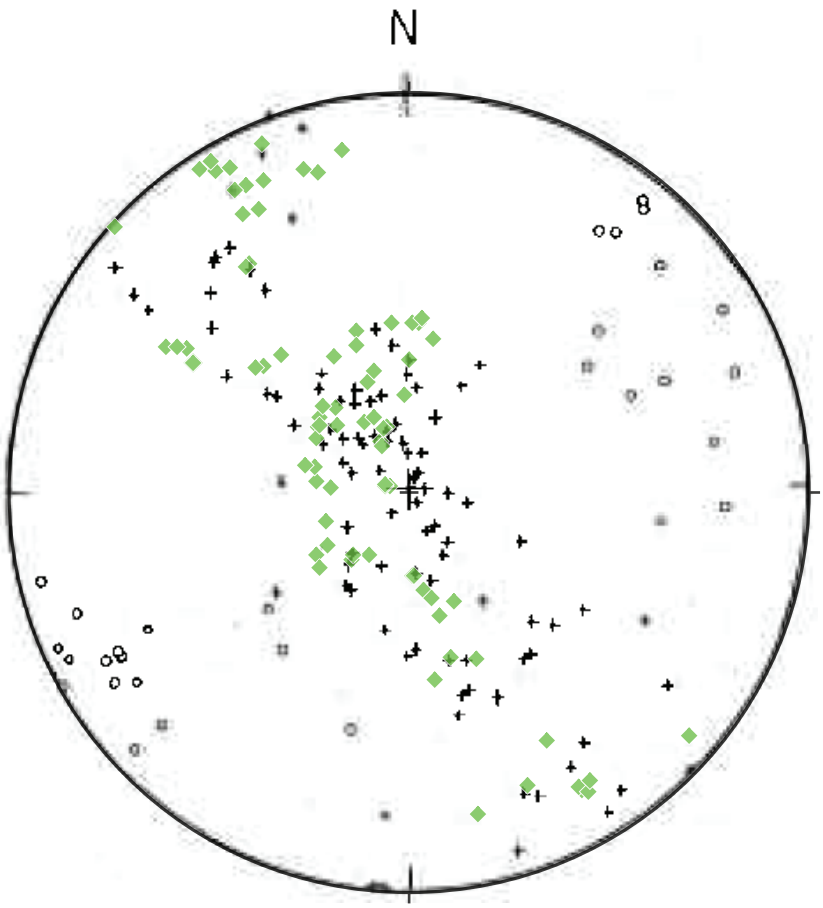

Figure 18: Equal area projection of poles to bedding from Unit B of Jap Bay. Green diamonds are measurements from this study (N=81) and black crosses are from Byrne (1982) (N=101). Also shown are the trend and plunge of fold axes (open circles). Adapted from Byrne (1982).

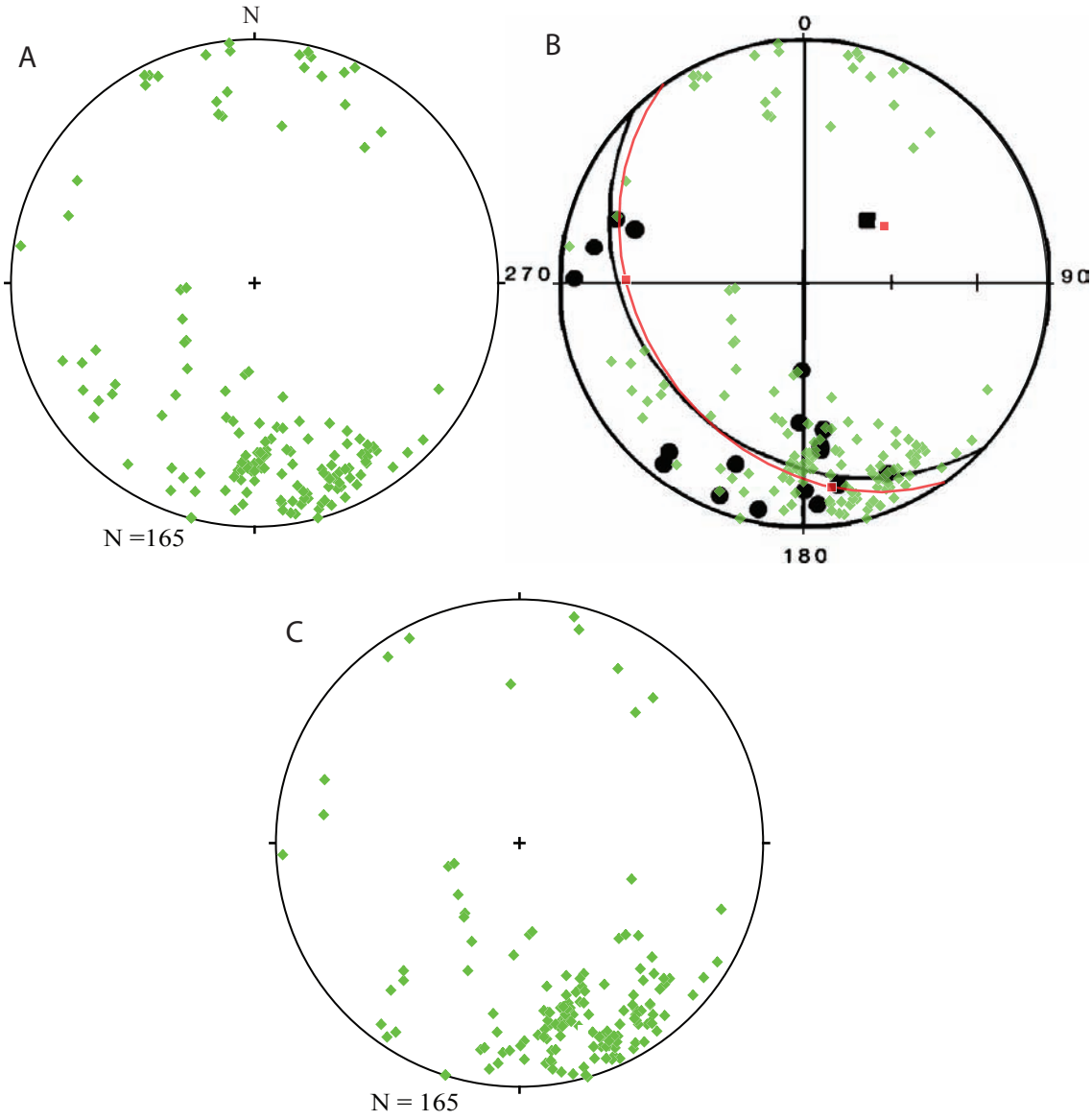

Figure 19: Equal area projections of poles to bedding in Alitak Bay. A. In-situ poles to bedding from this study. B. In-situ poles to bedding from this study (green diamonds) with cylindrical best fit overlain on the poles to bedding from Plumley et al. (1983) (black dots). Note similar orientations of poles to cylindrical best fits. C. Orientation of poles to bedding after corrected for ridge block rotation.

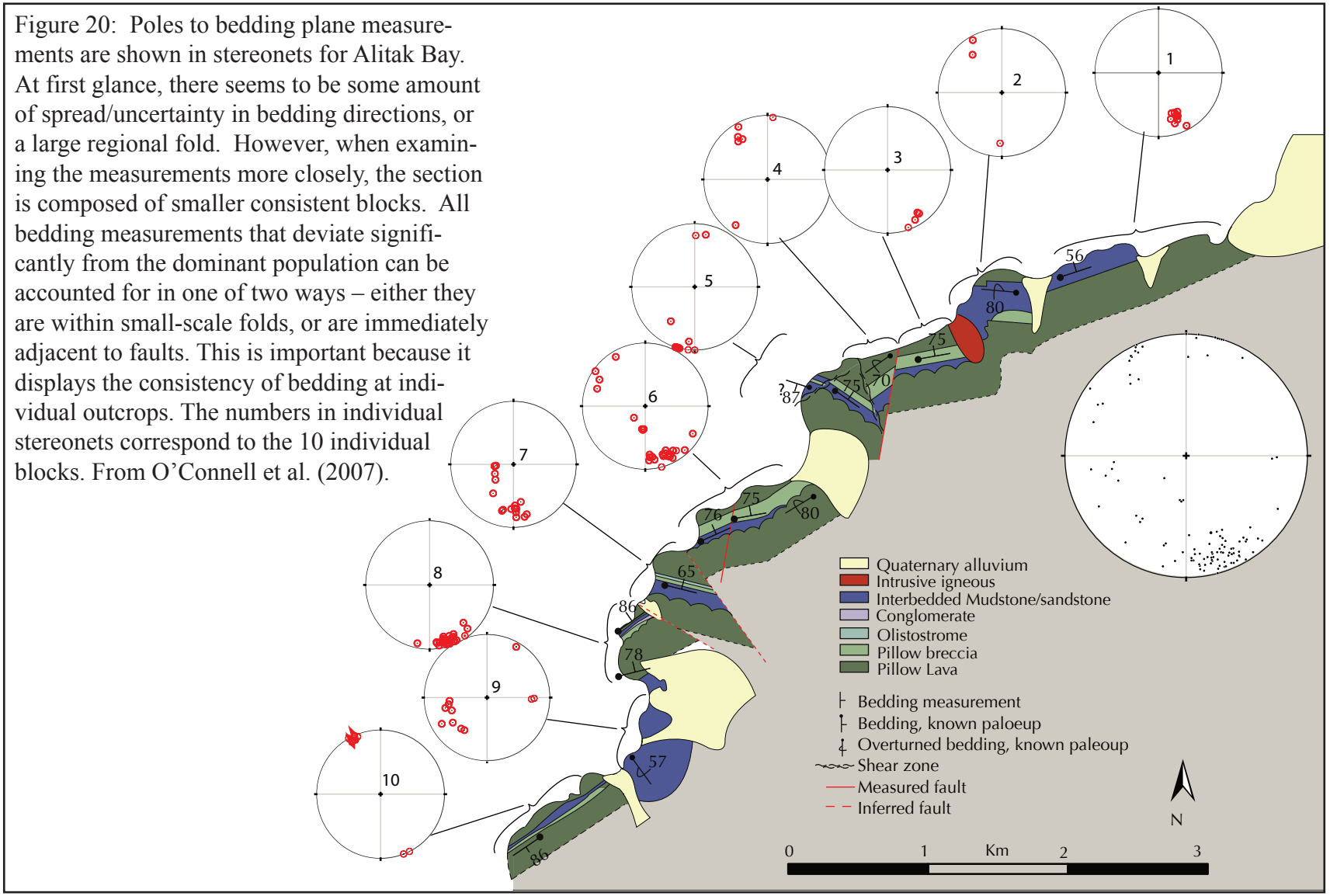

Figure 20: Poles to bedding plane measurements are shown in stereonets for Alitak Bay. At first glance, there seems to be some amount of spread/uncertainty in bedding directions, or a large regional fold. However, when examining the measurements more closely, the section is composed of smaller consistent blocks. All bedding measurements that deviate significantly from the dominant population can be accounted for in one of two ways – either they are within small-scale folds, or are immediately adjacent to faults. This is important because it displays the consistency of bedding at individual outcrops. The numbers in individual stereonets correspond to the 10 individual blocks. From O'Connell et al. (2007).

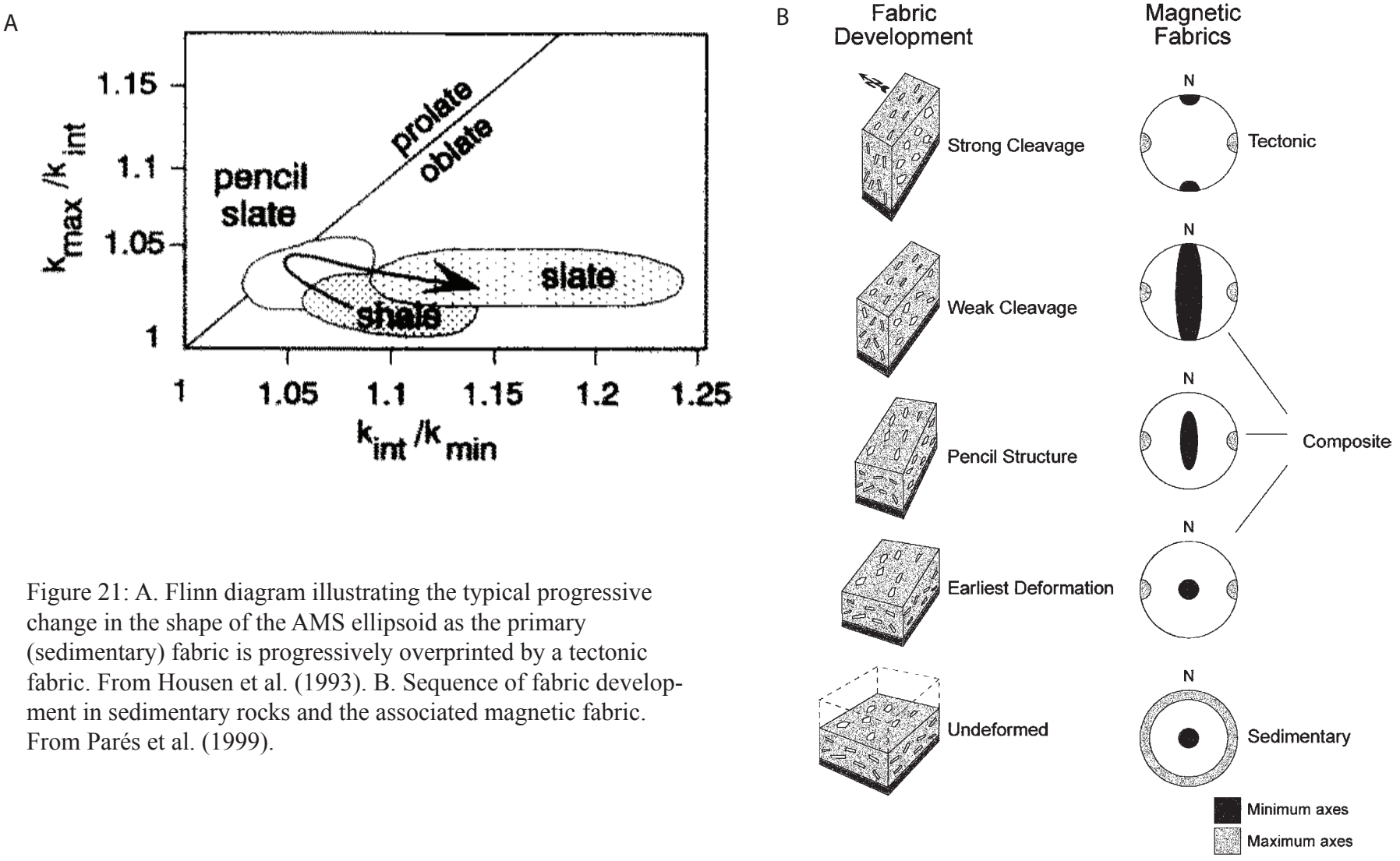

Figure 21: A. Flinn diagram illustrating the typical progressive change in the shape of the AMS ellipsoid as the primary (sedimentary) fabric is progressively overprinted by a tectonic fabric. From Housen et al. (1993). B. Sequence of fabric development in sedimentary rocks and the associated magnetic fabric. From Parés et al. (1999).

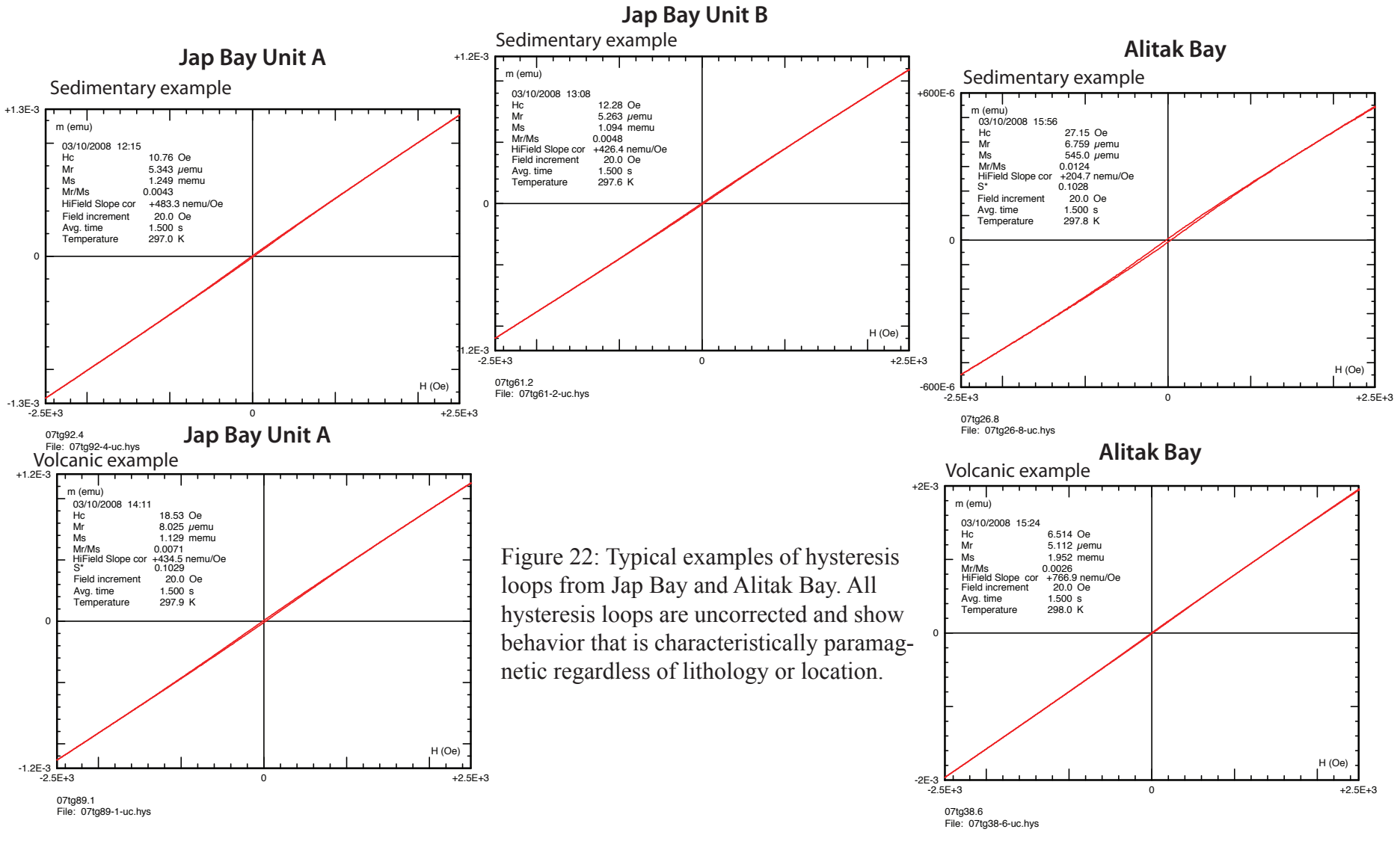

Figure 22: Typical examples of hysteresis loops from Jap Bay and Alitak Bay. All hysteresis loops are uncorrected and show behavior that is characteristically paramagnetic regardless of lithology or location.

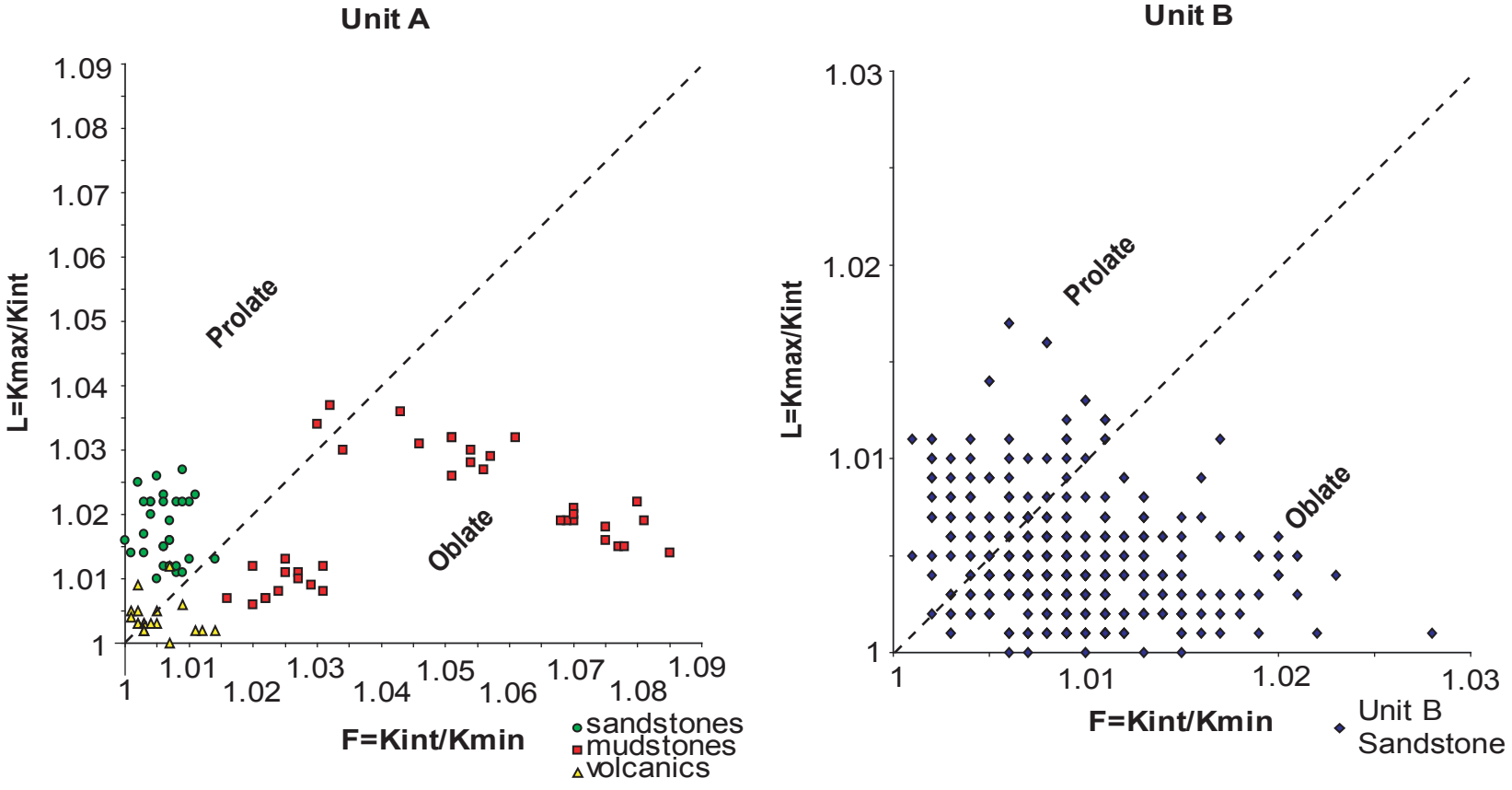

Figure 23: Flinn diagrams of all individual specimen data from Jap Bay Unit A and Unit B. Note the scale on each Flinn diagram is different.

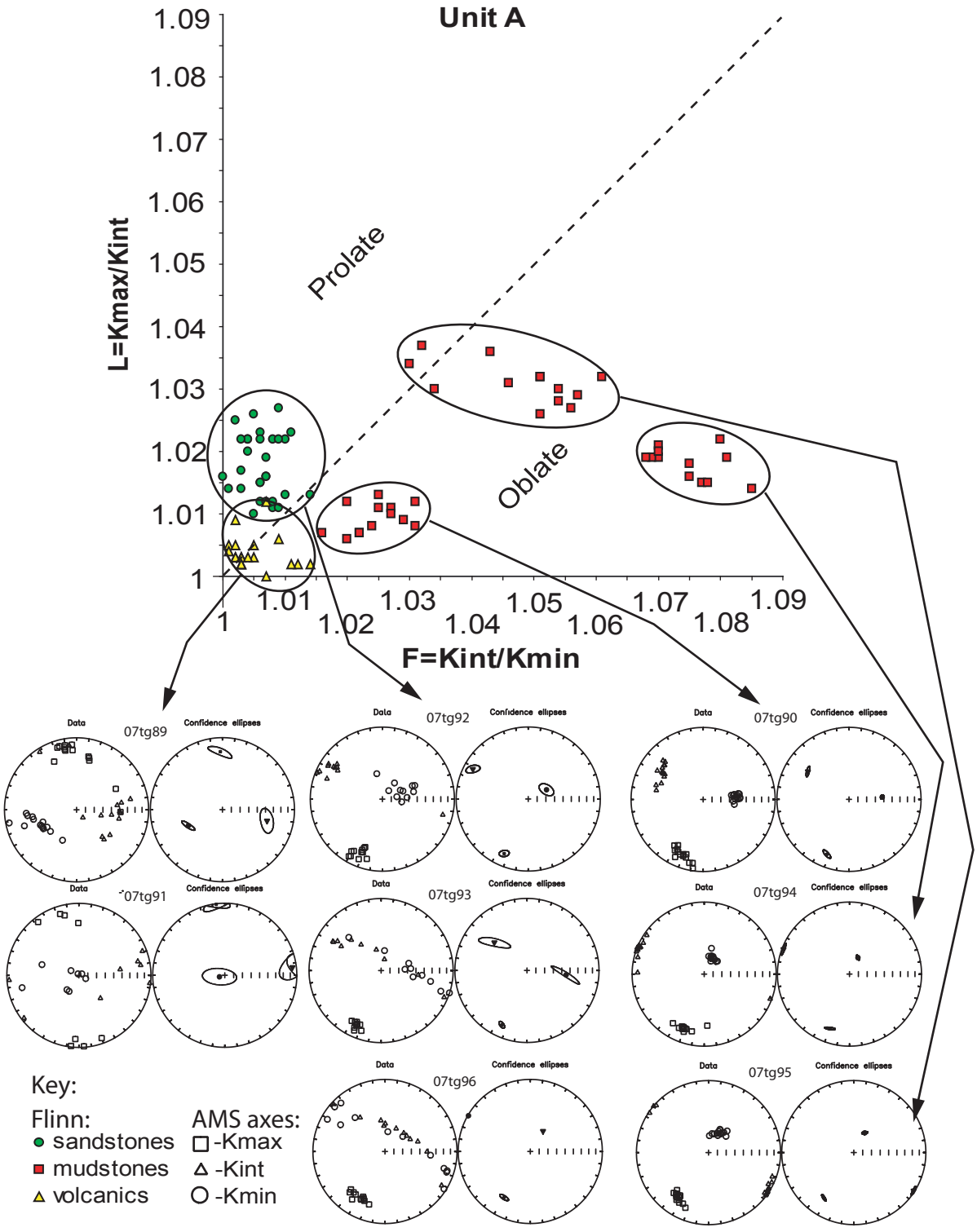

Figure 24: Flinn diagram and lower hemisphere equal area plots of AMS data in-situ coordinates from Unit A. 95% confidence ellipses are shown for data with significant clustering; small ellipses are simple bootstrap plotted using Tauxe (1998) plotams.exe program. Note the distinct differences in AMS ellipsoid shape and relative orientations of ellipsoid axes and the consistency of the Kmax directions of the sedimentary rocks.

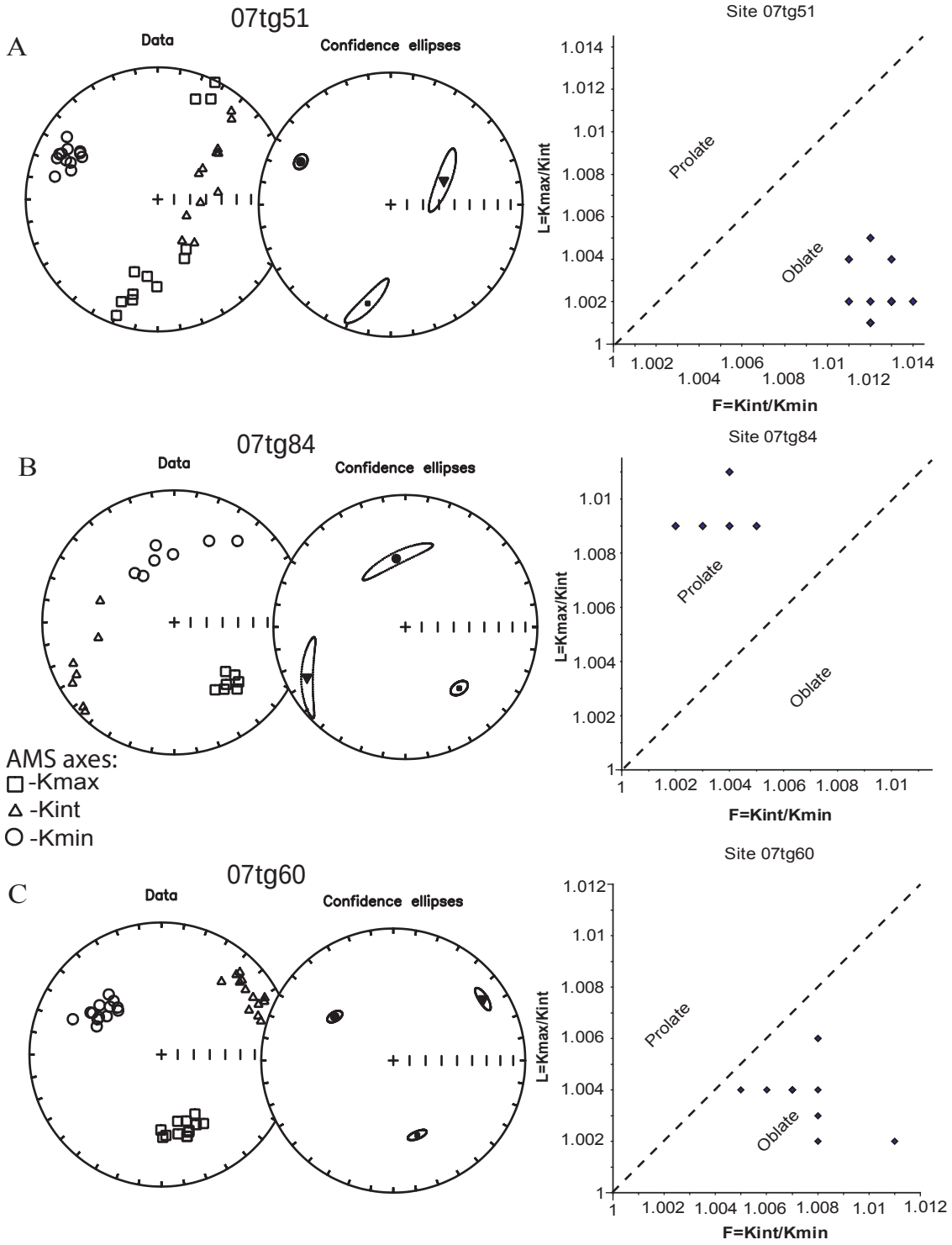

Figure 25: Equal area plots in in-situ coordinates of AMS data and Flinn diagrams of AMS data from two sites of sandstone from Unit B of Jap Bay. A and B are examples of oblate and prolate end-members respectively. C. Shows a typical example of the majority of site AMS ellipsoid sample directions and shapes. 95% confidence ellipses are shown for data with significant clustering; small ellipses are simple bootstrap. All AMS data was plotted using Tauxe (1998) plotams.exe program. Note the scale on each Flinn diagram is different.

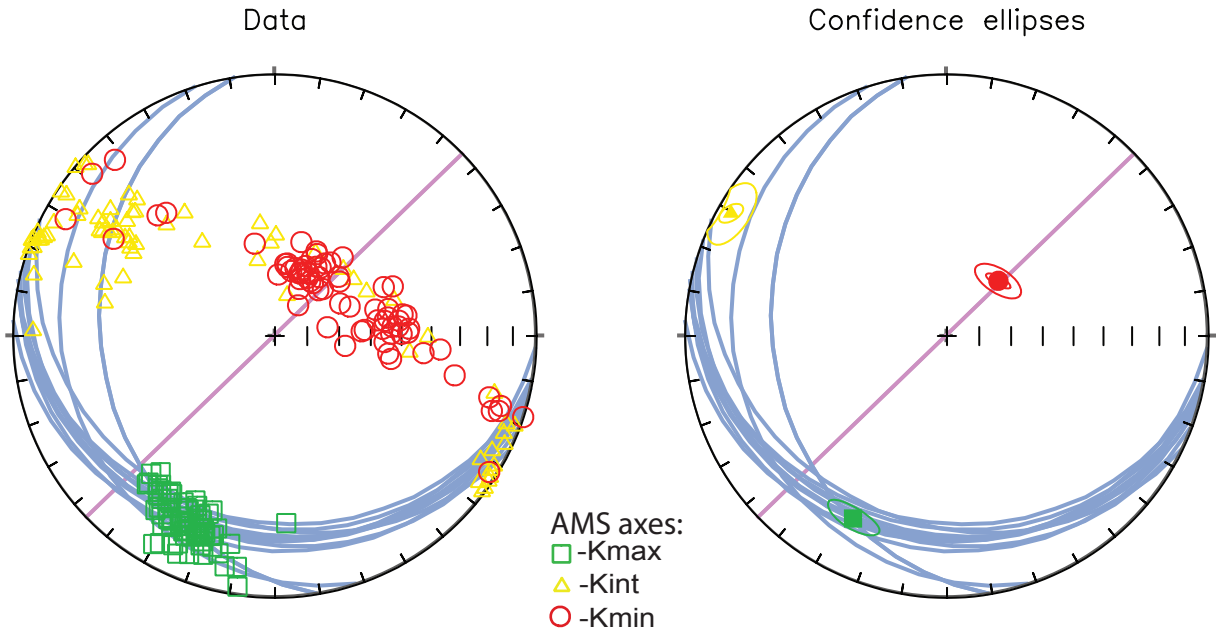

Figure 26: Equal area projections of AMS directional data of individual specimens from the sedimentary rocks of Unit A. An over lay of bedding planes measured in this study (blue great circles) and the average orientation of axial planar cleavage (purple great circle) determined by Byrne (1982) are shown for comparison of results. 95% confidence ellipses are shown for data with significant clustering; smaller ellipses are simple bootstrap and larger ellipses are parametric bootstrap plotted using Tauxe (1998) plotams.exe program.

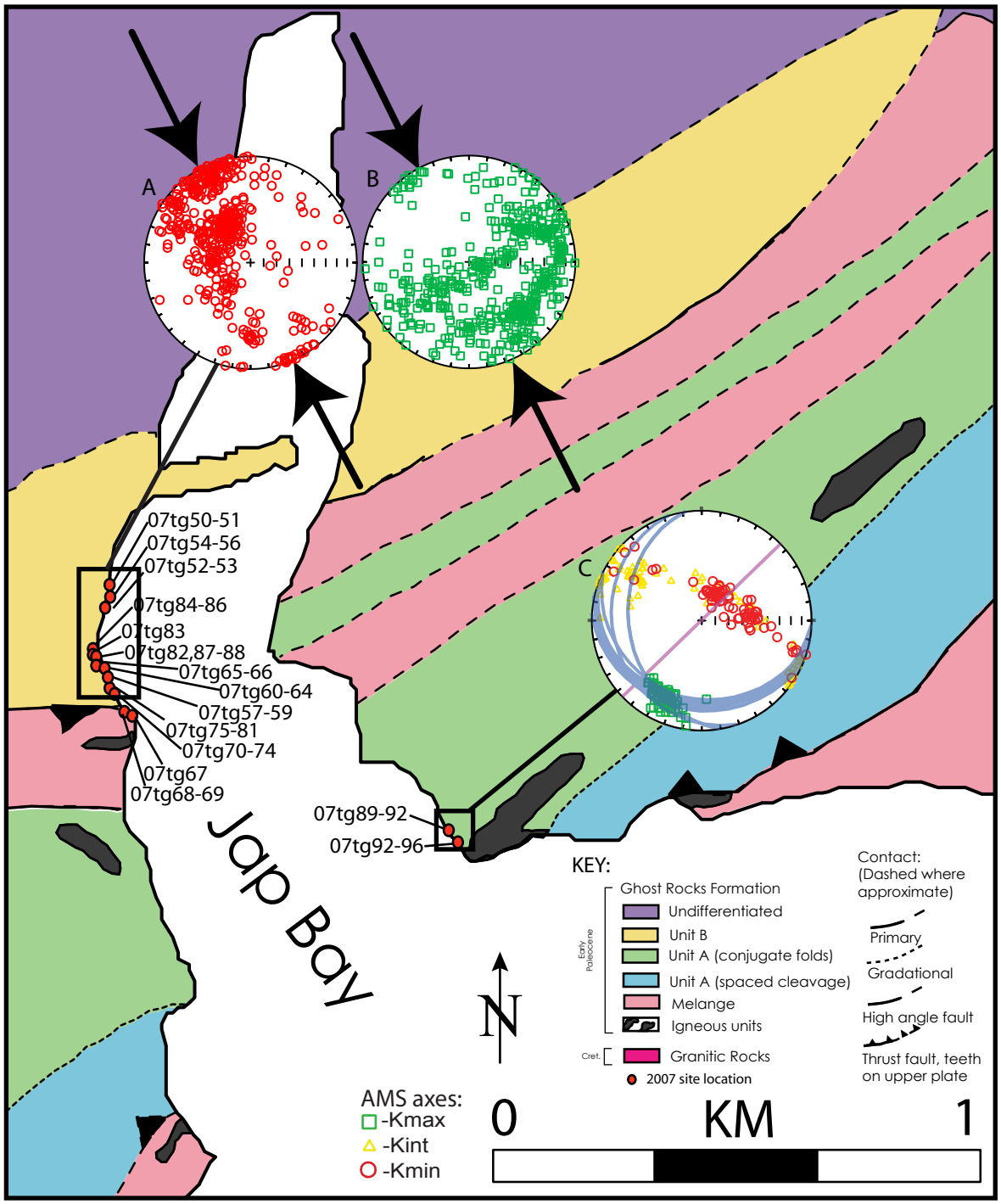

Figure 27: Simplified geologic map of Jap Bay. Showing 2007 site locations of this study and AMS results from sedimentary units in the coherent terranes, Unit A and Unit B. Lower hemisphere equal area projections A. and B. show AMS specimen data of Kmin and Kmax, respectively from Unit B. C. Unit A AMS specimen data from sedimentary units and structural data from Byrne (1982). The large black arrows correspond to the approximate shortening direction of ~334° of D2 determined from fold and fault data by Byrne (1982).

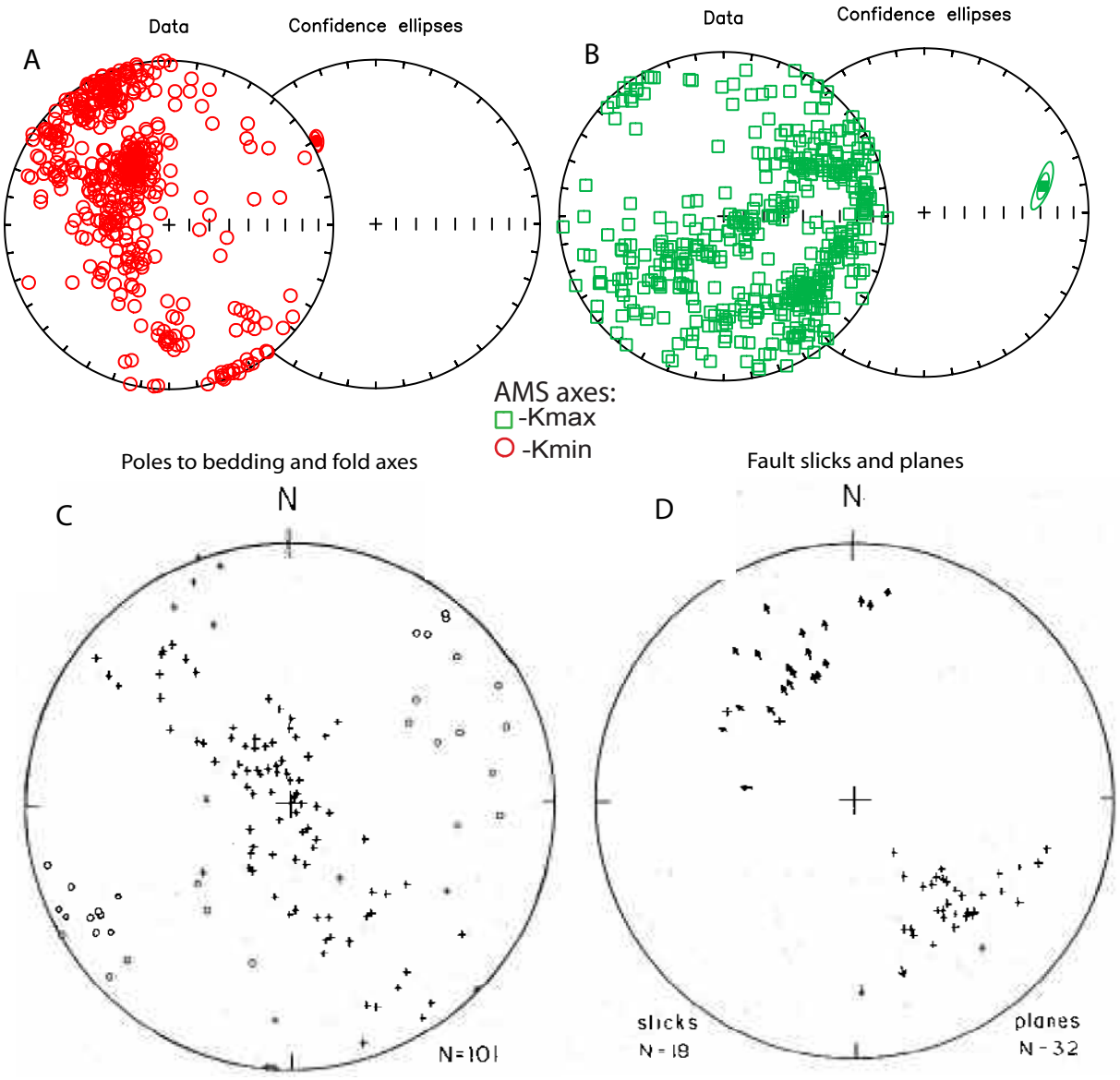

Figure 28: AMS individual specimen data and Structural data from Jap Bay Unit B. A. Individual specimen and mean Kmin directions, B. individual specimen and mean Kmax directions. C. Poles to bedding (crosses) and trend and plunge of fold axes (circles). C. Poles to fault planes (crosses) and slickenlines (arrows) from thrust faults in Jap Bay. (C and D from Byrne 1982). 95% confidence ellipses of AMS data are shown for data with significant clustering; smaller ellipses are simple bootstrap and larger ellipses are parametric bootstrap plotted using Tauxe (1998) plotams.exe program.

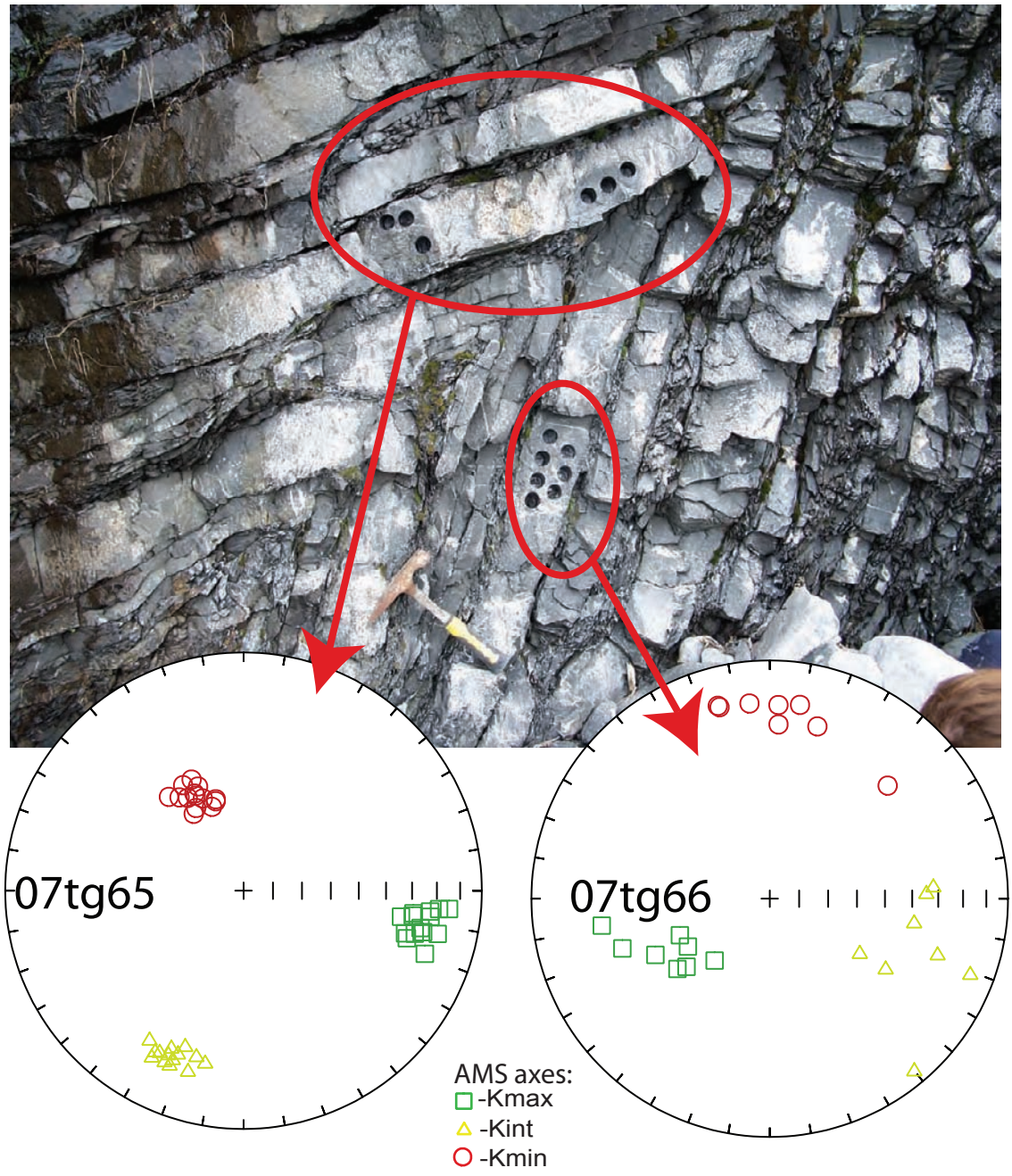

Figure 29: Photo of a tight fold from Unit B of Jap Bay and lower hemisphere equal area projections of AMS results from sites 07tg65 and 07tg66. Note the clear magnetic lineation of both sites. See text for details.

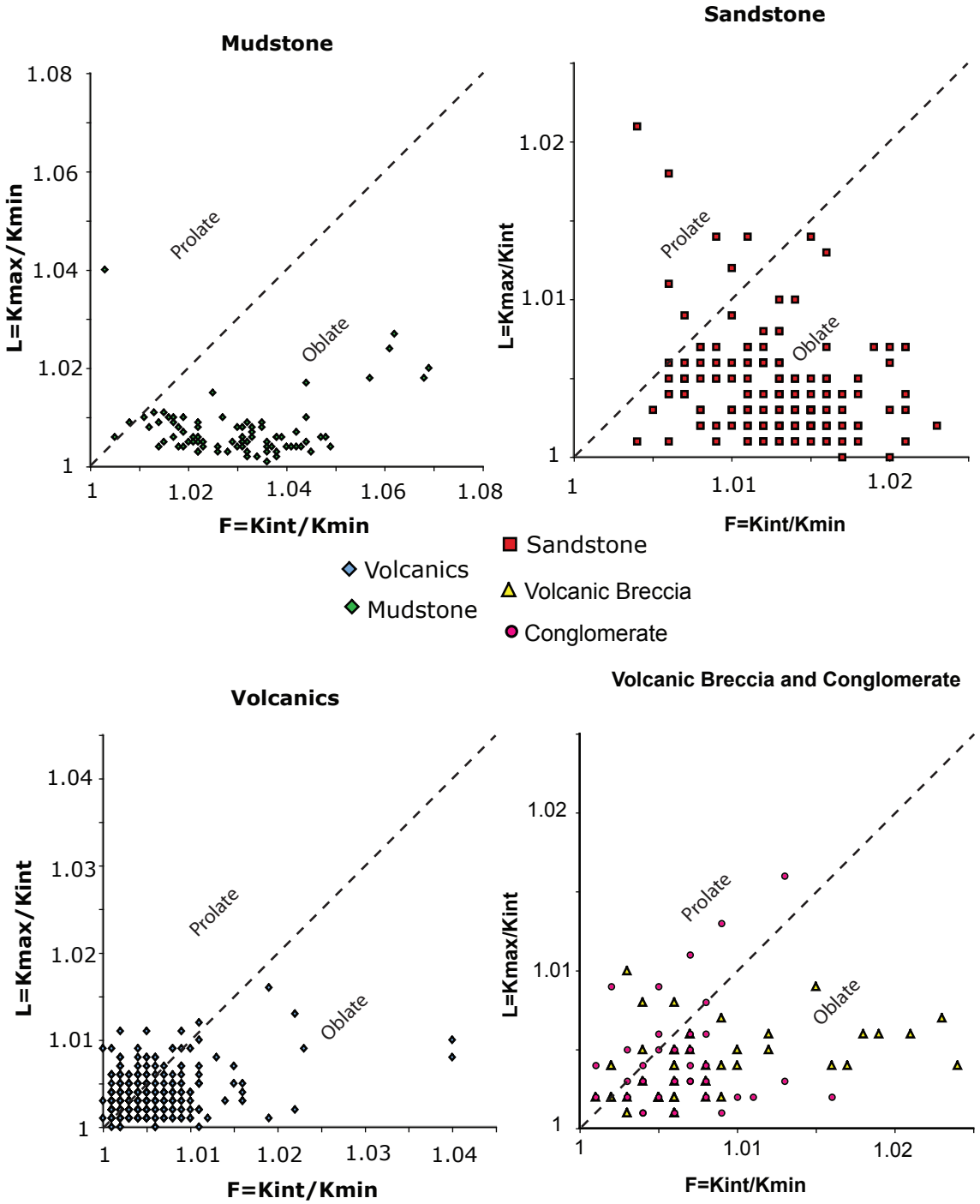

Figure 30: Flinn diagrams of AMS data of individual specimens from Alitak Bay divided by lithology. Note the scale on each Flinn diagram is different.

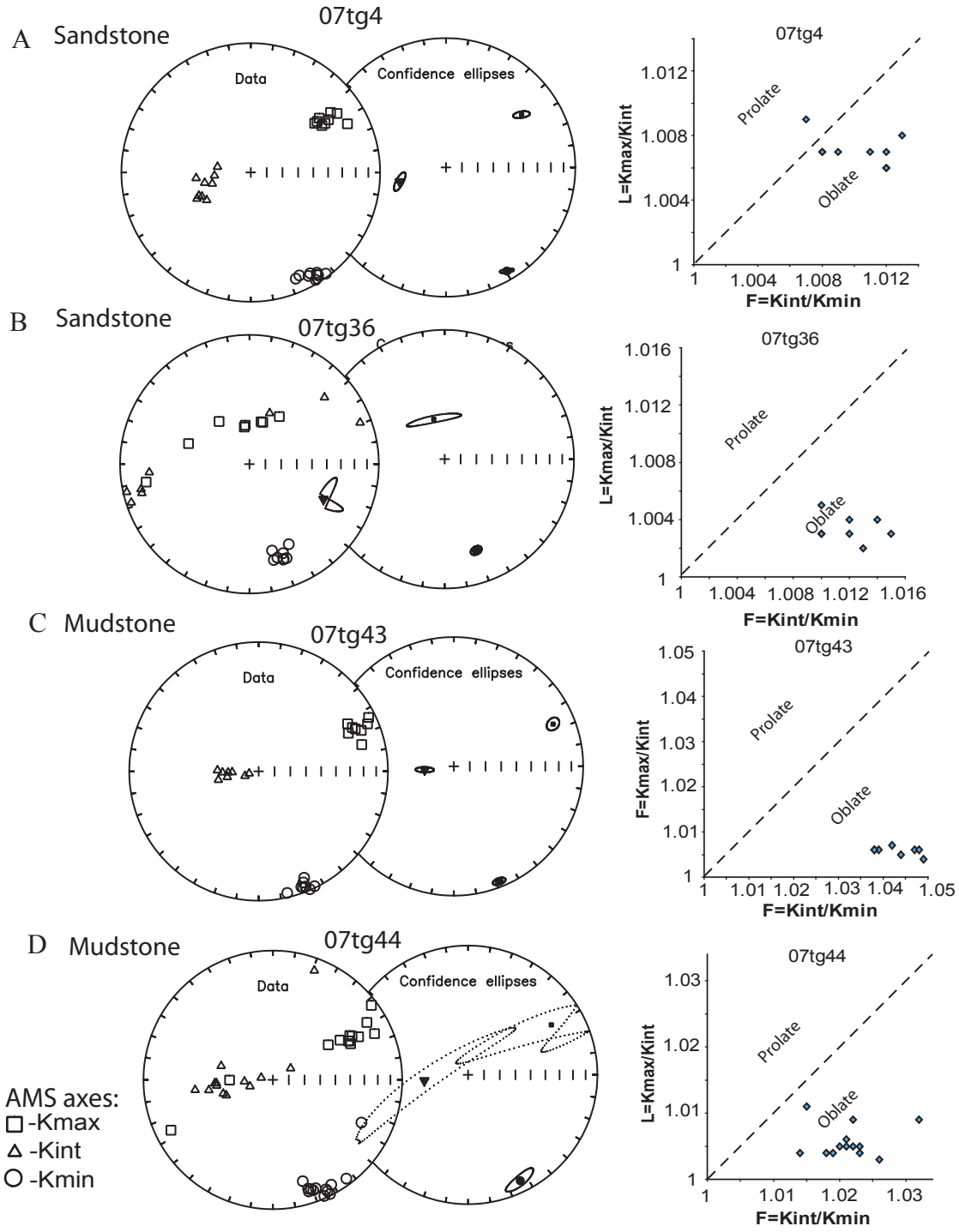

Figure 31: Lower hemisphere equal area projections of AMS data in in-situ coordinates and Flinn diagrams of AMS results from specimens of given sites from the sedimentary units of Alitak Bay. A and B show the end-members of the range in of principal axes orientations for sandstones and C and D show end-member cases of the mudstones. 95% confidence ellipses are shown for data with significant clustering; small ellipses are simple bootstrap. All AMS data was plotted using Tauxe (1998) plotams.exe program. Note the scale on each Flinn diagram is different.

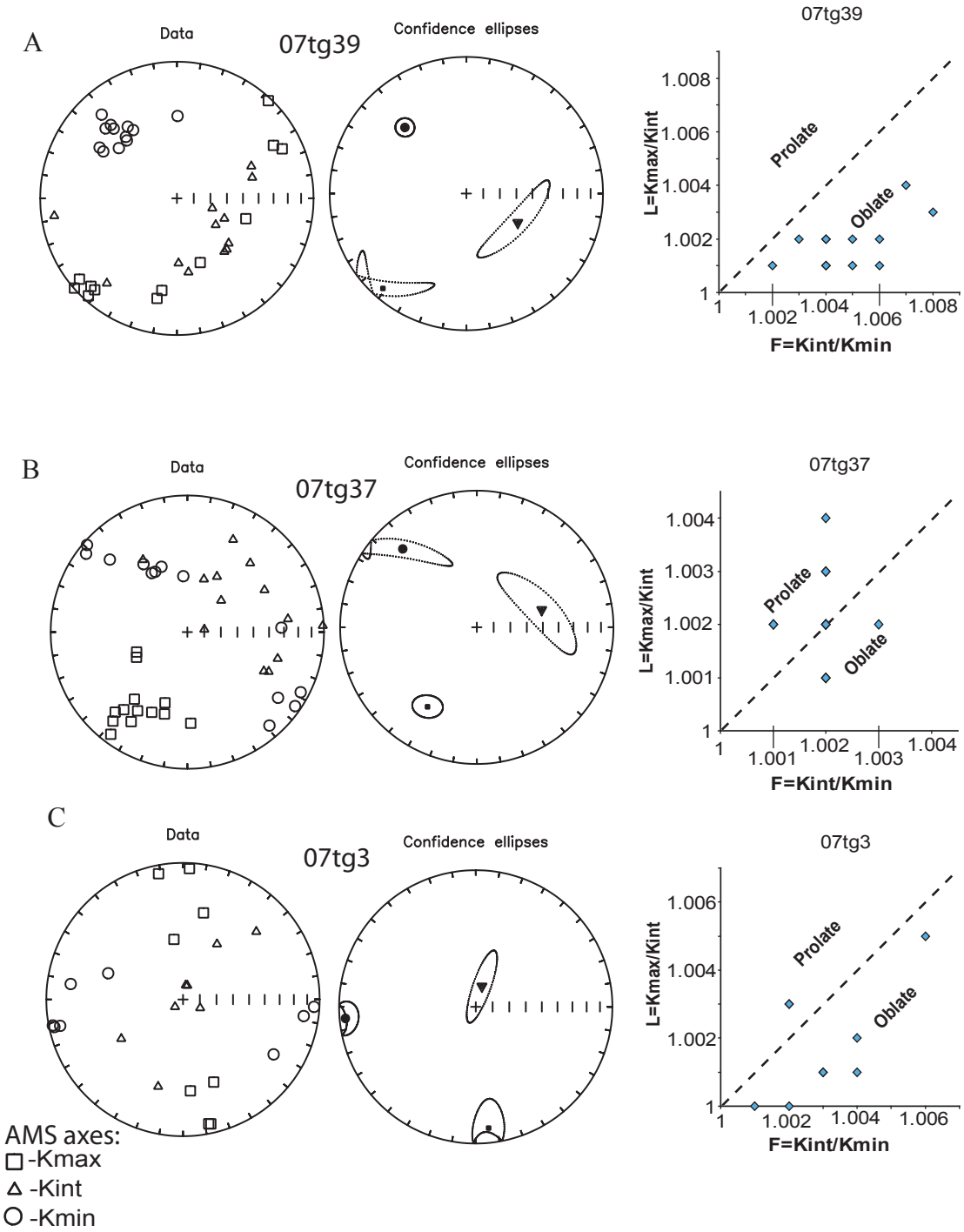

Figure 32: Lower hemisphere equal area plots of AMS ellipsoid principle axes of specimens and site means with 95% confidence ellipses and Flinn diagrams of site specimen results. A,B,&C are typical examples of the three general magnetic fabrics, foliation, lineation, and scatter respectively, observed in the pillow andesites from Alitak Bay. Note the scale on each Flinn diagram is different.

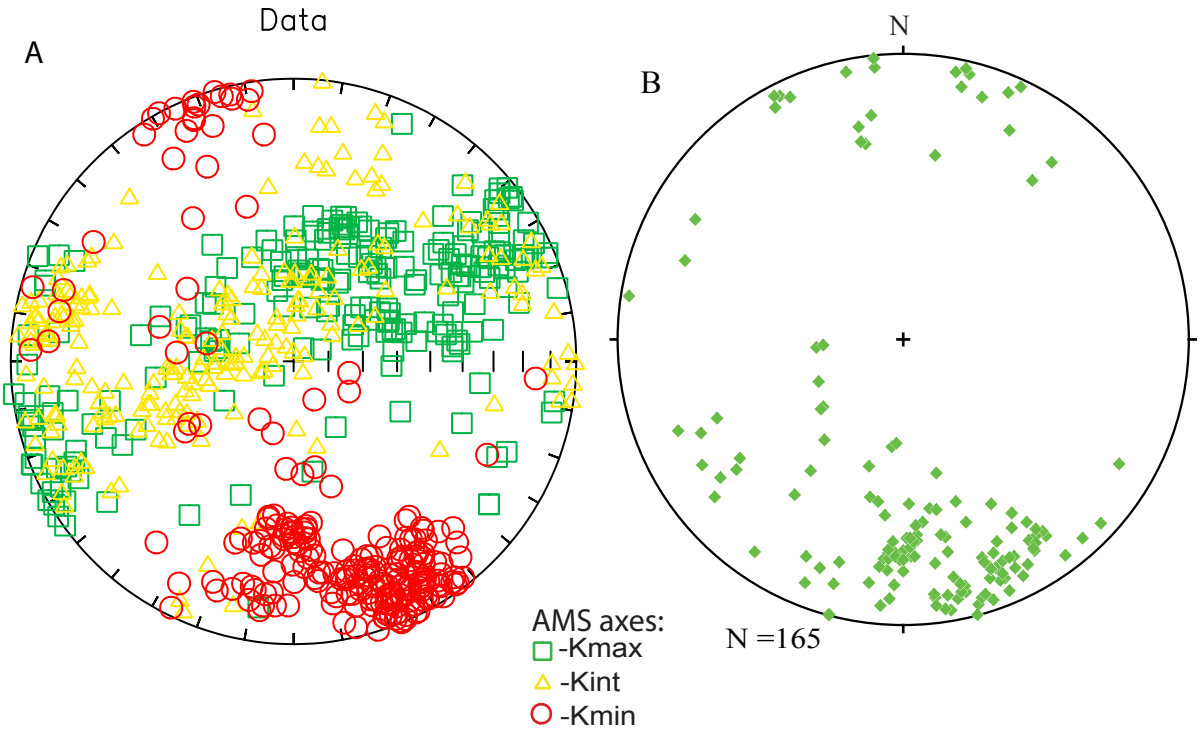

Figure 33: Lower hemisphere equal area plots of A. individual specimen AMS data from the sedimentary rocks from Alitak Bay and B. all of the poles to bedding from this study. Note the similar orientation of Kmin and the bedding poles.

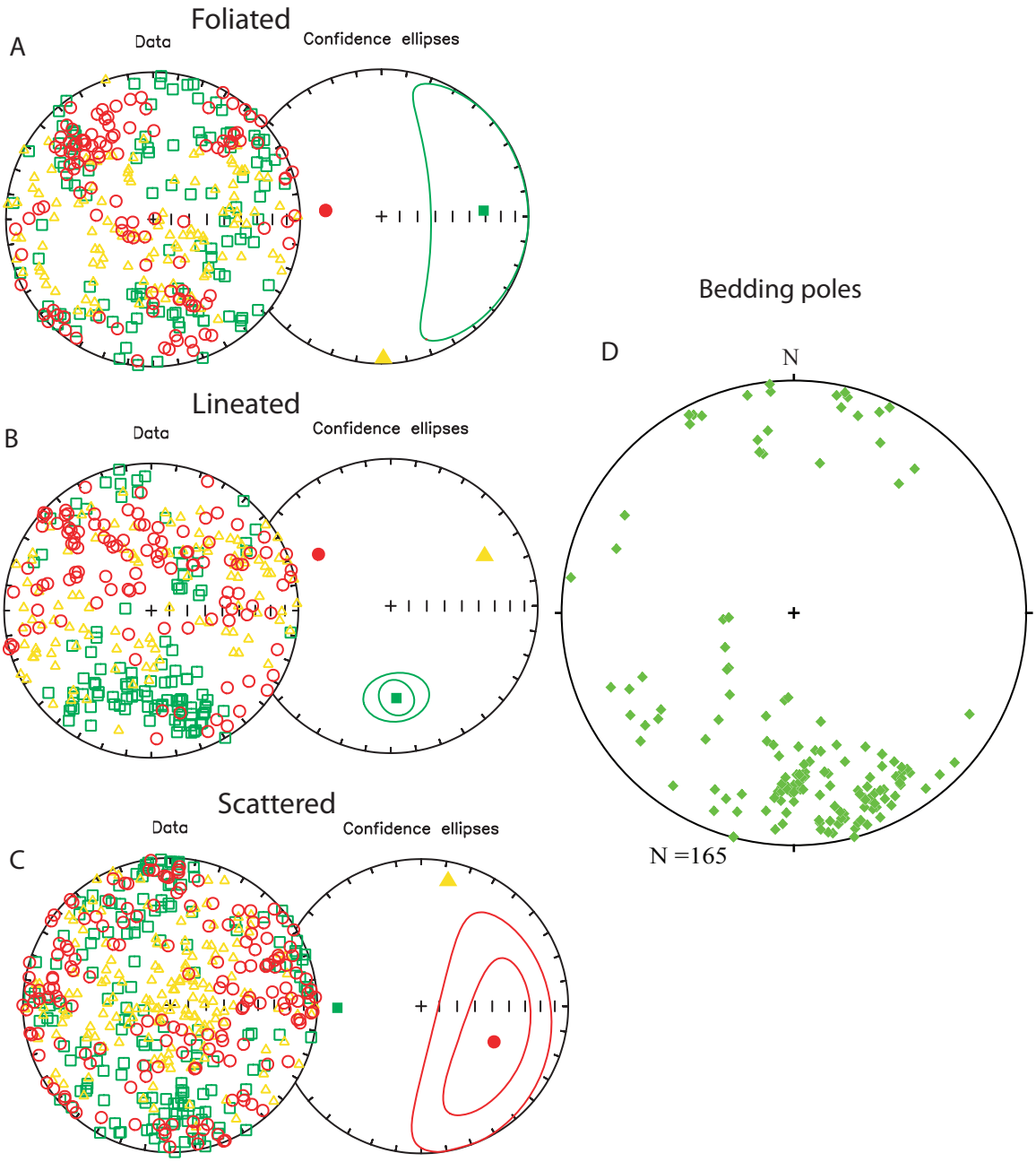

Figure 34: Lower hemisphere equal area projections of AMS directional data of individual specimens from the volcanic units divided qualitatively by type of magnetic fabric (A,B,&C). D. shows the poles to bedding from Alitak Bay. 95% confidence ellipses are shown for data with significant clustering; smaller ellipses are simple bootstrap and larger ellipses are parametric bootstrap plotted using Tauxe (1998) plotams.exe program.

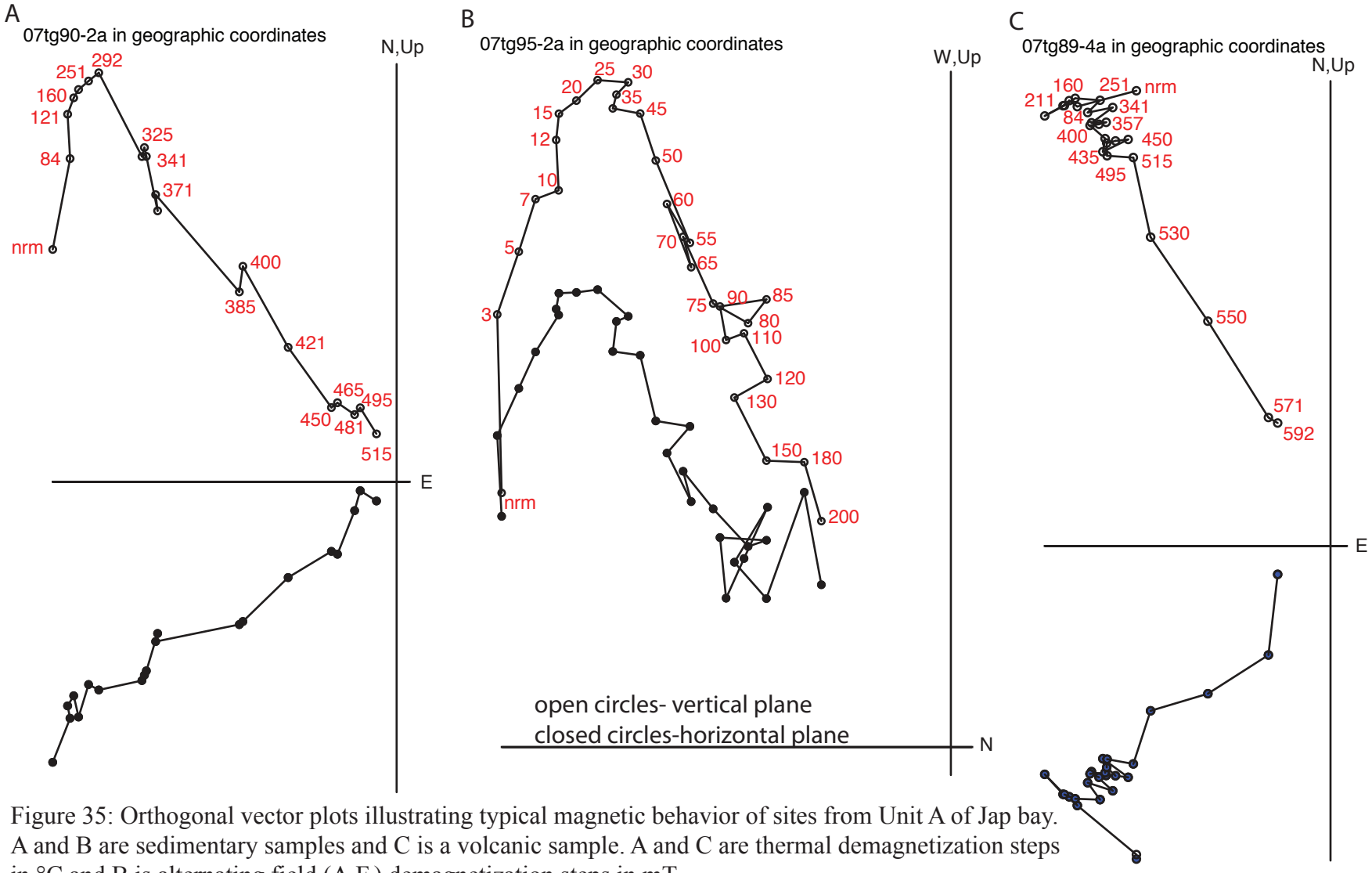

Figure 35: Orthogonal vector plots illustrating typical magnetic behavior of sites from Unit A of Jap bay. A and B are sedimentary samples and C is a volcanic sample. A and C are thermal demagnetization steps in °C and B is alternating field (A.F.) demagnetization steps in mT.

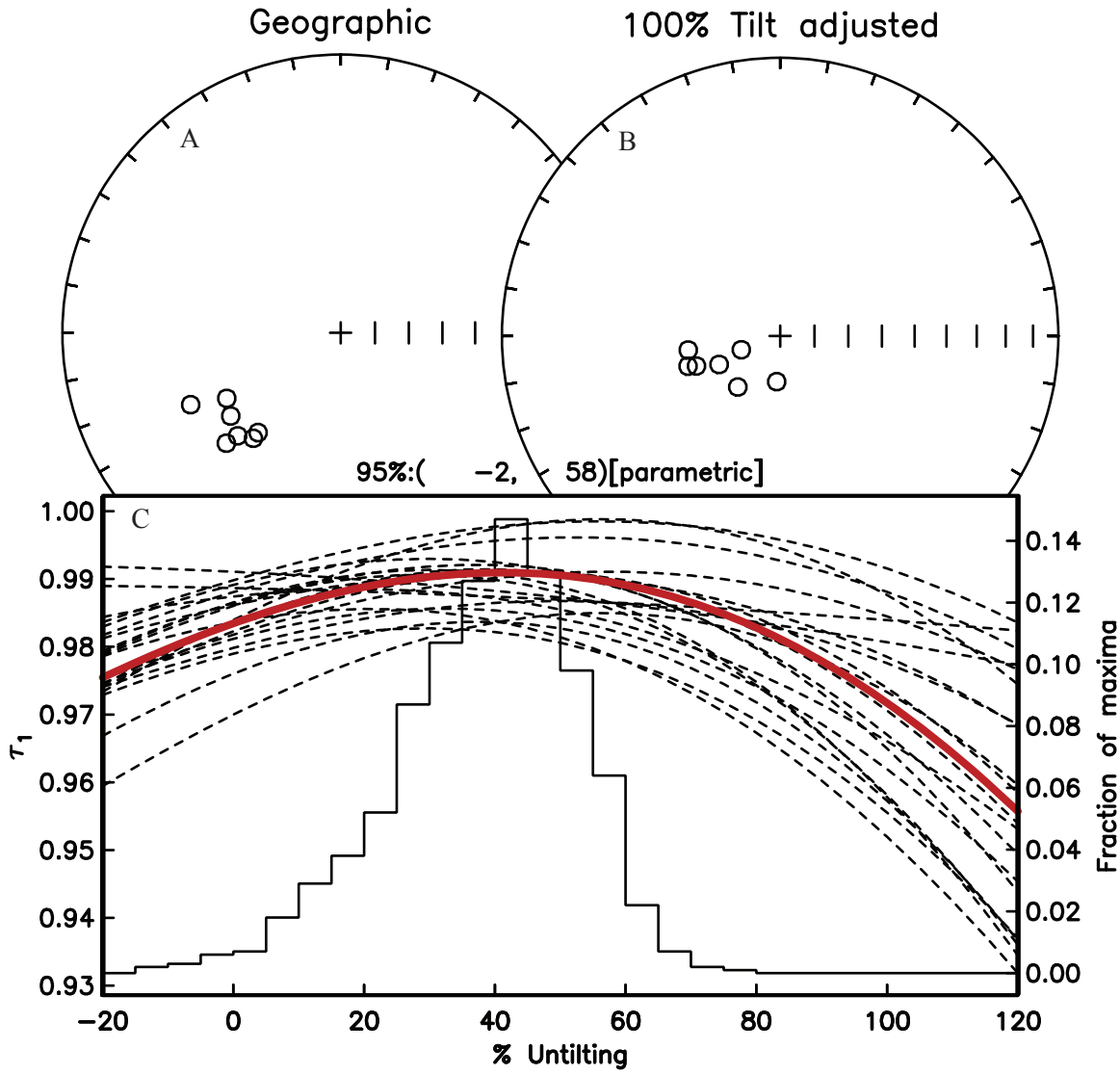

Figure 36: Paleomagnetic results from volcanic and sedimentary rocks from Unit A of Jap Bay. A. Site means in in-situ coordinates, and B. tilt-corrected coordinates. C. Results of Tauxe and Watson, (1994) fold test, showing best clustering of site means at 40% un-tilting, the red line shows the best fit correction and dash lines represent bootstrap trials.

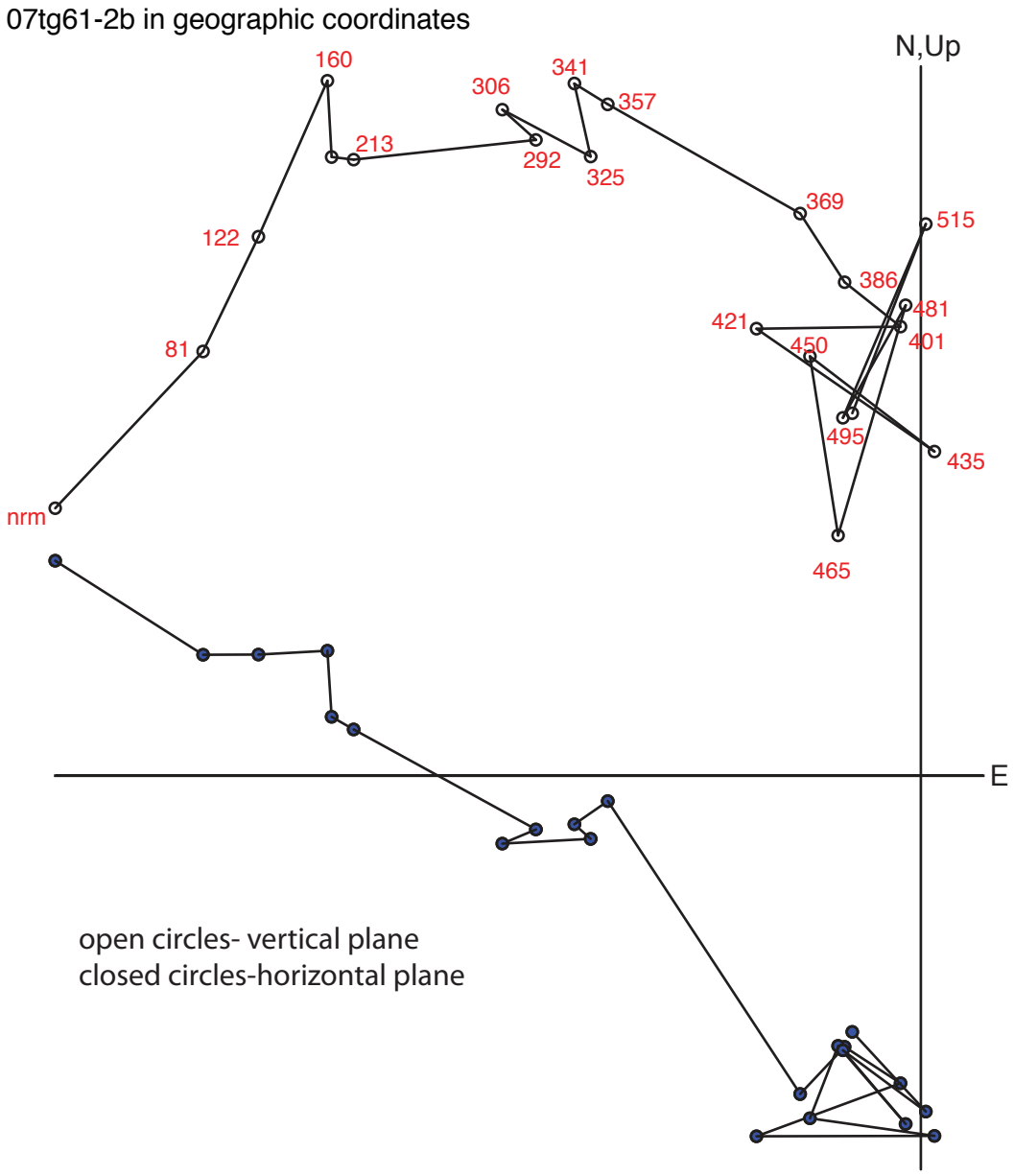

Figure 37: Orthogonal vector plot of stepwise thermal demagnetization in °C illustrating the typical magnetic behavior of most samples from Unit B of Jap Bay, which remains stable to ~280-355°C. Open circles represent inclination and closed circles represent declination.

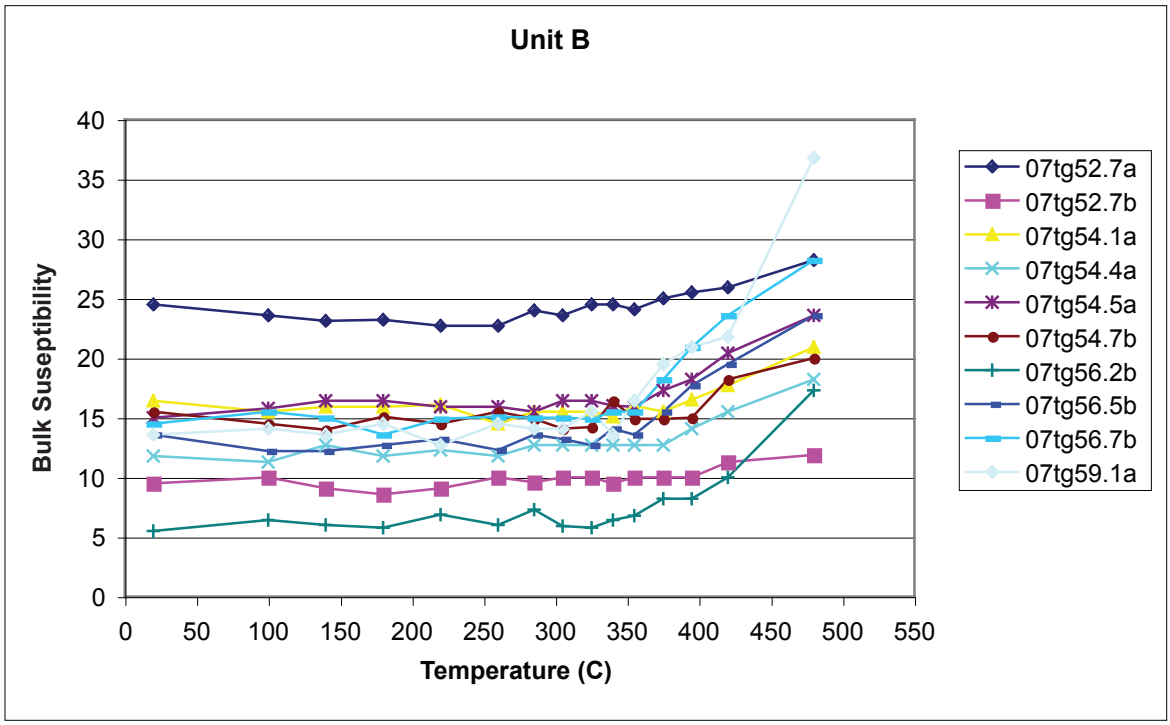

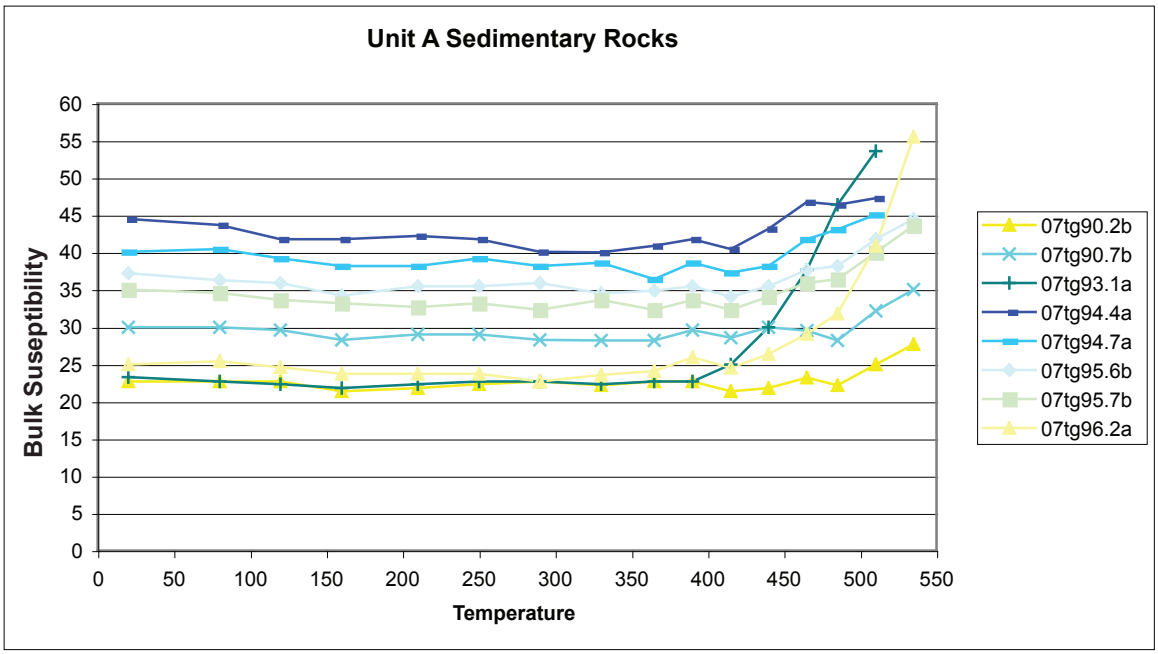

Figure 38: Bulk susceptibility vs. temperature plots of a group of representative specimens from Unit B and Unit A sedimentary rocks. Unit B begins to show changes in bulk susceptibility between ~300-330°C. Unit A show changes beginning at ~>400°C.

A

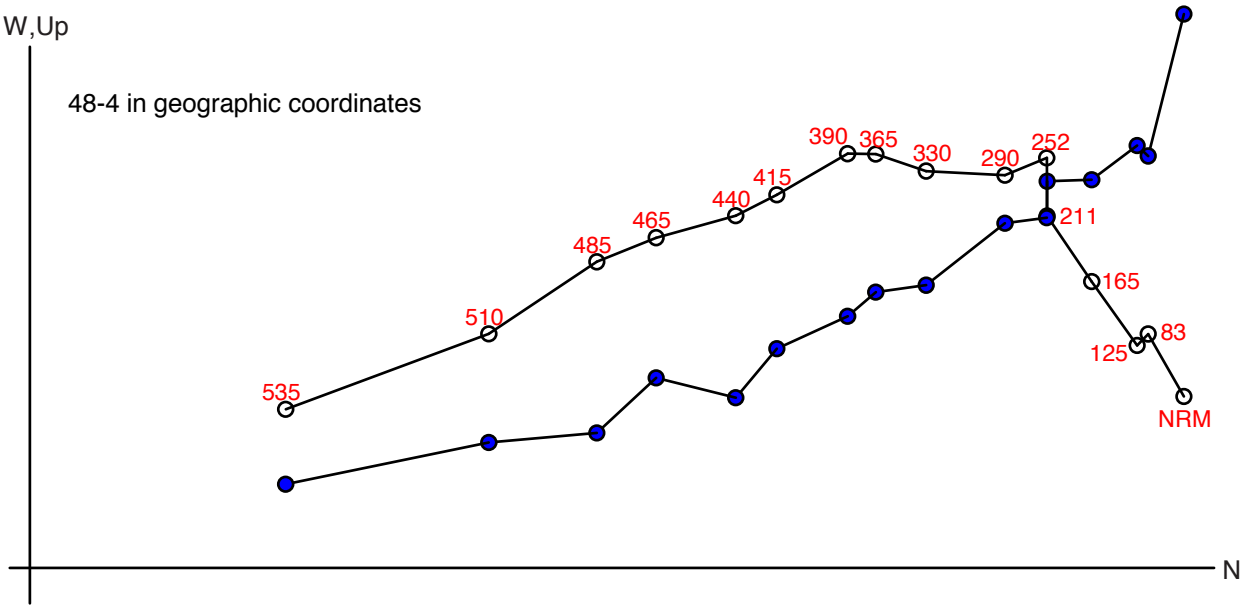

B

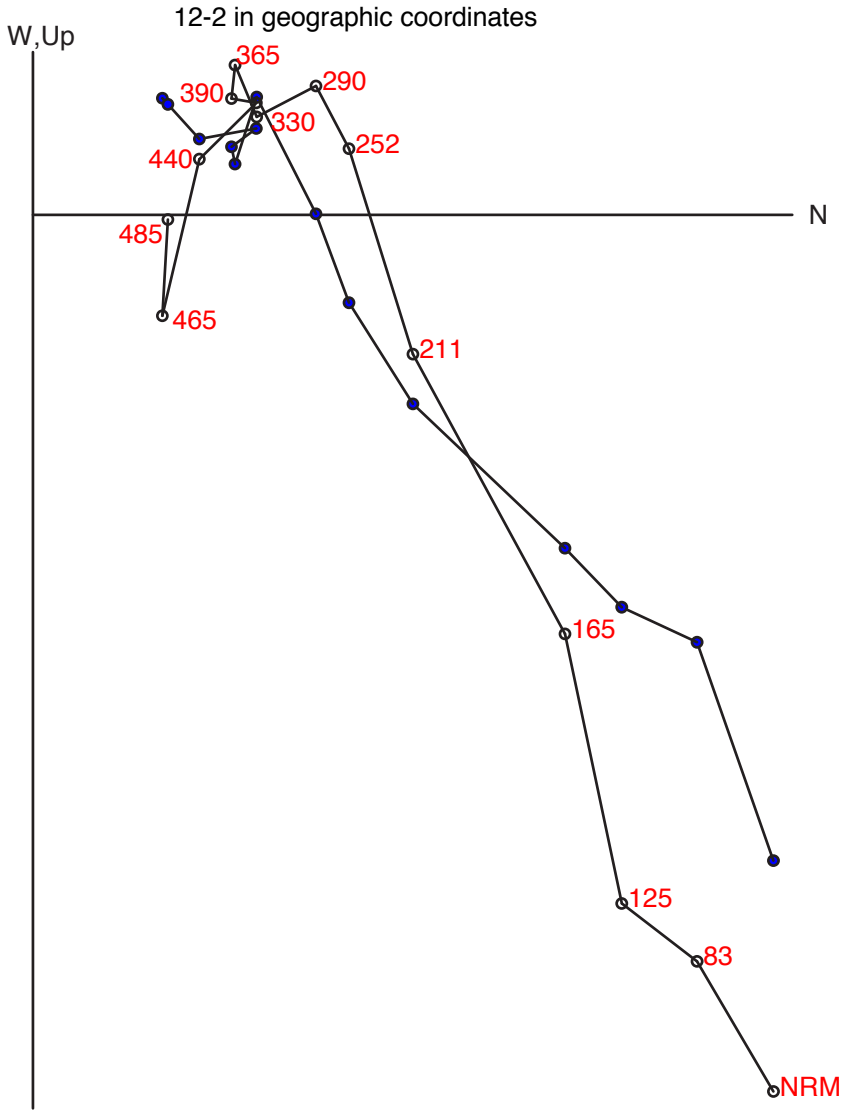

open circles- vertical plane
closed circles-horizontal plane

Figure 39: Orthogonal vector plots of thermal demagnetization in °C of typical examples if the magnetic behaviors of sedimentary rocks from Alitak Bay. A. Stable magnetic vectors that decay to the origin, B. stable magnetic vectors up to ~300 °C.

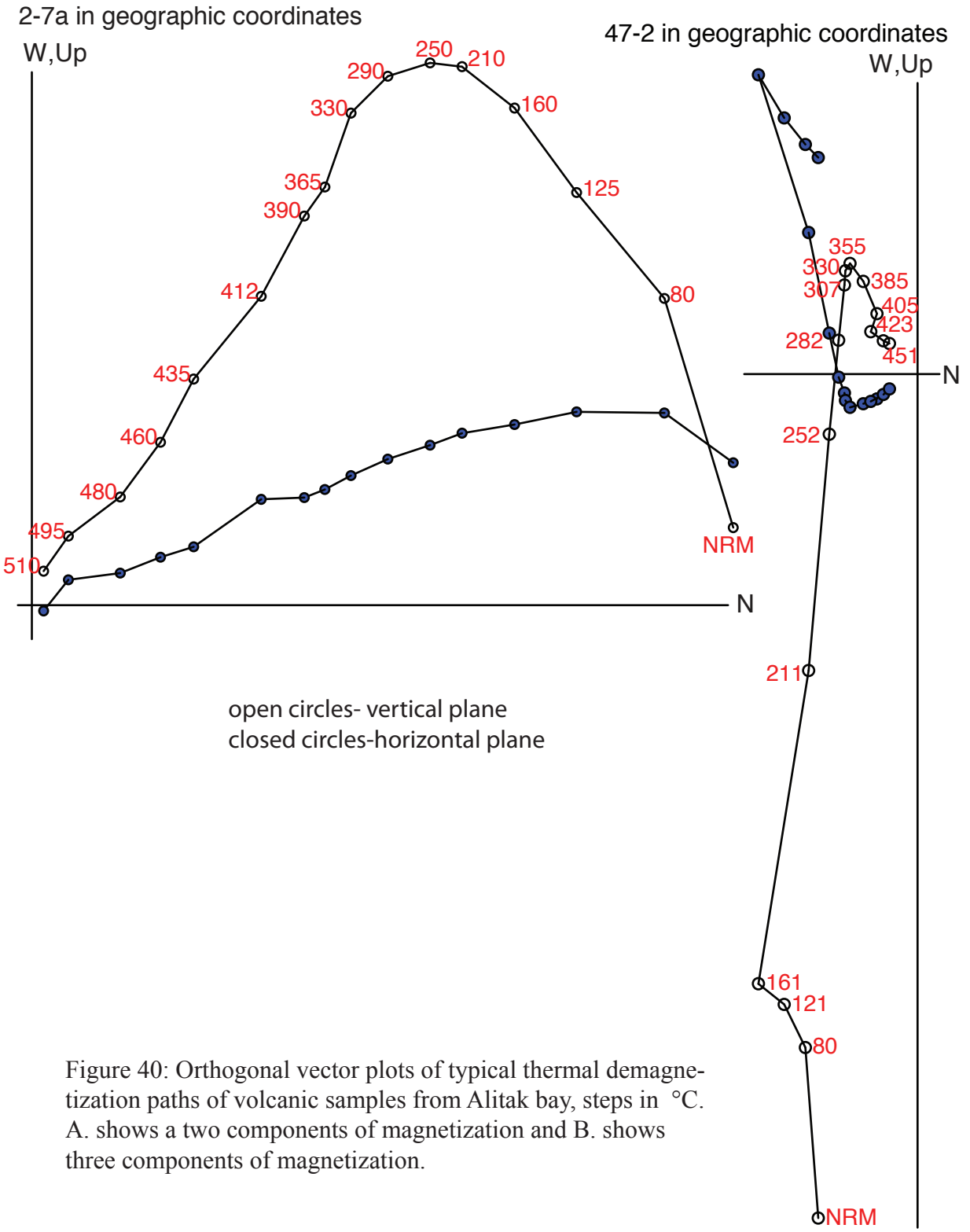

Figure 40: Orthogonal vector plots of typical thermal demagnetization paths of volcanic samples from Alitak bay, steps in °C. A. shows a two components of magnetization and B. shows three components of magnetization.

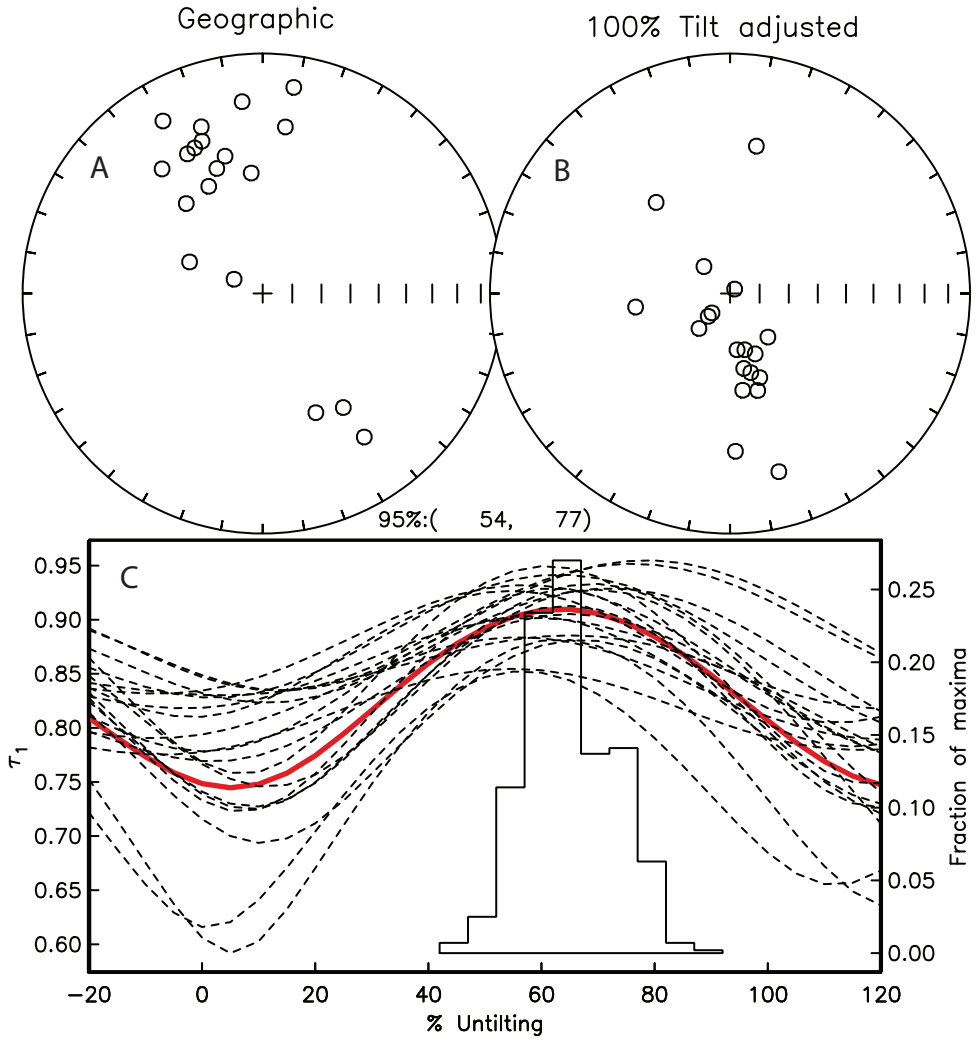

Figure 41: Paleomagnetic directions of the high unblocking temperature components from Alitak Bay of this study. Equal area projections of site mean directions A. in-situ coordinates and B. tilt-corrected coordinates. C. Results of the Tauxe and Watson (1994) fold test, the red line shows the best fit correction and dash lines represent bootstrap trials.

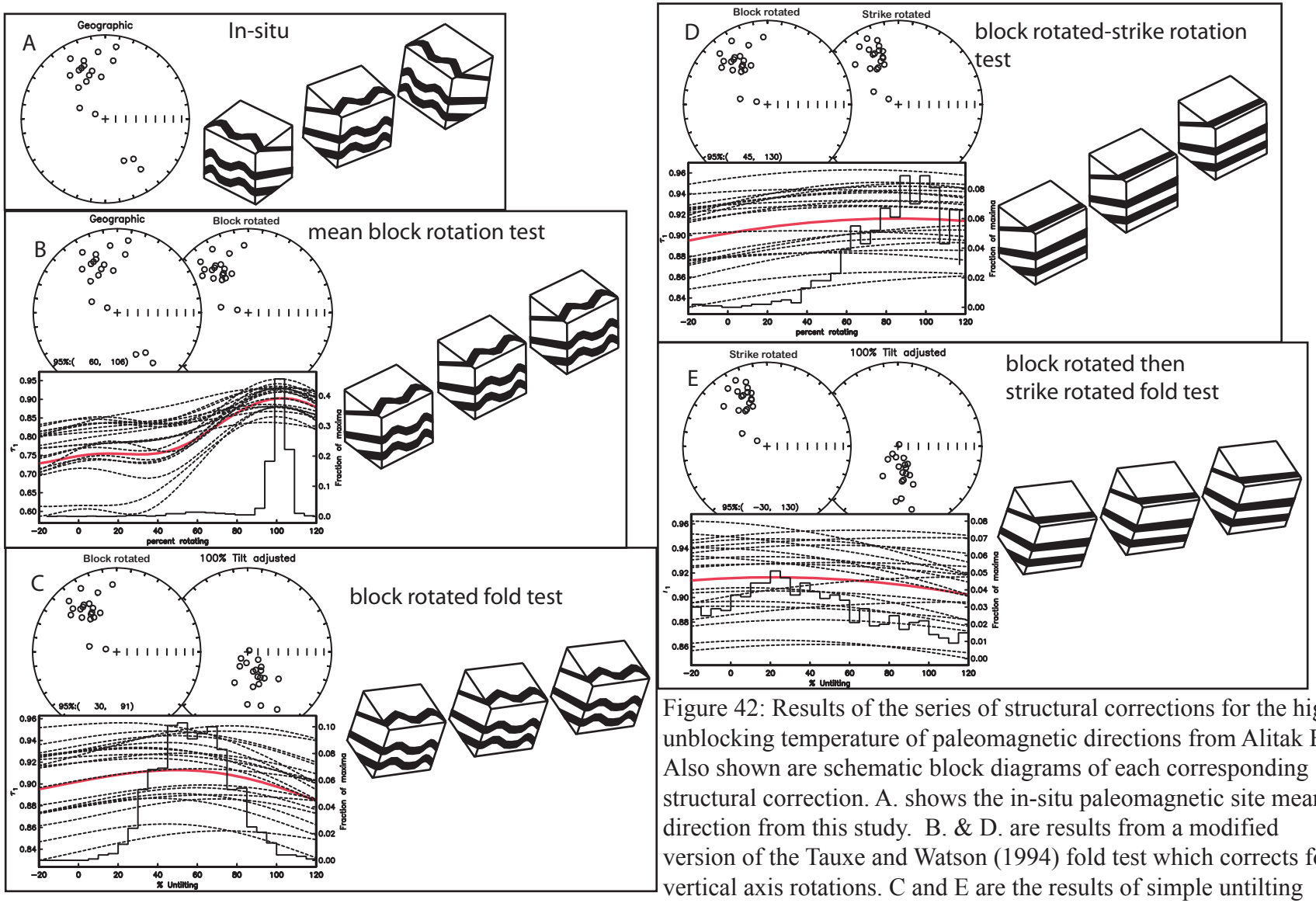

Figure 42: Results of the series of structural corrections for the high unblocking temperature of paleomagnetic directions from Alitak Bay. Also shown are schematic block diagrams of each corresponding structural correction. A. shows the in-situ paleomagnetic site mean direction from this study. B. & D. are results from a modified version of the Tauxe and Watson (1994) fold test which corrects for vertical axis rotations. C and E are the results of simple untilting using the fold test of Tauxe and Watson (1994).

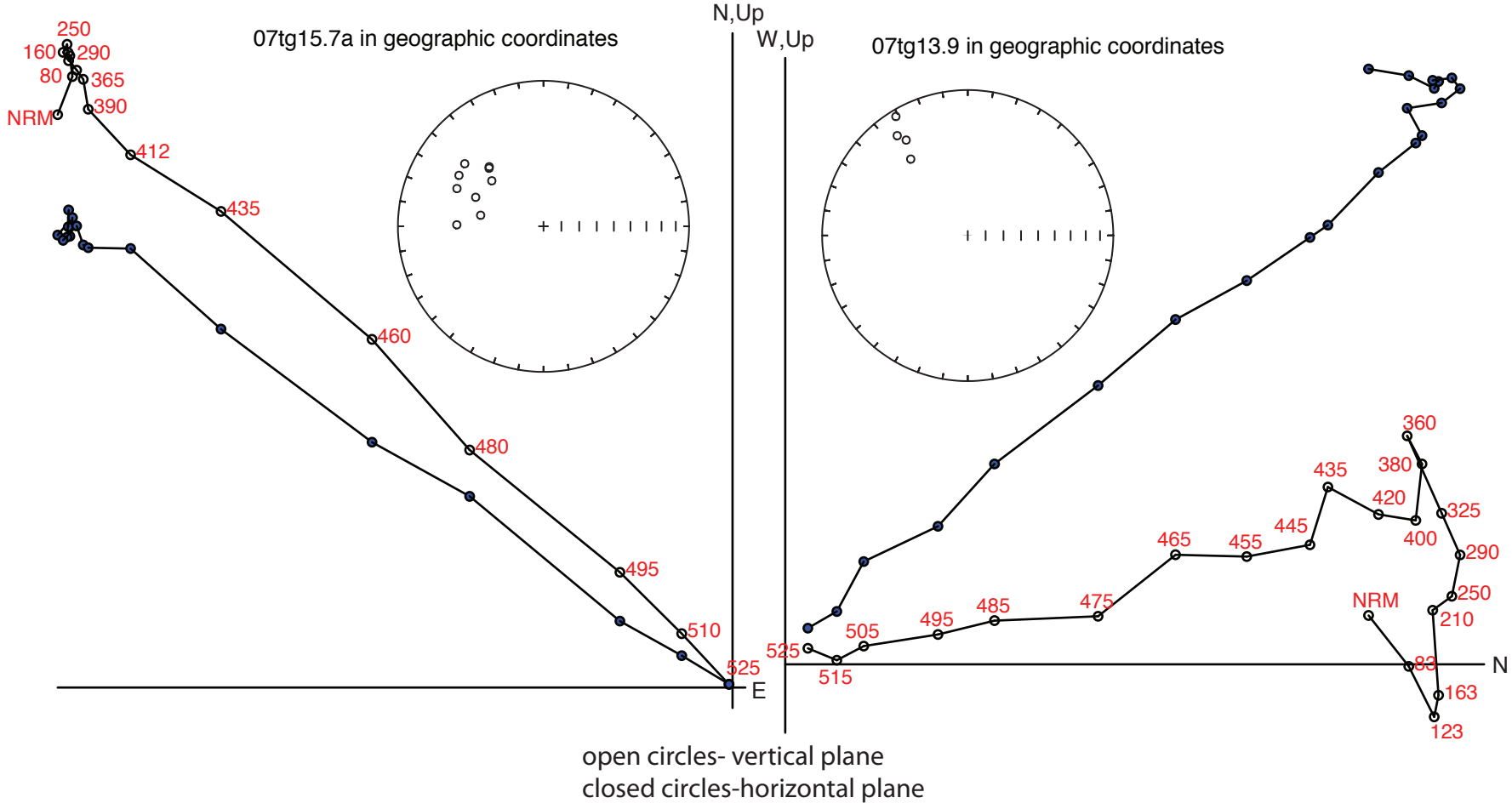

Figure 43: Orthogonal vector plots of thermal demagnetization in °C. Showing the typical magnetic behavior of volcanic clasts of volcanic breccia taken for the conglomerate test. The inset equal area plots show the magnetic directions from all well-defined characteristic components from corresponding sites. The directions are not sufficiently scattered and thus fail the conglomerate test.

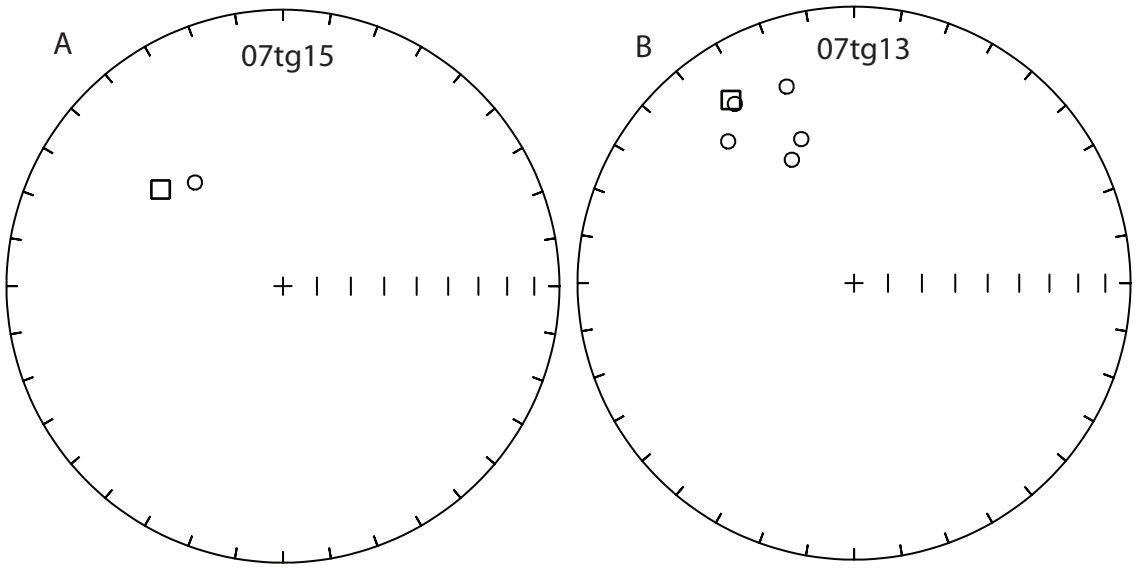

Figure 44: Equal area projections of paleomagnetic site mean directions. The squares represent volcanic breccia sites A. 07tg15 and B. 07tg13 from the pervious figure. The circles are near by pillow lava sites. See text for details.

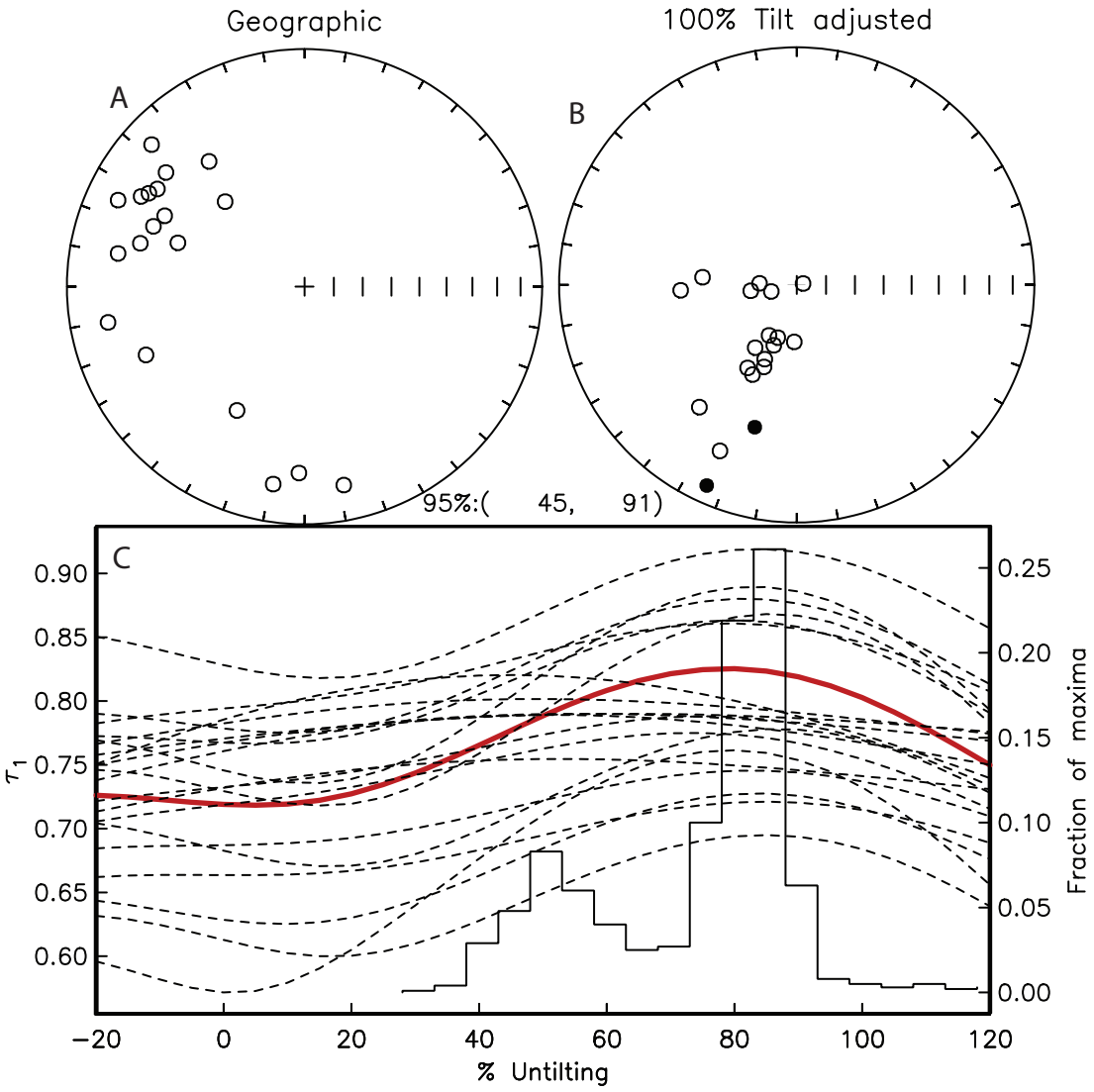

Figure 45: Hypothetical results following the structural interpretation of Plumley et al. (1983). Data was first corrected in two stages; first correcting for the plunge of a hypothetical regional scale fold, and second restoring fold to paleohorizontal. A. Plunge corrected coordinates and B. tilt-corrected coordinates. C. Results of the Tauxe and Watson (1994) fold test, the red line shows the best fit correction and dash lines represent bootstrap trials.

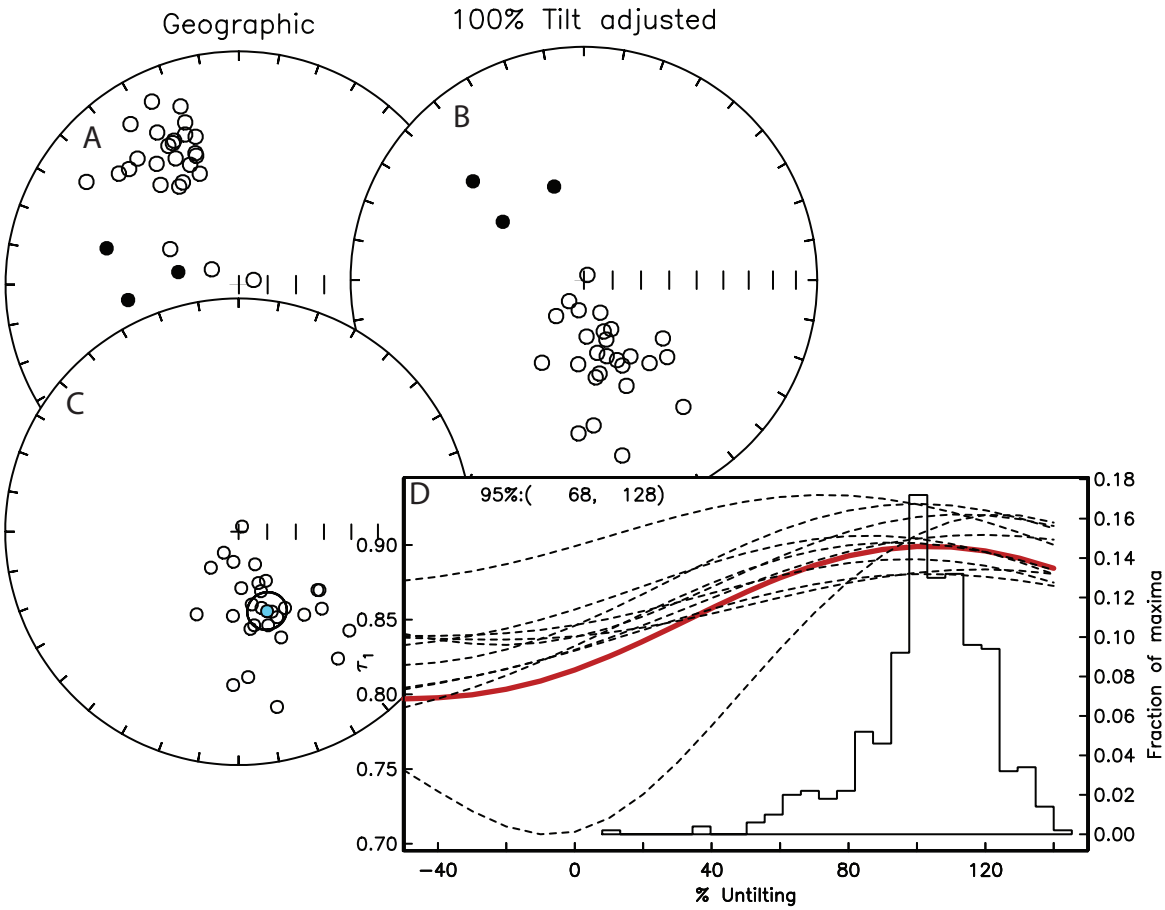

Figure 46: Combined paleomagnetic results of Alitak Bay after corrected from rotation from this study and Kiliuda Bay from the previous study by Plumley et al. (1983) A. Site means in-situ coordinates and B. tilt-corrected coordinates. C. Locality mean direction after all directions are changed to reverse-polarity, in tilt-corrected coordinates. D. Results of the Tauxe and Watson (1994) fold test, the red line shows the best fit correction and dash lines represent trial attempts. Blue circle represents the hypothetical Ghost Rocks Formation mean paleomagnetic direction of D = 162.2, I = -60.3, k =18.1, a95 =6.5. Large open circle show the 95% confidence ellipses of the tilt corrected mean direction.

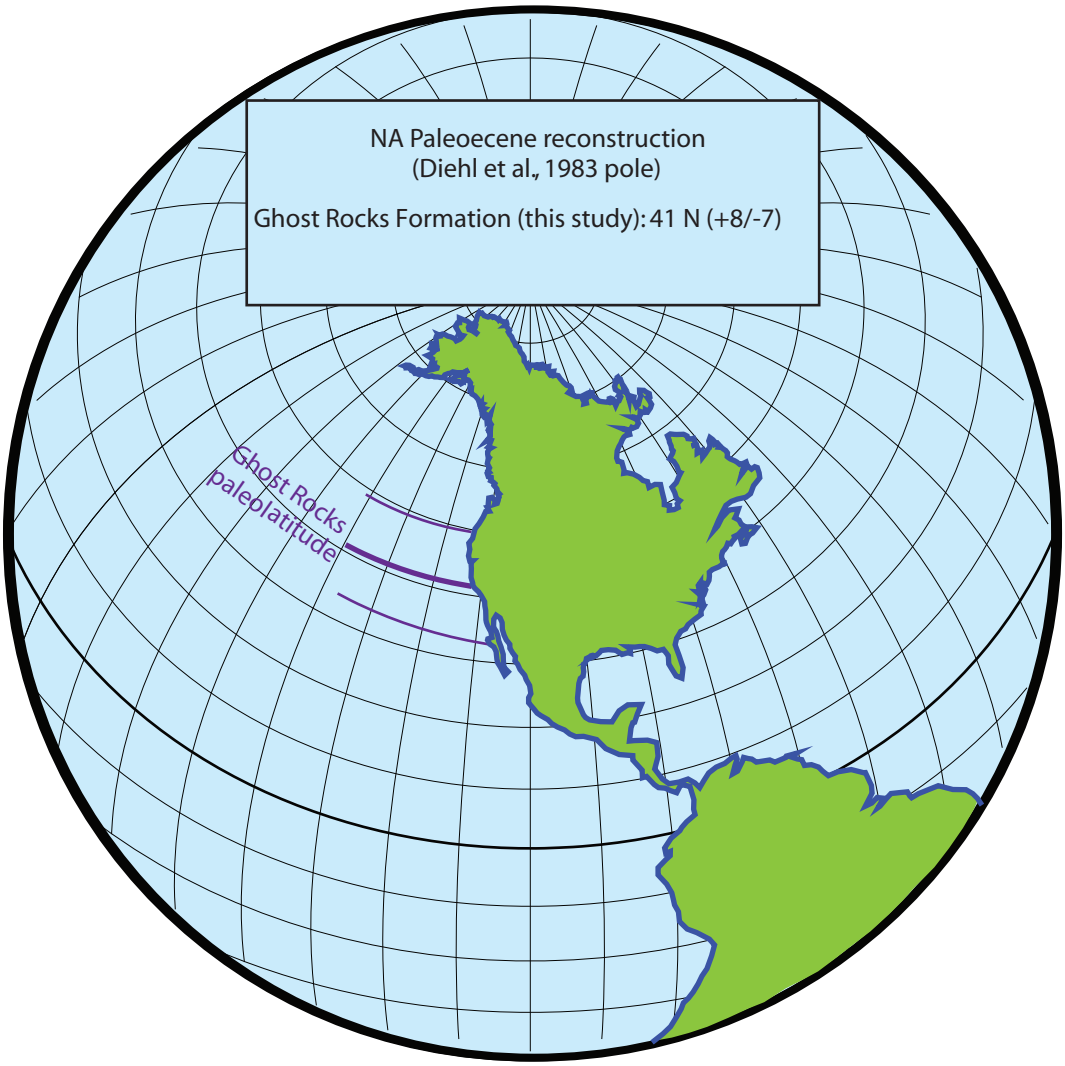

Figure 47: Paleo-geographic reconstruction using the pole of Diehl et al. (1983) of the mean paleomagnetic direction of the Ghost Rocks Formation. The Ghost Rocks mean direction used for this reconstruction was found using the tilt-corrected results of both the "rotation-corrected" paleomagnetic directions from Alitak Bay of this study and the in-situ Kiliuda Bay paleomagnetic directions from Plumley et al. (1983). Note the southerly Paleocene latitude. See text for explanation.

References

Aubourg, C., Rochette, P., Stephan, J., Popoff, M. & Chabert-Pelline, C. 1999, The magnetic fabric of weakly deformed Late Jurassic shales from the southern subalpines chains (French Alps); evidence for SW-directed tectonic transport direction; Applications of magnetic anisotropies to fabric studies of rocks and sediments, *Tectonophysics,* vol. 307, no. 1-2, pp. 15-31.

Babcock, R.S., Burmester, R.F., Engebretson, D.C., Warnock, A. & Clark, K.P. 1992, A rifted margin origin for the Crescent basalts and related rocks in the northern Coast Range volcanic province, Washington and British Columbia, *Journal of Geophysical Research,* vol. 97, no. B5, pp. 6799-6821.

Bol, A.J., Coe, R.S., Gromme, C.S. & Hillhouse, J.W. 1992, Paleomagnetism of the Resurrection Peninsula, Alaska; implications for the tectonics of southern Alaska and the Kula-Farallon Ridge, *Journal of Geophysical Research,* vol. 97, no. B12, pp. 17-17,232.

Borradaile, G.J. 1987, Anisotropy of magnetic susceptibility; rock composition versus strain, *Tectonophysics,* vol. 138, no. 2-4, pp. 327-329.

Borradaile, G.J. & Henry, B. 1997, Tectonic applications of magnetic susceptibility and its anisotropy, *Earth-Science Reviews,* vol. 42, no. 1-2, pp. 49-93.

Borradaile, G.J. 1988, Magnetic susceptibility, petrofabrics and strain, *Tectonophysics,* vol. 156, no. 1-2, pp. 1-20.

Bowman, J.R., Sisson, V.B., Valley, J.W. & Pavlis, T.L. 2003, Oxygen isotope constraints on fluid infiltration associated with high-temperature-low-pressure metamorphism (Chugach metamorphic complex) within the Eocene Southern Alaska forearc; Geology of a transpressional orogen developed during ridge-trench interaction along the North Pacific margin, *Special Paper - Geological Society of America,* vol. 371, pp. 237-252.

Bradley, D.C., Kusky, T.M., Haeussler, P.J., Goldfarb, R.J., Miller, M.L., Dumoulin, J.A., Nelson, S.W. & Karl, S.M. 2003, Geologic signature of early Tertiary ridge subduction in Alaska; Geology of a transpressional orogen developed during ridge-trench interaction along the North Pacific margin, *Special Paper - Geological Society of America,* vol. 371, pp. 19-49.

Breitsprecher, K., Thorkelson, D.J., Groome, W.G. & Dostal, J. 2003, Geochemical confirmation of the Kula-Farallon slab window beneath the Pacific Northwest in Eocene time, *Geology (Boulder)*, vol. 31, no. 4, pp. 351-354.

Bunge, H. & Grand, S.P. 2000, Mesozoic plate-motion history below the Northeast Pacific Ocean from seismic images of the subducted Farallon slab, *Nature (London)*, vol. 405, no. 6784, pp. 337-340.

Byrne, T. 1984, Early deformation in melange terranes of the Ghost Rocks Formation, Kodiak Islands, Alaska; Melanges; their nature, origin and significance, *Special Paper - Geological Society of America*, vol. 198, pp. 21-51.

Byrne, T. 1982, Structural evolution of coherent terranes in the Ghost Rocks Formation, Kodiak Island, Alaska; Trench-Forearc geology; sedimentation and tectonics on modern and ancient active plate margins, conference, *Special Publication - Geological Society of London*, vol. 10, pp. 229-242.

Byrne, T. & Fisher, D. 1987, Episodic growth of the Kodiak convergent margin, *Nature (London)*, vol. 325, no. 6102, pp. 338-341.

Cifelli, F., Rossetti, F., Mattei, M., Hirt, A.M., Funiciello, R. & Tortorici, L. 2004, An AMS, structural and paleomagnetic study of Quaternary deformation in eastern Sicily, *Journal of Structural Geology*, vol. 26, no. 1, pp. 29-46.

Cowan, D.S. 2003, Revisiting the Baranof-Leech River hypothesis for early Tertiary coastwise transport of the Chugach-Prince William Terrane, *Earth and Planetary Science Letters*, vol. 213, no. 3-4, pp. 463-475.

Dickinson, W.R. & Snyder, W.S. 1979, Geometry of subducted slabs related to San Andreas transform, *Journal of Geology*, vol. 87, no. 6, pp. 609-627.

Dickinson, W.R. 2004, Evolution of the North American Cordillera, *Annual Review of Earth and Planetary Sciences*, vol. 32, pp. 13-45.

Diehl, J.F., Beck, M.E.,Jr, Beske-Diehl, S., Jacobson, D. & Hearn, B.C.,Jr 1983, Paleomagnetism of the Late Cretaceous-early Tertiary north-central Montana alkalic province, *Journal of Geophysical Research*, vol. 88, no. B12, pp. 10593-10609.

Ellwood, B.B. 1978, Flow and emplacement direction determined for selected basaltic bodies using magnetic susceptibility anisotropy measurements, *Earth and Planetary Science Letters,* vol. 41, no. 3, pp. 254-264.

Engebretson, D.C., Cox, A. & Gordon, R.G. 1985, Relative motions between oceanic and continental plates in the Pacific Basin, *Special Paper - Geological Society of America,* vol. 206, pp. 59.

Farris, D.W., Haeussler, P., Friedman, R., Paterson, S.R., Saltus, R.W. & Ayuso, R. 2006, Emplacement of the Kodiak Batholith and slab-window migration, *Geological Society of America Bulletin,* vol. 118, no. 11-12, pp. 1360-1376.

Fisher, D. & Byrne, T. 1987, Structural evolution of underthrusted sediments, Kodiak Islands, Alaska, *Tectonics,* vol. 6, no. 6, pp. 775-793.

Fisher, R. A. 1953, Dispersion on a sphere, *Proceedings of the Royal Society London, Series A,* vol. 217, pp. 295-305.

Groome, W.G., Thorkelson, D.J., Friedman, R.M., Mortensen, J.K., Massey, N.W.D., Marshall, D.D. & Layer, P.W. 2003, Magmatic and tectonic history of the Leech River Complex, Vancouver Island, British Columbia; evidence for ridge-trench intersection and accretion of the Crescent Terrane; Geology of a transpressional orogen developed during ridge-trench interaction along the North Pacific margin, *Special Paper - Geological Society of America,* vol. 371, pp. 327-353.

Haeussler, P.J., Bradley, D.C., Wells, R.E. & Miller, M.L. 2003, Life and death of the Resurrection Plate; evidence for its existence and subduction in the northeastern Pacific in Paleocene-Eocene time, *Geological Society of America Bulletin,* vol. 115, no. 7, pp. 867-880.

Helwig, J. & Emmet, P. 1981, Structure of the early Tertiary Orca Group in Prince William Sound and some implications for the plate tectonic history of southern Alaska, *Journal of the Alaska Geological Society,* vol. 1, pp. 12-35.

Hill, M., Morris, J. & Whelan, J. 1981, Hybrid granodiorites intruding the accretionary prism, Kodiak, Shumagin, and Sanak islands, southwest Alaska; Granites and rhyolites, *Journal of Geophysical Research,* vol. 86, no. B11, pp. 10569-10590.

Housen, B.A., Richter, C. & van der Pluijm,Ben A. 1993, Composite magnetic anisotropy fabrics; experiments, numerical models, and implications for the quantification of rock fabrics, *Tectonophysics*, vol. 220, no. 1-4, pp. 1-12.

Housen, B.A. & van der Pluijm,Ben A. 1991, Slaty cleavage development and magnetic anisotropy fabrics, *Journal of Geophysical Research*, vol. 96, no. B6, pp. 9937-9946.

Hrouda, F. 1982, Magnetic anisotropy of rocks and its application in geology and geophysics, *Geophysical Surveys*, vol. 5, no. 1, pp. 37-82.

Kusky, T.M., Bradley, D.C., Donely, D.T., Rowley, D. & Haeussler, P.J. 2003, Controls on intrusion of near-trench magmas of the Sanak-Baranof Belt, Alaska, during Paleogene ridge subduction, and consequences for forearc evolution; Geology of a transpressional orogen developed during ridge-trench interaction along the North Pacific margin, *Special Paper - Geological Society of America*, vol. 371, pp. 269-292.

Jelinek, V., 1978, Statistical processing of anisotropy of magnetic susceptibility measured on groups of specimens. *Studies of Geophysics and Geodesy*, vol. 22, pp. 50-62.

Johnston, S.T. & Thorkelson, D.J. 1997, Cocos-Nazca slab window beneath Central America, *Earth and Planetary Science Letters*, vol. 146, no. 3-4, pp. 465-474.

Kanamatsu, T., Herrero-Bervera, E. & Taira, A. 2001, Magnetic fabrics of soft-sediment folded strata within a Neogene accretionary complex, the Miura Group, central Japan, *Earth and Planetary Science Letters*, vol. 187, no. 3-4, pp. 333-343.

Kirscvink, J.L. 1980, The least-squares line and plane and the analysis of paleomagnetic data *Geophysical Journal of the Royal Astronomical Society*, vol.62, no. 3, pp. 699-718.

Lonsdale, P.F. 1988, Paleogene history of the Kula Plate; offshore evidence and onshore implications, *Geological Society of America Bulletin*, vol. 100, no. 5, pp. 733-754.

Madsen, J.K., Thorkelson, D.J., Friedman, R.M. & Marshall, D.D. 2006, Cenozoic to Recent plate configurations in the Pacific Basin; ridge subduction and slab

window magmatism in western North America, *Geosphere*, vol. 2, no. 1, pp. 11-34.

Marshak, R.S. & Karig, D.E. 1977, Triple junctions as a cause for anomalously near-trench igneous activity between the trench and volcanic arc, *Geology (Boulder)*, vol. 5, no. 4, pp. 233-236.

McFadden, P.L. & Reid, A.B. 1982, Analysis of palaeomagnetic inclination data, *Geophysical Journal of the Royal Astronomical Society*, vol. 69, no. 2, pp. 307-319.

Moore, J.C., Byrne, T., Plumley, P.W., Reid, M., Gibbons, H. & Coe, R.S. 1983, Paleogene evolution of the Kodiak Islands, Alaska; consequences of ridge-trench interaction in a more southerly latitude, *Tectonics*, vol. 2, no. 3, pp. 265-293.

O'Connell, K. 2008, Sedimentology, structural geology, and paleomagnetism of the ghost rocks formation; kodiak islands, Alaska; M.S. Thesis, University of California at Davis, Davis, CA, United States, (USA).

O'Connell, K., Housen, B. & Roeske, S. 2007, Revisiting the paleomagnetism of a Paleocene trench-ridge-trench triple junction; kodiak islands, Alaska; Geological Society of America, 2007 annual meeting, *Abstracts with Programs - Geological Society of America*, vol. 39, no. 6, pp. 490.

Pares, J.M., van der Pluijm,Ben A. & Dinares Turell, J. 1999, Evolution of magnetic fabrics during incipient deformation of mudrocks (Pyrenees, northern Spain); Applications of magnetic anisotropies to fabric studies of rocks and sediments, *Tectonophysics*, vol. 307, no. 1-2, pp. 1-14.

Pares, J.M. & Moore, T.C. 2005, New evidence for the Hawaiian Hot Spot plume motion since the Eocene, *Earth and Planetary Science Letters*, vol. 237, no. 3-4, pp. 951-959.

Pares, J.M. & van der Pluijm,Ben A. 2002, Evaluating magnetic lineations (AMS) in deformed rocks, *Tectonophysics*, vol. 350, no. 4, pp. 283-298.

Pavlis, T.L. & Sisson, V.B. 2003, Development of a subhorizontal decoupling horizon in a transpressional system, Chugach metamorphic complex, Alaska; evidence for rheological stratification of the crust; Geology of a transpressional

orogen developed during ridge-trench interaction along the North Pacific margin, *Special Paper - Geological Society of America*, vol. 371, pp. 191-216.

Pavlis, T.L. & Sisson, V.B. 1995, Structural history of the Chugach metamorphic complex in the Tana River region, eastern Alaska; a record of Eocene ridge subduction, *Geological Society of America Bulletin*, vol. 107, no. 11, pp. 1333-1355.

Plafker, G., Moore, J.C. & Winkler, G.R. 1994, Geology of the Southern Alaska margin in *The geology of Alaska*, eds. G. Plafker & H.C. Berg, Geological Society of America, Boulder, CO, United States (USA), United States (USA).

Plumley, P.W., Coe, R.S. & Byrne, T. 1983, Paleomagnetism of the Paleocene Ghost Rocks Formation, Prince William terrane, Alaska, *Tectonics*, vol. 2, no. 3, pp. 295-314.

Roeske, S.M., Snee, L.W. & Pavlis, T.L. 2003, Dextral-slip reactivation of an arc-forearc boundary during Late Cretaceous-early Eocene oblique convergence in the northern Cordillera; Geology of a transpressional orogen developed during ridge-trench interaction along the North Pacific margin, *Special Paper - Geological Society of America*, vol. 371, pp. 141-169.

Rosa, J.W.C., Molnar, P. & Orcutt, J.A. 1988, Uncertainties in reconstructions of the Pacific, Farallon, Vancouver, and Kula plates and constraints on the rigidity of the Pacific and Farallon (and Vancouver) plates between 72 and 35 Ma; Special section; tribute to H. W. Menard, *Journal of Geophysical Research*, vol. 93, no. B4, pp. 2997-3008.

Sample, J.C. & Reid, M.R. 2003, Large-scale, latest Cretaceous uplift along the Northeast Pacific Rim; evidence from sediment volume, sandstone petrography, and Nd isotope signatures of the Kodiak Formation, Kodiak Islands, Alaska; Geology of a transpressional orogen developed during ridge-trench interaction along the North Pacific margin, *Special Paper - Geological Society of America*, vol. 371, pp. 51-70.

Sisson, V.B., Pavlis, T.L., Roeske, S.M. & Thorkelson, D.J. 2003, Introduction; an overview of ridge-trench interactions in modern and ancient settings; Geology of a transpressional orogen developed during ridge-trench interaction along the North Pacific margin, *Special Paper - Geological Society of America*, vol. 371, pp. 1-18.

Stock, J. & Molnar, P. 1988, Uncertainties and implications of the Late Cretaceous and Tertiary position of North America relative to the Farallon, Kula, and Pacific plates, *Tectonics,* vol. 7, no. 6, pp. 1339-1384.

Tarduno, J.A., Duncan, R.A., Scholl, D.W., Cottrell, R.D., Steinberger, B., Thordarson, T., Kerr, B.C., Neal, C.R., Frey, F.A., Torii, M. & Carvallo, C. 2003, The Emperor Seamounts; southward motion of the Hawaiian Hotspot plume in Earth's mantle, *Science,* vol. 301, no. 5636, pp. 1064-1069.

Tarling, D.H. & Hrouda, F. 1993, *The magnetic anisotropy of rocks,* Chapman & Hall, London, United Kingdom (GBR), United Kingdom (GBR).

Tauxe, L. & Watson, G.S. 1994, The fold test; an eigen analysis approach, *Earth and Planetary Science Letters,* vol. 122, no. 3-4, pp. 331-341.

Tauxe, L. 1998, Paleomagnetic principles and practice, *Modern Approaches in Geophysics,* vol. 17, pp. 299.

Thorkelson, D.J. 1996, Subduction of diverging plates and the principles of slab window formation, *Tectonophysics,* vol. 255, no. 1-2, pp. 47-63.

Thorkelson, D.J. & Taylor, R.P. 1989, Cordilleran slab windows, *Geology (Boulder),* vol. 17, no. 9, pp. 833-836.

Vrolijk, P., Myers, G. & Moore, J.C. 1988, Warm fluid migration along tectonic melanges in the Kodiak accretionary complex, Alaska, *Journal of Geophysical Research,* vol. 93, no. B9, pp. 10-10,324.

Weinberger, J. & Sisson, V.B. 2003, Pressure and temperature conditions of brittle-ductile vein emplacement in the greenschist facies, Chugach metamorphic complex, Alaska; evidence from fluid inclusions; Geology of a transpressional orogen developed during ridge-trench interaction along the North Pacific margin, *Special Paper - Geological Society of America,* vol. 371, pp. 217-235.